Medium Effects on Charge Transfer in Metal Complexes

Pingyun Chen and Thomas J. Meyer*

Department of Chemistry, University of North Carolina, Chapel Hill, North Carolina 27599–3290

Received July 29, 1997 (Revised Manuscript Received January 8, 1998)

Contents

I. Introduction

The solvent plays an important role in many chemical reactions, especially charge transfer where there is typically a substantial change in electronic distribution between the initial and final states.[1−3] Surrounding solvent molecules respond to this change and can influence both energetics and dynamics to a substantial degree. Changes in solvent can change the rate constant for electron transfer or cause dramatic shifts in absorption or emission, for example.[1−8] Transition metal complexes have provided useful probes for studying solvent effects.[5,8−15] They have easily measured spectroscopic properties and can be varied by making changes in the surrounding ligands.[16−19] The goal of this account is to summarize the results of solvent dependence studies on metal complexes, especially d^6 polypyridyl and ammine complexes relying on a survey of the literature to late 1996. They will be compared with relevant organic examples and both will be examined critically in light of available theories. There is a rich panoply of solvent-dependent, charge-transfer behavior in these molecules and our goal is to describe them and analyze them systematically with a section at the end for overview and conclusions.

II. Role of the Solvent: A Theoretical Background

A. Solvent Models

In the absence of an electric field, solvent molecules are randomly oriented (in H-bonding solvents structured clusters exist which are, themselves, randomly oriented).[20−22] The electric field of an added ion induces partial alignments of permanent dipoles of neighboring solvent molecules, distortion of electron

S0009-2665(94)01180-5 CCC: $30.00
Published on Web 05/23/1998

Pingyun Chen was born in 1962 in Gansu, China. He received a B.S. degree from Lanzhou University, Lanzhou, China, in 1982 and a Ph.D. degree from the University of North Carolina at Chapel Hill in 1989. He remained at the University of North Carolina for three years as a research associate with Professor Thomas J. Meyer and broadened his background in inorganic photochemistry, electron-transfer theories, and laser spectroscopy. He then spent one year with Dr. Richard Holroyd at Brookhaven National Laboratory. In 1994, he was appointed an instructor at Duke University where he also worked with Professor Richard A. Palmer on applications of step-scan, Fourier-transform infrared spectroscopy. In the fall of 1996, he returned to the University of North Carolina at Chapel Hill as a Laser Application Specialist. In 1998, he joined Nicolet Instrument Corporation as a Product Specialist. The research interests of Dr. Chen extend over a broad range of areas that include excited state electron and energy transfer in condensed media, laser spectroscopy, Fourier-transform infrared spectroscopy.

Professor Thomas J. Meyer is Vice Provost for Graduate Studies and Research, and Kenan Professor of Chemistry at the University of North Carolina at Chapel Hill. He was born in 1941 in Dennison, OH, received the B.S. degree summa cum laude from The Ohio University in 1963, and a Ph.D. degree from Stanford University in 1966. At Stanford his research director was Professor Henry Taube. After leaving Stanford, he spent a year as a NATO Postdoctoral Fellow at University College—London and worked with the late Sir R. S. Nyholm. In January, 1968, Professor Meyer was appointed Assistant Professor at the University of North Carolina at Chapel Hill where he has remained throughout his academic career. He has served as chair of Chemistry and of the Applied Sciences Curriculum and is currently on the Boards of the NC Board of Science and Technology, Research Triangle Institute, NC Biotechnology Center, and Triangle Universities Center for Advanced Studies Inc. Professor Meyer has served as visiting lecturer or visiting scholar at many universities throughout the United States and abroad, and has been recipient of a number of awards which have recognized his contributions as a teacher and scholar, including induction into both the National Academy of Sciences and the American Academy of Arts & Sciences. The research interests of Professor Meyer and his group extend over a number of areas of chemistry. They include mechanisms and catalysis of oxidation-reduction reactions, photochemical electron and energy transfer, artificial photosynthesis, and interfacial chemistry in thin films and molecular layers.

clouds and bonds, and translational displacements of solvent molecules from their equilibrium positions. The magnitude of the polarization depends on the individual and collective properties of the solvent molecules and the strength of the electric field.[3,21−23] The total polarization is a sum of contributions from changes in electronic, local translational oscillations, and orientational displacements. Their response times are $\sim 10^{-15}$, $\sim 10^{-13}$, and $\sim 10^{-11}$ s, respectively.[1,3,21−24] The local translational oscillations are analogous to phonon motions in the solid state and the orientations are collective rotations of solvent dipoles.[25−27]

In dielectric continuum treatments, the solvent is modeled as a structureless continuum characterized by its macroscopic dielectric constant. Because of the different time scales of the contributors, the dielectric constant (or relative permittivity) depends on the frequency of the applied electric field.[3,21−24] For some polar organic solvents the frequency dependence can be described by the Debye function,

$$\epsilon^*(\omega) = \epsilon_\infty + (\epsilon_o - \epsilon_\infty)/(1 + i\omega\tau_D) \qquad (1)$$

$\epsilon^*(\omega)$ is the dielectric constant at ω ($= 2\pi\nu$), the angular frequency of the applied field. ϵ_∞ ($= D_{op}$) and ϵ_o ($= D_s$) are the dielectric constants at very high (optical) and zero (static) frequencies. $\epsilon_o > \epsilon_\infty$ because in an oscillating electric field of very high frequencies, orientational changes are too slow to follow the field and do not contribute to $\epsilon^*(\omega)$. τ_D is the Debye relaxation time. ϵ_o can be measured from the change in capacitance in the presence and absence of the dielectric, and $\epsilon_\infty \approx n^2$ where n is the refractive index of the solvent.

Equation 1 is valid only for simple liquids at low frequencies. In short-chain alcohols which form H-bonded clusters, as many as three Debye-like terms are needed to describe frequency-dependent dielectric properties.[28−30] They have been attributed to hydrogen-bonding dynamics in molecular aggregates, monomer reorientation, and rotation of terminal C−OH groups.

A quantum treatment of the solvent was proposed by Levich and Dogonadze and applied to electron transfer.[26,31] In this model, molecules in liquids were assumed to perform diffusive jumps between temporary equilibrium positions and collective rotations about temporary equilibrium positions (orientations) determined locally by molecular symmetry and intermolecular interactions. The effects of diffusive jumps on electron transfer were neglected because they occur on a longer time scale ($\sim 10^{-10}$ s). Orientations were treated as harmonic oscillators and treated analogously to lattice vibrations in crystals (phonons).[32−34] The quantum spacings for these modes are small for common organic solvents (<50 cm^{-1}) and they were treated classically at or near room temperature.[3,8,35]

There is a well-established theoretical basis for treating liquids as a set of simple harmonic oscillators.[27] Following the initial work of Zwanzig,[36] new theoretical approaches have been developed on the

basis of quenched normal modes[37] and instantaneous normal modes[27] and applied to the description of liquid properties. These models give insight into the origin of solvation and solvent dynamics on short time scales. They are partitioned into collective rotations and fast, phonon-like translations.

Implementing these models computationally is difficult because of the large number of solvent molecules involved. There is still considerable value in describing solvent motions as a collection of coupled harmonic oscillators. A quantum mechanical description of solvent polarization is provided and, with it, useful quantitative relationships emerge which are applicable to electron transfer and spectroscopy. These relationships originate from physically transparent models which incorporate temperature and entropic effects. More sophisticated models and their applications to solvation and solvent dynamics have been summarized in recent reviews.[38−42]

B. Classical Theories of Electron Transfer

The rate constant for intramolecular electron transfer at a defined separation distance, in the limit that solvent dynamics are not rate limiting, is given by[6,8,43−48]

$$k_{ET} = \nu_{ET} \exp(-\Delta G^*/RT) = \kappa \nu_n \exp(-\Delta G^*/RT) \quad (2)$$

ΔG^* is the free energy of activation and ν_{ET} is the frequency factor for electron transfer. It is the product of the effective frequency for nuclear motion (or motions) along the reaction coordinate (ν_n) and the probability that electron transfer will occur at the nuclear coordinates of the activated complexes (κ).

For a bimolecular reaction in which electron transfer occurs at close contact and well below the diffusion-controlled limit, the experimentally observed rate constant, k_{obs}, is the product of the rate constant for electron transfer within the association complex of the reactants (k_{ET}) and the equilibrium constant for its formation K_A:[8,43,44,49−51]

$$k_{obs} = K_A k_{ET} \quad (3)$$

More generally, electron transfer can occur over a range of internuclear separations (d), not just at close contact, and $K_A k_{ET}$ is replaced by the result of integration over a distribution function of separation distances weighted by a distance dependent k_{ET}.[8,43,44,47,50]

Preassociation between ions in a bimolecular reaction introduces a solvent dependence because of the electrostatic work required to bring the ions together (w). From the Eigen−Fuoss equation for spherical ions in a dielectric continuum:[52−54]

$$K_A = \frac{4\pi N_A d^3}{3000} \exp[-(w/RT)] \quad (4)$$

$$w = \frac{Z_1 Z_2 e^2}{d\mathrm{D}} \frac{1}{(1 + \beta d\sqrt{\mu})} \quad (4a)$$

K_A depends on the separation distance between the centers of the ions (d), their radii (a_1 and a_2) and charges (Z_1 and Z_2), the static dielectric constant (D_s) and the ionic strength (μ). N_A is Avogadro's number, β is the Debye length, $(8\pi N_A e^2/1000\, D_s RT)^{1/2}$, and w is the electrostatic work required to bring the ions together, e is the unit electron charge. Equation 4 is valid only if $a_1 = a_2$.

Near the diffusion-controlled limit, diffusion (k_D) and electron transfer ($k_{ET}K_A$) are comparable in magnitude and kinetically coupled:[8,43,44,49−53]

$$\frac{1}{k_{obs}} = \frac{1}{k_D} + \frac{1}{k_{ET}K_A} \quad (5)$$

This introduces an additional solvent dependence through k_D and the solvent viscosity (η) since for spherical ions:[50,55−57]

$$k_D = \left(\frac{2RT}{3000\eta}\right)\left(2 + \frac{a_1}{a_2} + \frac{a_2}{a_1}\right)\delta \quad (6)$$

$$\delta = \frac{w/RT}{\exp(w/RT) - 1} \quad (6a)$$

For the electron-transfer step Marcus and Hush derived a quadratic dependence for the activation free energy (ΔG^*) on the free energy change ($\Delta G°$) and reorganizational energy (λ):[6,8,9,43−48,58−65]

$$\Delta G^* = (\lambda + \Delta G°)^2/4\lambda \quad (7)$$

λ is the sum of intramolecular (λ_i) and solvent (λ_o) reorganizational energies:

$$\lambda = \lambda_i + \lambda_o \quad (8)$$

λ_o was calculated by dielectric continuum theory in which the discrete character of individual solvent molecules is neglected and the solvent is treated as a structureless continuum. Electronic polarization does not contribute to λ_o because its response time is rapid compared to electron transfer and it always remains in equilibrium with the charge distribution of the system during the transition. Reorganization is required in the translational and orientational parts of the polarization. Marcus devised a two-step thermodynamic cycle for calculating λ_o.[24,58] In the first step, reactant charges are changed to those appropriate for electron transfer in the activated complex. In the second, charges are returned to those of the reactants but having the translational and orientational polarizations of the activated complex. The form derived for λ_o depends on the geometrical model chosen to represent the charge distribution. For spherical reactants, λ_o is given by[3,6,8,9,26,31,43−48,58−67]

$$\lambda_o = e^2\left(\frac{1}{2a_1} + \frac{1}{2a_2} - \frac{1}{d}\right)\left(\frac{1}{D_{op}} - \frac{1}{D_s}\right) \quad (9)$$

As we shall see in later sections, dielectric continuum theory breaks down if there are specific solute−solvent interactions,[68] dielectric saturation,[69−73] or coupled quantum modes in the solvent.[74]

Intramolecular vibrations have higher energy quantum spacings than coupled solvent modes and, in general, must be treated quantum mechanically. If $\hbar\omega < k_B T$, they can be treated as classical harmonic oscillators and λ_i is given by[6,8,43,48,61,75]

$$\lambda_i = \sum_j \frac{1}{2} f_j (\Delta Q_{e,j})^2 \tag{10}$$

The summation is over all coupled modes, j, with f_j the force constant for mode j assumed to be the same in the initial and final states, and $\Delta Q_{e,j}$ the change in equilibrium displacement. The only contributors to λ_i are those that have $\Delta Q_{e,j} \neq 0$.

In the *nonadiabatic* limit, nuclear motions are rapid on the electron-transfer time scale, the populations in coupled intramolecular and solvent vibrations remain in thermal equilibrium as electron transfer occurs, and[8,43,44,76]

$$\nu_{ET} = \frac{2\pi {H_{DA}}^2}{\hbar}\left(\frac{1}{4\pi\lambda RT}\right)^{1/2} \tag{11}$$

H_{DA} is the electron-transfer matrix element. It is the resonance energy arising from orbital mixing between the donor and acceptor.

In the *adiabatic* limit, H_{DA} is sufficiently large that the exchanging electron is always in equilibrium with the nuclear coordinates and $\kappa = 1$, and $\nu_{ET} = \nu_n$ in eq 2. In the classical limit, ν_n is given by the weighted average of the frequencies of the coupled solvent and intramolecular modes (ν_j):[8,43,77,78]

$$\nu_n = \left(\frac{\sum_j \lambda_j {\nu_j}^2}{\sum_j \lambda_j}\right)^{1/2}$$

with $\lambda_j = 1/2 f_j (\Delta Q_{e,j})^2$. If ν_n is dictated by longitudinal relaxation in the solvent:[28,79−98]

$$\nu_n = \frac{1}{\tau_l} A \tag{12}$$

τ_l is the longitudinal relaxation time. For solvents that are described by eq 1, τ_l is related to the Debye relaxation time by $\tau_l = \tau_D(\epsilon_\infty/\epsilon_o)$. The constant A depends on the model and assumptions used in the analysis.[79−98]

Classical theories are adequate for reactions in which there are no coupled high- or medium-frequency modes and at high temperature. In general, there *are* coupled high- or medium-frequency modes and they must be treated quantum mechanically in order to include transitions from low-lying vibrational levels (nuclear tunneling).

C. Theory of Time-Dependent Processes

The probability per unit time that a transition will occur between two electronic states is given by the "Golden Rule" result in eq 13.[3,99−104]

$$w = \frac{2\pi}{\hbar}\langle \Psi' | H' | \Psi \rangle^2 \delta(E' - E) \tag{13}$$

Ψ, Ψ', E, and E' are wave functions and energies of the two states and $\hat{H}'$ the perturbation that induces the transition. The Dirac delta function $\delta(E' - E)$ ensures that the transition occurs with energy conservation. This result is valid only in the weak coupling limit where the perturbation is small and the transition probability low.

For molecular systems, application of the Born−Oppenheimer and Condon approximations allow the integral in eq 13 to be partitioned between nuclear and electronic parts:

$$w = \frac{2\pi}{\hbar}\langle \psi'_{el} | \hat{H}' | \psi_{el} \rangle^2 \langle \psi'_{vib} | \psi_{vib} \rangle^2 \delta(E' - E) \tag{14}$$

This is a general result applicable to light absorption, emission, electron transfer, and excited-state decay.[3,9,26,51,102−108] $\hat{H}'$ is different for the different processes. The ψ'_{el} and ψ_{el} are electronic wave functions for the final and initial states. It is assumed that the electronic matrix element, $\langle \psi'_{el} | \hat{H}' | \psi_{el} \rangle$, is independent of nuclear coordinates.

ψ'_{vib} and ψ_{vib} are *total* vibrational wave functions for the final and initial states. They are products of wave functions for *all* normal modes including collective solvent vibrations:[99,109,110]

$$\psi_{vib} = \prod_j \chi_{v_j} \tag{15}$$

$$\psi'_{vib} = \prod_j \chi_{v_j'} \tag{16}$$

χ_{v_j} and $\chi_{v_j'}$ are wave functions for mode j in the initial and final states. v_j and v_j' are the associated vibrational quantum numbers.

For harmonic oscillators with no frequency change ($\hbar\omega_j = \hbar\omega_j'$), the vibrational overlap integrals have the form:[3,99]

$$\langle \chi_{v_j'} | \chi_{v_j} \rangle = \exp(-S_j) S_j^{(v_j' - v_j)} \frac{v_j!}{v_j'!} [L_{v_j}^{(v_j' - v_j)}(S_j)]^2 \tag{17}$$

$L_{v_j}^{(v_j' - v_j)}(S_j)$ is a Laguerre polynomial:

$$L_{v_j}^{(v_j' - v_j)}(S_j) = \sum_{v=0}^{v_j} \frac{v_j'! \, (-S_j)^v}{(v_j - v)!(v_j' - v_j + v)! v!} \tag{18}$$

S_j is the electron-vibrational coupling constant, or Huang−Rhys factor:[99,105]

$$S_j = \frac{1}{2}\left(\frac{M_j \omega_j}{\hbar}\right)(\Delta Q_{e,j})^2 \tag{19}$$

M_j is the reduced mass. The physical significance of the vibrational overlap integrals is that they give the extent to which the final and initial states coincide along the normal coordinate.

The population in level v_j is given by

$$p(v_j) = \exp[-(v_j\hbar\omega_j/k_BT)]/Z_j = \exp[-(v_j\beta_j)]/Z_j \quad (20)$$

with $\beta_j = \hbar\omega_j/k_BT$ and Z_j the vibrational partition function,

$$Z_j = \sum_{v_j} \exp\left[-\left(v_j + \frac{1}{2}\right)\beta_j\right] \quad (21)$$

If $\hbar\omega_j \gg k_BT$, only $v_j = 0$ is appreciably populated and

$$\langle\chi_{v_j'}|\chi_{v_j=0}\rangle^2 = \exp(-S_j)\frac{S_j^{v_j'}}{v_j'!} \quad (22)$$

The only modes coupled to a transition between states are those that have $S_j \neq 0$ and/or $\hbar\omega_j \neq \hbar\omega_j'$. The sum of the $\Delta Q_{e,j}$ changes for these modes adds up to the differences in molecular structure between states. These coupled modes determine the band shape in absorption and emission, define the barrier to electron transfer, and act as energy acceptors in excited-state decay. For all other modes, $\langle\chi_{v_j'}|\chi_{v_j}\rangle = 1$ for $v_j = v_j'$ or 0 for $v_j \neq v_j'$ and they have no effect on band shapes or barriers.

Quantum spacings for the solvent modes (orientations and translations) are typically small with $k_BT \gg \hbar\omega$.[3] Their energy levels form a continuum or near continuum at or near room temperature and the solvent can be treated classically. The solvent adds to the barrier through λ_o and provides a continuum or near continuum distribution of levels required for energy conservation through individual reaction channels.

D. Electron Transfer

Application of the Golden rule result in eq 14 to electron transfer in the nonadiabatic limit gives[3,8,26,76,102,111−120]

$$k_{ET} = \frac{2\pi}{\hbar}\frac{H_{DA}^2}{(4\pi\lambda_oRT)^{1/2}}\prod_j\sum_{v_j}\sum_{v_j'}p(v_j)\exp(-S_j)S_j^{(v_j'-v_j)}\frac{v_j!}{v_j'!}[L_{v_j}^{(v_j'-v_j)}(S_j)]^2 \times \exp[-(\Delta G° + \sum_j(v_j'-v_j)\hbar\omega_j + \lambda_o)^2/4\lambda_oRT] \quad (23)$$

k_{ET} is the Boltzmann weighted sum of k's for transitions through a series of vibrational channels from a set of initial levels v_j to final levels v_j'. The solvent is treated classically and included in the exponential distribution function. It gives the fraction of molecules surrounded by solvent polarizations having the required appropriate energy to achieve energy conservation for a given channel.

In eq 23 it is assumed that $\hbar\omega = \hbar\omega'$ for the high-frequency modes included in the summation. Frequency changes in the solvent modes (and low-frequency vibrations) are included in $\Delta G°$ (see section II.H).[8,115−117,121−124] In the classical limit with $\hbar\omega_j \ll k_BT$ and $\lambda = \lambda_i + \lambda_o$:[8,43]

$$k_{ET} = \frac{2\pi}{\hbar}\frac{H_{DA}^2}{(4\pi\lambda RT)^{1/2}}\exp[-[(\Delta G° + \lambda)^2/4\lambda RT]] \quad (24)$$

The classical result works reasonably well for metal complexes where the reaction barrier is dominated by coupled low-frequency metal−ligand vibrations and the solvent.[8−13,77,125−130]

With one coupled medium- or high-frequency mode (or averaged mode), only the $v = 0$ vibrational level is appreciably populated at room temperature ($\hbar\omega \gg k_BT$), and[8,43,112,115,131]

$$k_{ET} = \frac{2\pi}{\hbar}\frac{H_{DA}^2}{(4\pi\lambda_oRT)^{1/2}}\sum_{v'}\exp(-S)\frac{S^{v'}}{v'!}\exp[-[(\Delta G° + v'\hbar\omega + \lambda_o)^2/4\lambda_oRT]] \quad (25)$$

In this limit the coupled vibration does not contribute to the temperature dependence since the only contributing reaction channels originate from $v = 0$. If there are coupled low-frequency vibrations, they can be treated classically and included in eq 25 by replacing λ_o with $\lambda_{o,L}$. It is defined by

$$\lambda_{o,L} = \lambda_o + \lambda_{i,L} \quad (26)$$

with

$$\lambda_{i,L} = \sum_l S_l\hbar\omega_l \quad (27)$$

This is the reorganizational energy contributed by the low-frequency modes. The summation is over the coupled modes.

In the adiabatic limit, a treatment by Burshtein et al. predicts that the frequency factor is controlled by repopulation at the crossing points of a few dominant reaction channels rather than by electronic coupling.[132] They can become depleted forming "holes" in the thermal distribution. If the holes are dynamically linked by energy interconversion, the individual channels are coupled and the total rate constant cannot exceed the rate constant through the fastest channel.[132,133]

E. Electron Transfer in the Inverted Region

The classical result in eq 24 predicts that k_{ET} should increase with $-\Delta G°$ (if $-\Delta G° < \lambda$) and reach a maximum at $\lambda = -\Delta G°$ with

$$k_{ET} = \frac{2\pi}{\hbar}\frac{H_{DA}^2}{(4\pi\lambda RT)^{1/2}} \quad (28)$$

Further increases in $-\Delta G°$ are predicted to decrease $\ln(k_{ET})$ quadratically. This is the well-known "inverted region" effect predicted by Marcus.[46,62]

With a single coupled high- or medium-frequency mode (or averaged mode), eq 25 applies and the dependence of $\ln(k_{ET})$ on $-\Delta G°$ in the inverted region is predicted to be less than quadratic. State-to-state vibrational transitions are dominated by channels through $v = 0$ and there is no requirement for barrier crossing. In the limit, $-\Delta G° \gg S\hbar\omega$ and $\hbar\omega \gg k_BT$,

a closed form expression for k_{ET} can be derived giving the approximate "energy gap law" result in eq 29:[113,131,134,135]

$$k_{ET} = \frac{2\pi}{\hbar}\frac{{H_{DA}}^2}{(\hbar\omega(|\Delta G°| - \lambda_o))^{1/2}} \exp\left[-S - \frac{\gamma(|\Delta G°| - \lambda_o)}{\hbar\omega} + \left(\frac{\gamma+1}{\hbar\omega}\right)^2 \lambda_o k_B T\right] \quad (29)$$

$$\gamma = \ln\left[\frac{|\Delta G°| - \lambda_o}{S\hbar\omega}\right] - 1 \quad (30)$$

This result predicts that $\ln(k_{ET})$ should decrease linearly with $-\Delta G°$.

There are some unusual features associated with the solvent in the inverted region. Solvent dynamical effects are small or negligible for all but the fastest reactions.[84,85,92,136−138] As for nonradiative decay, electron transfer can continue to occur even in frozen media (section VI.B).[139−141] For bimolecular reactions in the normal region, k_{ET} is predicted to decrease with separation distance d and to reach a maximum at close contact.[142,143] This is because H_{DA} decreases with d (section III.A) and λ_o increases (eq 9). In the inverted region λ_o appears in the energy gap term, $\exp[-[(\gamma/\hbar\omega)(|\Delta G°|-\lambda_o)]$, and this favors electron transfer at longer distances. The value of d that maximizes k_{ET} represents a balance between the distance dependences of H_{DA} and λ_o.[142,143]

F. Excited State Decay

Rate constants for radiative (k_r) and nonradiative (k_{nr}) excited-state decay can be evaluated from lifetime (τ) and emission quantum yield (Φ_{em}) measurements:

$$\tau^{-1} = k_r + k_{nr} \quad (31a)$$

$$k_r = \Phi_{em}\tau^{-1} \quad (31b)$$

1. Radiative Decay

The rate constant for radiative decay by spontaneous emission is given by[104,134,144,145]

$$k_r = 8\pi\hbar c n^3 \langle\bar{\nu}^{-3}\rangle^{-1} B \quad (32)$$

n is the index of refraction of the solvent and $\langle\bar{\nu}^{-3}\rangle^{-1}$ is defined as

$$\langle\bar{\nu}^{-3}\rangle^{-1} = (\int I(\bar{\nu})\, d\bar{\nu})/(\int I(\bar{\nu})\bar{\nu}^{-3}\, d\bar{\nu})$$

$\bar{\nu}$ is the average emission energy (in cm^{-1}) and $I(\bar{\nu})$ is the emission intensity in quanta per energy interval per second at $\bar{\nu}$.[134] The Einstein B coefficient is related to the transition moment, $\vec{M}$, by

$$B = \frac{8\pi^3}{3\hbar^2 c}|\vec{M}|^2 = \frac{2303}{\hbar n N_A}\int \epsilon(\bar{\nu})\, d(\ln\bar{\nu}) \quad (33)$$

N_A is Avogadro's number and $\epsilon(\bar{\nu})$ the molar extinction coefficient at $\bar{\nu}$. It follows from eqs 32 and 33 that k_r is related to $\vec{M}$ by

$$k_r = \frac{64\pi^4 n^3}{3\hbar}|\vec{M}|^2\langle\bar{\nu}^{-3}\rangle^{-1} \quad (34)$$

2. Nonradiative Decay

In nonradiative decay, the initial electronic energy of the excited state appears in vibrational and solvent modes of the ground state.[51,134,135,146−156] The transition between states is induced by "promoting modes" which perturb the electron clouds and induce the transition. The excess energy of the excited state is channeled into the "acceptor" modes and the solvent. If there is a single coupled high- or medium-frequency acceptor mode (or average mode) with $\hbar\omega = \hbar\omega'$, $\hbar\omega \gg k_B T$, k_{nr} is given by[131,134,147]

$$k_{nr} = \frac{2\pi}{\hbar}\frac{{V_k}^2}{(4\pi\lambda_o RT)^{1/2}}\sum_{v'}\exp(-S)\frac{S^{v'}}{v'!}\exp[-[(|\Delta G°| - v\hbar\omega - \lambda_o)^2/4\lambda_o RT]] \quad (35)$$

In this equation, the solvent is treated classically and frequency changes in solvent modes are included in $\Delta G°$, section II.G.2. The solvent influences the magnitudes of the vibrational overlap integrals through its effect on the energy gap and it also acts as an energy acceptor.[135,151,152]

If there is a single promoting mode of quantum spacing $\hbar\omega_k$ and coordinate Q_k,[134,153−156]

$$V_k = \frac{\hbar^2}{M_k}\langle\psi_{el}'|\partial/\partial Q_k|\psi_{el}\rangle\langle\chi_{v_k'}|\partial/\partial Q_k|\chi_{v_k}\rangle = \frac{\hbar}{{M_k}^{1/2}}\langle\psi_{el}'|\partial/\partial Q_k|\psi_{el}\rangle(\hbar\omega_k/2)^{1/2} = C_k(\hbar\omega_k/2)^{1/2} \quad (36)$$

M_k is the reduced mass of the promoting mode k. V_k is the vibrationally induced electronic coupling matrix element. It arises from the effect of selected vibrations in mixing the excited and ground-state electronic wave functions and is a breakdown of Born−Oppenheimer approximation. Equation 36 is applicable to internal conversion. For intersystem crossing, the effect of spin−orbit coupling on the mixing of the electronic wave functions must be included.

The energy gap law form of eq 35 for nonradiative decay with E_o ($= |\Delta G°|-\lambda_o$) $\gg S\hbar\omega$ and $\hbar\omega \gg k_B T$ is given by[102,134,135]

$$k_{nr} = \frac{\sqrt{\pi}\omega_k {C_k}^2}{(2\hbar\omega E_o)^{1/2}}\exp\left[-S - \frac{\gamma E_o}{\hbar\omega} + \left(\frac{\gamma+1}{\hbar\omega}\right)^2\lambda_o k_B T\right] \quad (37)$$

$$\gamma = \ln\left[\frac{E_o}{S\hbar\omega}\right] - 1 \quad (38)$$

The solvent enters this expression both through λ_o and its effect on the energy gap, E_o. Related forms of the energy gap law have been derived[134,135,150−156] and applied to nonradiative decay in organic,[157−162] lanthanide,[163−165] and other transition metal complex excited states.[134,166−172]

G. Absorption and Emission

Application of the Golden rule to single photon absorption gives[90,100,104−107]

$$w(\nu) = \frac{2\pi}{3\hbar^2 n^2}|\vec{M}|^2 W(\nu) \quad (39)$$

$W(\nu)$ is the energy density of the electromagnetic field at frequency ν, $\vec{M}$ is the transition moment, and n, the refractive index. For an electric-dipole allowed transition with higher order terms negligible, $\vec{M}$ is given by

$$\vec{M} = \langle\psi'_{\rm el}|e\sum_n \vec{r}_n|\psi_{\rm el}\rangle\langle\psi'_{\rm vib}|\psi_{\rm vib}\rangle = \vec{\mu}\langle\psi'_{\rm vib}|\psi_{\rm vib}\rangle \quad (40)$$

$$\vec{\mu} = \langle\psi'_{\rm el}|e\sum_n \vec{r}_n|\psi_{\rm el}\rangle \quad (41)$$

The absorption intensity is determined by the magnitude of the transition dipole, $\vec{\mu}$. The sum is over all of the electronic coordinates, $\psi'_{\rm vib}$ and $\psi_{\rm vib}$ are the total vibrational wave functions in eqs 15 and 16.

1. Franck–Condon Analysis of Spectral Band Shapes

The integrated absorption spectrum is related to $\vec{M}$ by

$$\int \epsilon(\nu)\,{\rm d}\nu = \frac{4\pi^2 N_{\rm A}\nu}{3000cn\hbar\ \ln 10}|\vec{M}|^2 \quad (42)$$

Evaluation of the vibrational overlap integrals in eq 40 gives[73,100,104,123]

$$\int \epsilon(\nu)\,{\rm d}\nu = \frac{2\pi N_{\rm A}}{3000\ \ln 10cn\hbar^2}\frac{|\vec{\mu}|^2}{(4\pi\lambda_{\rm o}k_{\rm B}T)^{1/2}}\prod_j\sum_{v_j}\sum_{v_j'}(\Delta G^\circ + \sum_j(v_j' - v_j)\hbar\omega_j + \lambda_{\rm o})p(v_j)\exp(-S_j)\frac{S_j^{v_j'}v_j!}{v_j'!}[L_{v_j}^{(v_j'-v_j)}]^2 \times \exp -[(h\nu - (\Delta G^\circ + \sum_j(v_j' - v_j)\hbar\omega_j + \lambda_{\rm o}))^2/4\lambda_{\rm o}k_{\rm B}T] \quad (43)$$

This assumes $\hbar\omega = \hbar\omega'$ with frequency changes in the solvent included in ΔG°.

For a single coupled vibration or averaged vibration with $\hbar\omega \gg k_{\rm B}T$

$$\int \epsilon(\nu)\,{\rm d}\nu = \frac{2\pi N_{\rm A}}{3000\ \ln 10cn\hbar^2}\frac{|\vec{\mu}|^2}{(4\pi\lambda_{\rm o}k_{\rm B}T)^{1/2}}\sum_{v'}(\Delta G^\circ + v'\hbar\omega + \lambda_{\rm o})\exp(-S)\times \frac{S^{v'}}{v'!}\exp\left[-\left[\frac{(h\nu - (\Delta G^\circ + v'\hbar\omega + \lambda_{\rm o}))^2}{4\lambda_{\rm o}k_{\rm B}T}\right]\right] \quad (44)$$

This is an equation for a series of vibronic lines at $\Delta G^\circ + \lambda_{\rm o}$, $\Delta G^\circ + \lambda_{\rm o} + \hbar\omega$, $\Delta G^\circ + \lambda_{\rm o} + 2\hbar\omega$, etc., each broadened by the exponential solvent distribution function. The full width at half-maximum for each vibronic component, $\Delta\bar{\nu}_{1/2}$, is given by[9,73,123,173]

$$(\Delta\bar{\nu}_{1/2})^2 = 16k_{\rm B}T\lambda_{\rm o}\ln 2 \quad (45)$$

The equivalent of eq 43 for emission is[73,104]

$$\int I(\nu)\,{\rm d}\nu = \frac{8\pi|\vec{\mu}|^2}{3c^3\hbar^3}\prod_j\sum_{v_j}\sum_{v_j'}\left[[|\Delta G^\circ| - \sum_j(v_j - v_j')\hbar\omega_j - \lambda_{\rm o}]^3 p(v_j')\frac{S_j^{v_j}v_j'!}{v_j!}[L_{v_j}^{(v_j-v_j')}]^2 \times \exp[-[h\nu - [|\Delta G^\circ| - \sum_j(v_j - v_j')\hbar\omega_j - \lambda_{\rm o}]]^2/4\lambda_{\rm o}k_{\rm B}T]\right] \quad (46)$$

The notation is the same as for absorption but the initial and final states are reversed. If there is a single coupled medium or high-frequency vibration

$$\int I(\nu)\,{\rm d}\nu = \frac{8\pi N_{\rm A}}{3c^3\hbar^3}\frac{|\vec{\mu}|^2}{(4\pi\lambda_{\rm o}k_{\rm B}T)^{1/2}}\sum_v(|\Delta G^\circ| - v\hbar\omega - \lambda_{\rm o})^3\exp(-S)\times \frac{S^v}{v!}\exp\left[-\left[\frac{(h\nu - (|\Delta G^\circ| - v\hbar\omega - \lambda_{\rm o}))^2}{4\lambda_{\rm o}k_{\rm B}T}\right]\right] \quad (47)$$

If $\hbar\omega_j = \hbar\omega_j'$, normalized absorption ($\epsilon(\nu)/\nu$) and emission spectra ($I(\nu)/\nu^3$) are mirror images. The crossing point between them defines the 0−0 energy $E(0{-}0)$ and $E(0{-}0) = |\Delta G^\circ|$.

2. Temperature and Solvent Dependence by Moment Analysis

Application of the generating function method of Kubo[106] and the moment analysis of Lax[107] gives, for the first two moments of an absorption band,[123]

$$M_1 = \Delta E^\circ + \sum_j\lambda_j' + {}^1/_2\sum_j\hbar\Omega_j\coth(\beta_j/2) \quad (48)$$

$$M_2 = \sum_j\frac{(\hbar\omega_j')^2}{\hbar\omega_j}\lambda_j'\coth(\beta_j/2) + {}^1/_2\sum_j(\hbar\Omega_j)^2\coth^2(\beta_j/2) \quad (49)$$

The first moment is the mean band energy and the second moment is related to the bandwidth. For a Gaussian-shaped band,

$$M_1 = E_{\rm abs} \quad (50)$$

$$M_2 = (\Delta\bar{\nu}_{1/2})^2/(8\ln 2) \quad (51)$$

where $E_{\rm abs}$ is the absorption maximum and $\Delta\bar{\nu}_{1/2}$ the width at half-maximum.

Equations 48 and 49 introduce frequency changes between states with Ω_j, λ_j', and β_j defined as

$$\Omega_j = \frac{(\omega_j')^2 - (\omega_j)^2}{2\omega_j} \quad (52)$$

$$\lambda_j' = \frac{1}{2}M_j(\omega_j')^2(\Delta Q_{{\rm e},j})^2 = S_j\hbar\omega_j' \quad (53)$$

$$\beta_j = \hbar\omega_j/k_{\rm B}T \quad (54)$$

λ_j' and $\hbar\omega_j'$ are the reorganizational energy and

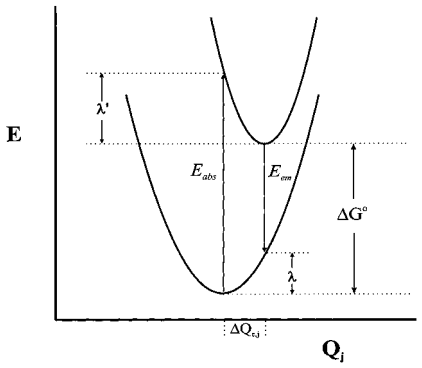

Figure 1. Schematic energy diagram along normal coordinate Q_j illustrating energy terms for absorption and emission. The energy surfaces are treated as harmonic oscillators with different frequencies for the ground and excited states. The reorganizational energy along the excited-state surface is λ' (for absorption) and that along the ground-state surface is λ (for emission). In the case illustrated, $\lambda' > \lambda$.

quantum spacing for mode j along the excited-state energy surface, λ_j and $\hbar\omega_j$ are the corresponding quantities for the ground-state surface. They are illustrated in Figure 1. λ_j and λ_j' are internal energy quantities, assumed to be temperature-independent. In the classical treatment of Marcus and Sutin, the reorganizational energies (λ) are free energies.[8,122] This distinction is of fundamental importance, but it remains to be resolved.

Changes in frequencies (and quantum spacings) for the coupled vibrations and solvent modes make M_1 and M_2 temperature dependent and introduce an entropic change, $\Delta S°$, which is defined in eq 55:[123]

$$T\Delta S° \approx -{}^1/_2\sum_j \hbar\Omega_j \coth(\beta_j/2) \tag{55}$$

Equation 55 is valid if $\Delta\omega_j = |\omega_j' - \omega_j| \ll \omega_j, \omega_j'$. It does not include the electronic entropy change (ΔS_{el}) arising from changes in electronic multiplicity.

In the classical limit, $\coth(\hbar\omega_j/2k_BT) \rightarrow 2k_BT\ \hbar\omega_j$, and

$$T\Delta S° \approx -k_BT\sum_j \frac{\Delta\omega_j}{\omega_j} \tag{56}$$

The ratio $\Delta\omega/\omega$ is usually small for high-frequency intramolecular vibrations. The solvent dominates because there are many coupled solvent modes of low frequency.

In the absence of pressure−volume work, $\Delta E° = \Delta H°$, and

$$M_1 = \Delta H° - T\Delta S° + \sum_j \lambda_j' = \Delta G° + \sum_j \lambda_j' = \Delta G° + \lambda \tag{57}$$

The temperature dependence of M_1 gives $-\Delta S°$,

$$\partial M_1/\partial T = -\Delta S° \tag{58}$$

If the second term in eq 49 is neglected ($\omega_j'^2 \gg (\omega_j')^2 - (\omega_j)^2$), M_2 is given by

$$M_2 = \sum_j \hbar\omega_j\lambda_j' \coth(\beta_j/2) \tag{59}$$

or, in the classical limit

$$M_2 = \sum_j 2\lambda_j'\ k_BT = 2\lambda'\ k_BT \tag{60}$$

It follows from eqs 51 and 60 that

$$(\Delta\bar{\nu}_{1/2})^2 = 16\lambda'\ k_BT \ln 2 \tag{61}$$

or, if only the solvent is treated classically

$$(\Delta\bar{\nu}_{1/2})^2 = 16\lambda_o'k_BT \ln 2 \tag{62}$$

This shows that λ_o' can be evaluated experimentally by measuring the bandwidth as a function of temperature.

An equivalent set of equations can be written for emission with λ_j and β_j' defined similarly to λ_j' and β_j, with ω_j' replacing ω_j and vice versa.[123] For the first moment

$$M_1{}^{em} = E_{em} = |\Delta G°| - \sum_j \lambda_j = |\Delta G°| - \lambda \tag{63}$$

$$\partial M_1{}^{em}/\partial T = -\Delta S° \tag{64}$$

For the second moment,

$$M_2{}^{em} = \sum_j \hbar\omega_j\lambda_j \coth(\beta_j'/2) \tag{65}$$

or, in the classical limit

$$M_2{}^{em} = 2\lambda k_BT \tag{66}$$

H. Spectral Evaluation of Vibrational Kinetic Parameters

1. Absorption and Emission

Electron transfer and nonradiative decay are spontaneous processes but are linked to light absorption or emission between the same two states since the same vibrations and solvent modes are coupled to the transitions.[9,73,101,103,123,134,135] The band-shape parameters S_j, $\hbar\omega_j$, λ_o, and $\Delta G°$ in eqs 43 and 46 also define the electron-transfer barrier in eq 23. Application of band-shape analysis to extract these parameters can be problematical because there tend to be many coupled vibrations. For charge-transfer absorption and emission this results in broad, featureless bands which are superpositions of many vibronic contributors, each broadened by coupling with the solvent.

Even in these cases it is possible to derive useful information by spectral fitting to only one or two modes by using mode averaging. In this procedure the coupled vibrations are grouped into average modes according to[102,134,135,147,174,175]

$$S = \sum_j S_j \tag{67}$$

and

$$\hbar\omega = \sum_j S_j \hbar\omega_j / \sum_j S_j \quad (68)$$

This procedure is reasonably accurate if the spread in vibrational energies is less than the weighted average. It allows parameters to be derived for use in single mode equations such as 25 and 29.

2. Resonance Raman

Resonance enhancement of Raman bands is observed when the frequency of the incident light is tuned into the absorption band of an electronic transition. Resonance enhancement occurs only for the coupled vibrations, those with $\Delta Q_{e,j} \neq 0$. Raman band energies give $\hbar\omega_j$ and S_j can be calculated from excitation profiles by use of Heller theory.[103,175−178] It uses wave packet dynamics to relate the Raman cross section for mode j, $\sigma(\nu_j)$, to the time-dependent overlap of the initial vibrational wave function on the excited-state surface, $\psi_f(0)$, with the evolving ground-state wave function, $\psi_i(t)$. The result is

$$\sigma(\nu_i) = A\int_0^\infty \mathrm{d}t\, \exp(2\pi i\Delta\nu - \Gamma)t\langle\psi_f(0)|\psi_i(t)\rangle \quad (69)$$

In this equation $\Delta\nu$ is the frequency difference between the incident light and the electronic transition, Γ is a damping factor, and A is a constant. Relative values of Δ_j ($= (2S_j)^{1/2}$) are obtained by fitting the excitation profile for each band by using eq 69. In certain limits the ratio of Raman intensities for two coupled vibrations is given by

$$\frac{I_i}{I_j} = \frac{\Delta_i^2\omega_i^2}{\Delta_j^2\omega_j^2} \quad (70)$$

Absolute values of the individual Δ_j's can be obtained by a normalization procedure which involves analysis of absorption or emission bandwidths.

Resonance Raman provides the mode-specific parameters S_j and $\hbar\omega_j$ required to calculate vibrational barriers to electron transfer and nonradiative decay on a mode-by-mode basis.[103,178−185] Straightforward application is limited to those cases where there is resonance enhancement from well−defined charge-transfer absorption bands free of spectral overlap with other transitions.

III. Solvent Effects on Charge-Transfer Absorption

Shifts in absorption band energies with solvent (solvatochromism) can be large for charge-transfer bands. For the organic dye 2,6-diphenyl-4-(2,4,6-triphenyl-1-pyridinio)phenolate (**1**), E_{abs} varies from 63.1 kcal/mol in water (453 nm) to 37.5 kcal/mol (762 nm) in diphenyl ether.[2,186,187]

A series of "solvent polarity" scales have been developed to correlate data of this kind.[2,68,187−192] Examples are the E_T scale of Dimroth-Reichardt which is defined as the energy of the lowest charge-transfer absorption band for **1** in (kcal/mol)[186,187] and the Donor Number scale of Gutmann, which is the molar reaction enthalpy in 1,2-dichloroethane for the formation of a 1:1 adduct between $SbCl_5$ and the added solvent as donor.[68] Others include the unified solvation model of Drago et al.[193−195] and the Z scale of Kosower.[196,197] These scales are commonly used in the literature and are of value empirically, but they are not well-defined in a fundamental sense.

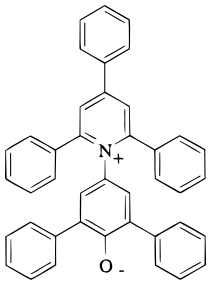

(**1**)

The results of section II provide a quantitative basis for accounting for solvent effects based on analysis of spectral band shapes. If dielectric continuum theory is applicable, the solvent contributions to $\Delta G°$ and λ_o can be calculated from the known geometry of the solute and the dielectric properties of the solvent. If specific interactions dominate, the solvent is still included in the relationships defining absorption and emission, but there is no general theory for relating these quantities to solvent properties.

A. Intervalence Transfer (IT)

For the mixed-valence complexes in eq 71, low-energy absorption bands are often observed in the near infrared (NIR) or visible which can be assigned to intervalence transfer (IT) or, as they are sometimes called, metal-to-metal charge transfer (MMCT) or even intervalence charge transfer (IVCT) transitions.[9,10,198−203] For the symmetrical example in eq 71 with L = pyrazine (pz), a broad, featureless band appears in CH_3CN at 1300 nm (7700 cm^{-1}) of bandwidth 4900 cm^{-1}.[204−208]

$$cis,cis\text{-}[(bpy)_2ClRu^{III}(L)Ru^{II}Cl(bpy)_2]^{3+} \xrightarrow{h\nu} cis,cis\text{-}[(bpy)_2ClRu^{II}(L)Ru^{III}Cl(bpy)_2]^{3+} \quad (71)$$

(L = pz, 4,4′-bpy, bpe)

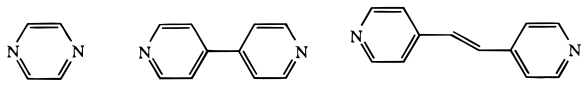
(pz) (4,4-bpy) (*trans*-bis(4-pyridyl)ethene; bpe)

The solvent dependences of IT bands have been analyzed by using the results of section II.G.2. For a Gaussian absorption in the classical limit (eq 57) with $\lambda = \lambda'$

$$E_{abs} = \Delta G° + \lambda \quad (72)$$

and

$$(\Delta\bar{\nu}_{1/2})^2 = 16(E_{abs} - \Delta G°)k_B T \ln 2 = 2310(E_{abs} - \Delta G°) \quad \text{(at RT in cm}^{-1}\text{)} \quad (73)$$

These equations were originally derived by Hush.[9,47,65] He also derived relationships between band-shape parameters and the electron-transfer barrier

$$\Delta G^* = \frac{(\Delta G^\circ + \lambda)^2}{4\lambda} = \frac{{E_{abs}}^2}{4(E_{abs} - \Delta G^\circ)} = \frac{578{E_{abs}}^2}{(\Delta\bar{\nu}_{1/2})^2} \quad \text{(at RT in cm}^{-1}\text{)} \quad (74)$$

If $\Delta G^\circ = 0$

$$E_{abs} = \lambda \quad (75)$$

$$(\Delta\bar{\nu}_{1/2})^2 = 2310E_{abs} \quad \text{(at RT in cm}^{-1}\text{)} \quad (76)$$

$$\Delta G^* = \frac{E_{abs}}{4} = \frac{\lambda}{4} \quad (77)$$

These relationships are valid only if $H_{DA} \ll \lambda$ with H_{DA} the electron-transfer matrix element, section II.B. For a Gaussian-shaped band, H_{DA} can be calculated from simple band-shape parameters[9,10,47,65,209]

$$H_{DA} = [(4.2 \times 10^{-4})\epsilon_{max}\Delta\bar{\nu}_{1/2}E_{abs}]^{1/2}/d \quad (78)$$

ϵ_{max} (in $M^{-1}cm^{-1}$) is the molar extinction coefficient at the maximum and d the charge-transfer distance (in Å).

This analysis provides a framework for using IT band measurements to calculate barriers and rate constants for electron transfer. This is important since for technical reasons it has proven difficult to measure the dynamics of intramolecular electron transfer for mixed-valence complexes by direct measurement.

1. Application of Continuum Models

The classical approximation is reasonable for intervalence transfer in metal complexes where the coupled vibrations are low-frequency metal−ligand modes.[8−13,125−130,182,183,210,211] With the electron donor and acceptor modeled as nonpenetrating spheres and $\Delta G^\circ = 0$, application of dielectric continuum theory to the solvent (eqs 8, 9, and 75) gives

$$E_{abs} = \lambda_i + \lambda_o = \lambda_i + e^2\left(\frac{1}{2a_1} + \frac{1}{2a_2} - \frac{1}{d}\right)\left(\frac{1}{D_{op}} - \frac{1}{D_s}\right) \quad (79)$$

or for a symmetrical mixed-valence complex with $a = a_1 \approx a_2$,

$$E_{abs} = \lambda_i + \lambda_o = \lambda_i + e^2\left(\frac{1}{a} - \frac{1}{d}\right)\left(\frac{1}{D_{op}} - \frac{1}{D_s}\right) \quad (80)$$

Equations 79 and 80 neglect the volume occupied by the acceptor next to the donor and vice versa (the excluded volume) and are only valid if $a < d$. They predict that (1) E_{abs} should vary linearly with the solvent dielectric function $(1/D_{op} - 1/D_s)$ with a slope of $e^2(1/a - 1/d)$ and intercept λ_i at $(1/D_{op} - 1/D_s) = 0$; and (2) in a single solvent with the bridge length varied, E_{abs} should decrease with $1/d$ (at fixed a with slope $e^2(1/D_{op} - 1/D_s)$.

The first solvent dependent study by Creutz and Taube, on $[(NH_3)_5Ru(pz)Ru(NH_3)_5]^{5+}$, led to a surprise.[212] An IT band was observed at 1570 nm in D_2O. However, it was structured, the bandwidth ($\Delta\bar{\nu}_{1/2} = 1250$ cm^{-1}) was narrower than predicted by eq 76 by $\sim 1/3$, and E_{abs} was nearly solvent independent. These properties are a consequence of strong electronic coupling accross the bridge as discussed in section III.D.3.

The predictions of eq 80 were verified for the polypyridyl complexes in eq 71.[204−208] Plots of E_{abs} vs $1/D_{op} - 1/D_s$ were linear ($R^2 = 0.92$ to 1.00) for each L with slopes within 20% of values calculated by assuming $a = 6.0-6.5$ Å (depending on the bridging ligand) and bridge lengths of 6.9, 11.1, and 13.2 Å for L = pz, 4,4′-bpy, and bpe. A plot of E_{abs} vs $1/d$ in CH_3CN was also linear with a slope of 4.7×10^3 cm^{-1}/Å, near the value calculated from $e^2(1/D_{op} - 1/D_s) = 6.1 \times 10^3$ cm^{-1}/Å for the complexes in eq 71.[204,207]

Extrapolation of E_{abs} vs $1/D_{op} - 1/D_s$ plots to $(1/D_{op} - 1/D_s) = 0$ for the complexes in eq 71 gave $\lambda_i = 5700-6300$ cm^{-1},[207] which was larger than $\lambda_i \sim 3900$ cm^{-1} estimated from known Ru−Cl and Ru−N bond distance changes.[213] In addition, experimental $\Delta\bar{\nu}_{1/2}$ values were larger than those calculated from eq 76 by 10−40%.[207] Both of these effects arise because there are actually three overlapping IT bands which result in a broad absorption manifold. They arise from transitions from the three dπ orbitals at Ru^{II} to the hole at Ru^{III}, dπ_1, dπ_2, dπ_3(Ru_a^{II}) → dπ_3(Ru_b^{III}).[214] The degeneracy of dπ orbitals is lifted by low symmetry and spin−orbit coupling at Ru_a^{III} produced in the transition. Separate IT bands have been observed for *cis,cis*-$[(bpy)_2ClOs^{II}(PPh_2CH_2PPh_2)Os^{III}Cl(bpy)_2]^{3+}$ ($PPh_2CH_2PPh_2$ is bis(diphenylphosphino)methane) and $[(bpy)_2ClOs^{II}(CN)Ru^{III}(NH_3)_5]^{3+}$.[215] The spin−orbit coupling constant for Os^{III} ($\zeta = 3200$ cm^{-1}) is greater than for Ru^{III} ($\zeta = 1200$ cm^{-1}) by ~ 3 and this splits the transitions sufficiently to observe separate bands.[215,216] The lowest energy band, dπ_3(M^{II}) → dπ_3(M^{III}), corresponds to the lowest energy electron-transfer pathway. The products of the other two transitions are formed in the interconfigurational excited states at M^{III}, dπ_1^2dπ_2^1dπ_3^2 or dπ_1^1dπ_2^2dπ_3^2.

In a related study on biferrocene cations, $[(C_5H_5)Fe^{III}(C_5H_4-C_5H_4)Fe^{II}(C_5H_5)]^+$, $[(C_5H_5)Fe^{III}(C_5H_4-C\equiv C-C_5H_4Fe^{II}(C_5H_5)]^+$, and $(C_5H_5)Fe(^{III}C_5H_4C\equiv C-C\equiv C-C_5H_4)Fe^{II}(C_5H_5)]^+$, a correlation was found between E_{abs} and the solvent dielectric function, but the slopes were too small by $\sim 1/3$.[217] These results were questioned because of possible ion-pairing effects (section III.C.3),[218,219] but they were later verified by McManis et al. who made measurements in relatively polar solvents at low concentrations where ion-pairing was negligible.[220] The smaller than expected slopes were explained by a mean spherical approximation with solvent molecules modeled as hard spheres with embedded dipoles rather than as a continuum. The decreased slopes may also be a consequence of extensive dπ(Fe^{II})−dπ(Fe^{III}) mixing across the ligand bridge, see below. Scatter in E_{abs} vs $(1/D_{op} - 1/D_s)$ plots correlated with the Acceptor Number of Gut-

mann (section III.C), suggesting that specific solute−solvent interactions also contribute to λ_o.

The two-sphere model is only applicable to nonpenetrating spheres. Ellipsoidal cavity models have been used to analyze solvent effects in nonspherical molecules, such as $[(NH_3)_5Ru(L)Ru(NH_3)_5]^{5+}$, and ion pairs, such as $[Ru(NH_3)_5(py)]^{3+}$ and $[Fe(CN)_6]^{4-}$.[221] Charge transfer is treated as a dipole inversion within a low dielectric cavity with the transition dipole length given by the charge-transfer distance. An analytical expression for λ_o derived by Brunschwig et al. is given in eq 81:[221]

$$\lambda_o = \frac{\Delta e}{R}\left[\left(\frac{1}{D_{in}} - \frac{1}{D_s}\right)\sum_{n=1}^{\infty}\frac{X_n}{I_n(D_{in},D_s)} - \left(\frac{1}{D_{in}} - \frac{1}{D_{op}}\right)\sum_{n=1}^{\infty}\frac{X_n}{I_n(D_{in},D_{op})}\right]$$

$$X_n = 2(2n+1)[1-(-1)^n]P_n^{\,2}(\xi_k)Q_n(l_o)/P_n(l_o)$$

$$I_n(D_\alpha, D_\beta) = 1 - \frac{D_\alpha}{D_\beta}\left[\frac{l_o - P_{n+1}(l_o)/P_n(l_o)}{l_o - Q_{n+1}(l_o)/Q_n(l_o)}\right]$$

$$l_o = \left[\frac{A^2}{A^2 - B^2}\right]^{1/2} \qquad (81)$$

In these equations D_{in} is the dielectric constant in the cavity; R, the interfocal length; $\xi_k = d/R$; d, the separation distance between the two redox sites; and P_n and Q_n are Legendre polynomials of the first and second kinds. $2A$ and $2B$ are the lengths of the major and two minor axes, respectively. With an appropriate choice of cavity parameters and D_{in} values from 1.8 to 2.2, good agreement was obtained between calculated and experimental slopes and intercepts of plots of E_{abs} vs the dielectric function in eq 81 for the complexes in eq 71, for example.

Electronic coupling across 4,4′-bipyridine in $[(NH_3)_5Ru(4,4'\text{-bpy})Ru(NH_3)_5]^{5+}$ is considerably less than for L = pz. E_{abs} is solvent dependent and varies with $(1/D_{op} - 1/D_s)$ as predicted by eq 79, but the slope was only ~ 40% of the value calculated from $a = 3.5$ Å, $d = 11.3$ Å.[10,221−224] One explanation advanced was that partial dielectric saturation occurs in the first solvation shell but this has been ruled out on the basis of an interpretation of selective solvation effects (section III.C.2).[225−227] Stark effect measurements give $d = 5.1 \pm 0.7$ Å rather than the 11.3 Å estimated from the molecular geometry.[228,229] The decreased charge-transfer distance was explained by dπ−π*(4,4′-bpy) mixing and electronic polarization of the dπ donor orbital onto the bridge.[230] With $d = 5.1$ Å, either the two-sphere or ellipsoidal cavity models satisfactorily account for the solvent dependence. Polarization effects along the ligand bridge are less important for the bpy complexes in eq 71 because of competing dπ−π*(bpy) mixing.

For unsymmetrical mixed-valence complexes,[231−233]

$$cis,cis\text{-}[(bpy)_2ClOs^{III}(L)Ru^{II}Cl(bpy)_2]^{3+} \xrightarrow{h\nu} cis,cis\text{-}[(bpy)_2ClOs^{II}(L)Ru^{III}Cl(bpy)_2]^{3+} \quad (82)$$

E_{abs} also depends on $\Delta G°$ (eq 72). Solvent dependences of λ_o and $\Delta G°$ were evaluated separately by spectral and electrochemical measurements. $\Delta G°$ was estimated from the difference in reduction potentials between the $Ru^{III/II}$ and $Os^{III/II}$ couples, measured electrochemically ($\Delta E_{1/2} = E_{1/2}(2) - E_{1/2}(1) \approx \Delta G°$) which is only an approximation (section III.D.1). The dependence of E_{abs} on $\Delta G°$ was verified by Curtis et al. in *cis,trans*-$[(bpy)_2ClRu^{II}(pz)Ru^{III}(NH_3)_4(L)]^{4+}$ (L = NH_3, pyridine, 4-methylpyridine, 3,5-dimethylpyridine, etc.) with $\Delta E_{1/2}$ found to vary through the series by 0.39 V in DMF and by 0.27 V in acetonitrile.[234] $\Delta E_{1/2}$ in $[(bpy)_2ClRu^{II}(pz)Ru^{III}(NH_3)_4(L)]^{4+}$ (L = NH_3 and pyridine) was also varied by solvent changes. The $Ru^{III/II}$ potential for the ammine couple was found to be more sensitive to solvent than the bpy couple because of specific H-bonding interactions with the ammines, section III.C.1.

2. Noncontinuum Effects

The continuum approximation breaks down if there are specific solvent effects or coupled high-frequency vibrations in the solvent ($\hbar\omega \gg k_BT$). The latter does occur as evidenced by the H_2O/D_2O kinetic isotope effects of ~2 for $Fe(H_2O)_6^{3+/2+}$ self-exchange[126,235,236] and nonradiative decay in $[Ru(bpy)_3]^{2+}$,[237] section V.B.1.

Coupled quantum modes were invoked to explain the fact that E_{abs} is 15−20% higher for *cis,cis*-$[(bpy)_2ClRu^{III}(4,4'\text{-bpy})Ru^{II}Cl(bpy)_2]^{3+}$ in H_2O than predicted by extrapolation of a plot of E_{abs} vs $(1/D_{op} - 1/D_s)$.[238] The dielectric properties of H_2O and D_2O are essentially the same as a function of frequency until the onset of the librational region.[20] It was suggested that H_2O librations at 450, 550, and 775 cm^{-1}, which are associated with rotations of individual H_2O molecules within five-membered water clusters,[20] may be coupled to intervalence transfer. If so, they contribute ~700 cm^{-1} to E_{abs} with $S \approx 1.2$.[238]

Ulstrup et al. noted that the dielectric function $1/D_{op} - 1/D_s$ incorporates the entire spectrum of solvent motions *including* librational and molecular O−H stretching and bending modes.[239] If the high-frequency modes are separated out (by using a lower cut-off frequency for D_{op} in eq 9), the deviation from dielectric continuum theory is even greater. They suggested two additional effects, a hydrophobic effect caused by H-bonding close to the ion and a structural effect which causes "solvent nonlocality" and "structure breaking".

Matyushov and Schmid have introduced a molecular solvent theory to explain solvent effects including water and hexamethylphosphoramide (HMPA) which systematically fail in applying dielectric continuum theory.[240−242] They separate λ_o into a component from orientational fluctuations of solvent dipoles (E_p) and one from density fluctuations (translations) (E_d)

$$\lambda_o = E_p + E_d \quad (83)$$

Individual solvent molecules (treated as spheres) are included by introducing their hard-sphere repulsive core diameters (σ) and dipole moments (μ). Corrections for excluded volume are made and equations derived based on two-sphere and ellipsoidal cavity models.

By using this approach, they could account for the solvent dependence of IT bands in $[(bpy)_2ClRu^{III}(bpe)Ru^{II}Cl(bpy)_2]^{3+}$, $[(NH_3)_5Ru^{II}(4,4'\text{-bpy})Ru^{III}(NH_3)_5]^{5+}$ (with $d = 5.8$ Å), and $[(C_5H_5)Fe^{III}(C_5H_4{-}C{\equiv}C{-}C_5H_4)Fe^{II}(C_5H_5)]^+$ including H_2O and HMPA.[240] The anomalous behavior of these two solvents in simple continuum treatments was attributed to their volumes, HMPA has the largest volume ($\sigma = 6.87$ Å) of the common solvents used and H_2O ($\sigma = 2.84$ Å) the smallest. For most common solvents, $\sigma = 4-5$ Å.

E_p and E_d are influenced by σ in opposite ways. According to this theory, it is the use of solvents of comparable molecular volumes that helps to account for the success of the continuum theories.

E_p is mainly enthalpic and temperature dependent because of the temperature dependences of D_{op} and D_s, largely from the orientational fluctuations of the latter. E_d is mainly entropic and temperature dependent because of the temperature dependence of the density.

3. Ionic Strength and Ion Pairing

Ion-atmosphere effects influence IT band energies and widths for $[(C_5H_5)Fe^{II}(C_5H_4{-}C{\equiv}C{-}C_5H_4)Fe^{III}(C_5H_5)]^+$ (Fc−C≡C−Fc$^+$) in low dielectric solvents such as nitrobenzene and dichloromethane[218] and for $[(bpy)_2ClRu^{II}(pz)Ru^{III}(NH_3)_4(L)]^{4+}$ (L = pyridine derivatives) in nitromethane.[234] Blackbourn and Hupp extended and verified the earlier results on biferrocene which had been questioned by Hendrickson et al.[217,218,243−245] They were able to discern separate IT bands for ion-paired and non-ion-paired forms of the mixed-valence ion:[245]

$$Fc^+{-}C{\equiv}C{-}Fc \xrightarrow{h\nu} Fc{-}C{\equiv}C{-}Fc^+ \quad (84)$$

$$X^-,Fc^+{-}C{\equiv}C{-}Fc \xrightarrow{h\nu} X^-,Fc{-}C{\equiv}C{-}Fc^+ \quad (85)$$

A shift to higher energy for the ion pair was attributed to an electrostatic asymmetry, $\Delta E'$, created by the switch in ion atmosphere caused by charge transfer:

$$E_{abs} = \lambda_i + \lambda_o + \Delta E' \quad (86)$$

A similar interpretation was advanced to explain the dependence of E_{abs} in **2** on added $[N(n\text{-}C_4H_9)_4](PF_6)$ in DMSO and *N*-methylformamide. E_{abs} was found to vary with the extended Debye−Huckel function, $\sqrt{\mu}/(1+\sqrt{\mu})$ (μ is the ionic strength).[246]

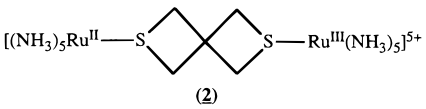

(2)

Ion pairing is more appropriately treated as a reorganizational energy since $\Delta G° = 0$ for the analogous thermal electron transfer:

$$X^-,Fc^+{-}C{\equiv}C{-}Fc \rightarrow Fc{-}C{\equiv}C{-}Fc^+,X^- \quad (87)$$

This introduces a new molecular motion, translation of X^- between the donor and acceptor, which adds an increment to the reorganizational energy, λ_{X^-}. E_{abs} is given by

$$E_{abs} = \lambda_i + \lambda_o + \lambda_{X^-} \quad (88)$$

The predicted dependence of λ_{X^-} on d is not quadratic.[247] The motion of X^- could also dictate ν_{ET} since translational diffusion is relatively slow ($10^{-9}-10^{-10}$ s).

In the series, $[(NH_3)_5Ru(L)Ru^{III}(NH_3)_5]^{5+}$, *trans*,*trans*-$[(py)(NH_3)_4Ru(L)Ru^{III}(NH_3)_4(py)]^{5+}$, $[(bpy)(NH_3)_3Ru(L)Ru^{III}(NH_3)_3(bpy)]^{5+}$ (L = pz, 4-cyanopyridine, 4,4′-bipyridine), solvent effects are dominated by specific solute−solvent interactions for most mixed-valence ions.[248] In nitromethane with added $[N(n\text{-}C_4H_9)_4](PF_6)$, electrolyte effects are clearly observable in the data but are of lesser magnitude than solvent effects. They arise from both ion pairing and diffuse ion−atmosphere effects with the latter maximized for $[(NH_3)_5Ru(4,4'\text{-bpy})Ru^{III}(NH_3)_5]^{5+}$.

B. Metal-to-Ligand Charge-Transfer (MLCT) Bands

The solvent dependences of absorption and emission have been examined both theoretically and experimentally by many authors.[3,9,73,249−261] Following the notation of Brunschwig et al.,[173] in the classical limit E_{abs} is given by

$$E_{abs} = \Delta G°(vac) + \lambda_i + \lambda_o + \Delta w(D_s) \quad (89)$$

$\Delta G°$(vac) is the free energy difference between excited and ground states in a vacuum and $\Delta w(D_s)$ the difference in solvation energies. As derived by Kirkwood, the solvation energy for a spherical ion is[262]

$$w(D_s) = \frac{Z^2e^2}{2a}\left(\frac{1}{D_s} - 1\right) + \frac{\vec{\mu}^2}{a^3}\left(\frac{1 - D_s}{2D + 1}\right) \quad (90)$$

with higher order terms (quadrupole, octupole, etc.) neglected. Application of this result to a spherical light absorber (the dipole-in-a-sphere model) gives

$$\Delta w(D_s) = \frac{1}{a^3}(\vec{\mu}_g{}^2 - \vec{\mu}_e{}^2)\frac{D_s - 1}{2D_s + 1} \quad (91)$$

The Born solvation energy terms cancel in this case because there is only a charge redistribution within the spherical cavity enclosing the solute. $\vec{\mu}_g$ and $\vec{\mu}_e$ are the point dipole vectors of the ground and excited states, a the radius of the spherical cavity, and $\Delta G°$(vac) and λ_i are taken to be solvent independent. The solvent reorganizational energy is given by

$$\lambda_o = \frac{1}{a^3}(\vec{\mu}_g - \vec{\mu}_e)^2\left(\frac{D_s - 1}{2D_s + 1} - \frac{D_{op} - 1}{2D_{op} + 1}\right) \quad (92)$$

and the shift in E_{abs} with solvent, ΔE_{abs}, by

$$\Delta E_{abs} = \lambda_o + \Delta w(D_s)$$
$$= \frac{1}{a^3}\left[2\vec{\mu}_g\cdot(\vec{\mu}_g - \vec{\mu}_e)\frac{D_s - 1}{2D_s + 1} - (\vec{\mu}_g - \vec{\mu}_e)^2\frac{D_{op} - 1}{2D_{op} + 1}\right] \quad (93)$$

In these equations the internal dielectric constant of the cavity is assumed to be 1 although a more realistic value of ~2 is probably appropriate for most molecules.[173]

There is an equivalent set of equations for emission:

$$E_{em} = \Delta G°(vac) - \lambda_i - \lambda_o + \Delta w(D_s) \quad (94)$$

$$\Delta E_{em} = \Delta w(D_s) - \lambda_o$$
$$= \frac{1}{a^3}\left[2\vec{\mu}_e\cdot(\vec{\mu}_g - \vec{\mu}_e)\frac{D_s - 1}{2D_s + 1} + (\vec{\mu}_e - \vec{\mu}_g)^2\frac{D_{op} - 1}{2D_{op} + 1}\right] \quad (95)$$

The energy difference between absorption and emission is given by

$$E_{abs} - E_{em} = 2(\lambda_i + \lambda_o)$$
$$= 2\lambda_i + \frac{2}{a^3}(\vec{\mu}_g - \vec{\mu}_e)^2\left(\frac{D - 1}{2D_s + 1} - \frac{D_{op} - 1}{2D_{op} + 1}\right) \quad (96)$$

Equation 93 was applied to the solvent dependence of MLCT absorption in $[Ru(bpy)_3]^{2+}$, $[Os(bpy)_3]^{2+}$, *cis*-$[Os(bpy)_2(py)_2]^{2+}$, *cis*-$[Os(bpy)_2(CH_3CN)_2]^{2+}$, and $[Os(bpy)_2(dppb)]^{2+}$ (dppb is 1,2-bis(biphenylphosphino)-benzene) in 19 solvents.[263] These are complex spectra which consist of a series of overlapping MLCT bands all of which have similar solvent dependences. For $[Ru(bpy)_3]^{2+}$, E_{abs} for the most intense MLCT feature varies from 21 910 cm^{-1} (nitrobenzene) to 22 220 cm^{-1} (H_2O). The tris-chelates have D_3 symmetry and $\vec{\mu}_g = 0$ in the ground state. If the MLCT transition is to a single bpy ligand, eq 97, a dipole is created in the excited state:

$$[Ru^{II}(bpy)_3]^{2+} \xrightarrow{h\nu} [Ru^{III}(bpy^{\bullet -})(bpy)_2]^{2+*} \quad (97)$$

From eq 93 with $\vec{\mu}_g = 0$,

$$\Delta E_{abs} = \frac{\vec{\mu}_e{}^2}{a^3}\left(\frac{1 - D_{op}}{2D_{op} + 1}\right) \quad (98)$$

A linear correlation was found to exist between E_{abs} and $(1 - D_{op})/(2D_{op} + 1)$ with a correlation coefficient of 0.94.[263] This agreement provides good evidence that MLCT excitation occurs to a single bpy ligand rather than to a π^* orbital delocalized over all three. The D_3 symmetry of the ground state would be retained in that case with $\vec{\mu}_e = 0$. From the slopes of the plots and a = 6.5 Å, excited-state dipole moments of 14.1 ± 6.1 and 13.3 ± 6.6 D were calculated for $[Ru(bpy)_3]^{2+*}$ and $[Os(bpy)_3]^{2+*}$. This gave 2.4−3.0 Å for the dipole length in the excited states. For the unsymmetrical complexes, $\vec{\mu}_g \neq 0$ and E_{abs} correlated with the full dielectric function in eq 93.[263]

A more complete treatment of the solvent has been given by McRae which includes mixing with transitions to upper excited states.[256] Mixing is especially important for high-energy bands where the spectrum is cluttered and many transitions lie close in energy. The visible MLCT bands for $[M(bpy)_3]^{2+}$ (M = Ru, Os) are of relatively low energy and well separated from other transitions. In the study on $[Ru(bpy)_3]^{2+}$, it was assumed that mixing with higher energy transitions played a minor role.[263] This conclusion was challenged by Milder.[264] On the basis of measurements in seven solvents, he suggested that the long-axis polarized $\pi \rightarrow \pi^*$ transitions in $[Ru(bpy)_3]^{2+}$, *cis*-$[Ru(bpy)_2Cl_2]$, and *cis*-$[Ru(bpy)_2(CN)_2]$ are ~4 times more sensitive to the solvent polarization function $(1 - D_{op})/(2D_{op} + 1)$ than the MLCT bands. He concluded that the MLCT solvent dependence arose through mixing with higher energy transitions. In a more detailed study it was found that the variation in E_{abs} for the MLCT bands in $[Ru(bpy)_2(CN)_2]$ are actually three times as large as the $\pi \rightarrow \pi^*$ bands (section III.C.2).[265] It was concluded that specific solvent effects dominate and that the solvent dependence of $\pi \rightarrow \pi^*$ arises largely by mixing with the lower energy MLCT transitions. Further, the variations of $\pi \rightarrow \pi^*$ with solvent for $[Ni(bpy)_3]^{2+}$ and $[Zn(bpy)_3]^{2+}$, where there are no low-lying MLCT bands, are ~1/2 those for $[Ru(bpy)_3]^{2+}$.

Milder also concluded that MLCT excitation in $[Ru(bpy)_3]^{2+}$ gave a delocalized excited state.[264] This conclusion is inconsistent with the results of other experiments. A "localized" transition in $[Ru(bpy)_3]^{2+}$ is supported by Stark effect measurements by Boxer et al.[266] and by time-resolved resonance Raman measurements on the excited state by Woodruff et al.[267−269] and, more recently, by time-resolved infrared measurements.[270]

"Pure" $\pi \rightarrow \pi^*$ bands usually have small solvent dependences because the transitions involve a redistribution of electron density within the same π-framework.[259,260,271,272] In the polypyridyl complexes they gain a solvent dependence by mixing with lower or higher energy MLCT transitions. The orbital basis for mixing in these nominally $\pi \rightarrow \pi^*$ transitions is by $d\pi(Ru^{III}, Ru^{II})$ mixing with π,π^*(bpy) with $d\pi-\pi$ mixing dominating, at least in this case.[265]

The dipole-in-a-sphere model has been applied to solvent shifts in *fac*-[Re(bpy)$(CO)_3$H], *fac*-[Re(bpy)-$(CO)_3$Ph], *trans*-$[Re(bpy)(PMe_2Ph)_2(CO)_2]^+$, and *cis*-$[Re(bpy)(PMe_2Ph)_2(CO)_2]^+$ (Ph = phenyl anion, PMe_2-Ph = dimethylphenylphosphine).[273] The shifts are large and reasonable correlations (R^2 = 0.75−0.86) exist between E_{abs} and the solvent dielectric function in eq 93. Variations in fitting coefficients for the different complexes could be reconciled qualitatively

by taking into account variations in molecular radii.

Large solvent shifts are observed in $[M(L\text{-}L)(CO)_4]$ (L-L = 2,2′-bypyridine, 1,10-phenanthroline, their derivatives, and in other diimines; M = Cr, Mo, W).[19,274−279] A new solvent polarity scale was pro-

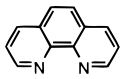

(1,10-phenanthroline; phen)

posed by Lees based on $[W(bpy)(CO)_4]$.[276] This scale correlates with other scales such as E_T, π^*, solvent polarizability α, or dipole moment. In these correlations, there is nearly always a separate correlation for alcohols, and it has been suggested that H-bonding between CO and the hydroxyl group of the alcohols is important.

In symmetrical dimers $[W(CO)_5]_2L$ (L = pyrazine, bpe, 4,4′-bipyrimidine, etc.) and $[M(CO)_4]_2(bpm)$ (M = W, Mo) there is no net dipole moment in the ground state.[280−283] Yet, MLCT solvatochromic shifts are

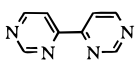

(4,4'-bipyrimidine)

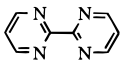

(2,2'-bipyrimidine; bpm)

comparable, or even larger in some cases than in the corresponding monomers. It was suggested that the shifts arose because of a difference in polarizability between the ground and excited states.

However, Dodsworth and Lever found that they could fit data for $[M(CO)_4]_2(bpm)$ and $[M(CO)_4(bpm)]$ (M = Mo, W) in 15 aprotic, nonaromatic, nonhalogenated solvents to the dielectric function:[284,285]

$$\Delta E_{abs} = (A + B)\frac{D_{op} - 1}{2D_{op} + 1} + C\left(\frac{D_s - 1}{D_s + 2} - \frac{D_{op} - 1}{D_{op} + 2}\right) \quad (99)$$

with

$$B = (\vec{\mu}_g{}^2 - \vec{\mu}_e{}^2)/a^3$$

$$C = 2\vec{\mu}_g\cdot(\vec{\mu}_g - \vec{\mu}_e)/a^3$$

The parameter A involves a sum over all the electronic transitions of the molecules. The parameter C was well-defined in the fits and its magnitude for $[Mo(CO)_4]_2(bpm)$ (4610 ± 409 cm^{-1}) was comparable to that for $[Mo(CO)_4(bpm)]$ (5490 ± 365 cm^{-1}), while that for $[W(CO)_4]_2(bpm)$ (2700 ± 525 cm^{-1}) was $\sim^1/_2$ that for $[W(CO)_4(bpm)]$.

The parallel responses of the mononuclear and dinuclear complexes to dielectric function in eq 99 was taken by the authors to imply that the same solute−solvent interactions are responsible for the solvent shifts, and that dipole−dipole interactions dominate, rather than the dispersion forces suggested earlier by Kaim.[280−283] With this interpretation, the dinuclear complexes can be envisioned as two halves, each of which has a dipole moment and interacts with surrounding solvent molecules. Formally, these symmetrical dimers have quadrupole moments which can be included in the dielectric continuum treatment by including a quadrupole term to the Kirkwood solvation energy (eq 90). The higher order terms are the origin of the solvent dependence for solvent molecules that do not possess a permanent dipole. This case has been treated by Newton et al.[286,287]

For optical charge transfer in betaine-26 (2,4,6-triphenyl-*N*-(di-*tert*-butyl-4-hydroxyphenyl)pyridinium ion, which is a derivative of **1**,[288,289] a low-energy

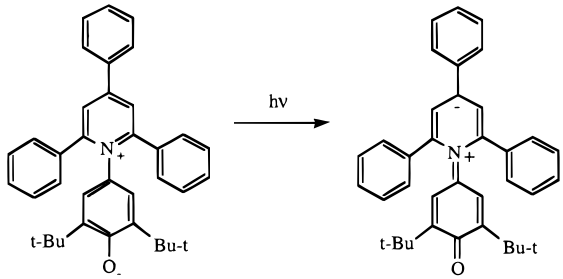

(100)

charge transfer (CT) band appears well-separated from other transitions at higher energy. E_{abs} varies from 587 nm in methanol to 907 nm in carbon disulfide. Application of a single-mode Franck−Condon result similar to eq 44 with $\hbar\omega = 1600$ cm^{-1} showed that $\Delta G°$ and λ_o are separately solvent dependent. In aprotic, polar solvents, a reasonable linear correlation was found between $(\Delta\bar{\nu}_{1/2})^2$ and $1/D_{op} - 1/D_s$ with λ_o varying from 0.22 to 0.40 eV (eq 62). The intercept gave a residual reorganizational energy of 0.02−0.03 eV which was attributed to low-frequency vibrations such as torsional motions of the butyl groups.

The correlation between bandwidth and dielectric function broke down in CS_2 or toluene which are nonpolar with $1/D_{op} - 1/D_s \sim 0$.[286−289] Bandwidths and λ_o (= 0.2 eV) were nearly solvent independent for solvents for which $1/D_{op} - 1/D_s < 0.4$. It was suggested that the residual bandwidth was induced by quadrupolar or dispersion forces, pressure−density effects, or pseudo-potential-like forces.

In normal alcohols, and some other H-bonding solvents, the single mode fit with $\hbar\omega = 2200$−2600 cm^{-1} gave bandwidths more than twice as large as in aprotic solvents. Better fits could be obtained by using a multimode equation with contributions from a distribution of modes between 1900 and 2200 cm^{-1}. It was suggested that in these solvents ν(O−H) is coupled to the transition by H-bonding.

C. Specific Solvent Effects

Dielectric continuum theory breaks down for charge transfer in ammine or cyano complexes where there are specific interactions between these ligands and individual solvent molecules.[265,290] These interactions coexist with continuum effects but tend to dominate when they exist and correlations with dielectric functions normally fail. Correlations are sometimes found with empirical solvent parameters such as, the E_T scale for $[Fe(bpy)_2(CN)_2]$ and the Z scale for $[M(bpy)(CO)_4]$ (M = Mo, W), demonstrating that charge-transfer transitions having different origins

can be influenced in parallel ways by the solvent.[186,190−192,274−279]

Specific-solvent effects have been discussed in a general way by Lay.[291] He noted that changes in oxidation state influence internal solvent structure, H-bonding, and π-stacking of ring systems in the solvent. He broadly outlined how such effects influence $\Delta G°$, λ_i, λ_o, and even H_{DA}.

Specific interactions arise from H-bonding or donor−acceptor interactions. In both cases, orbital mixing occurs between individual ligands and solvent molecules.[265,290] This leads to weak, pseudo-bonding, by electron pair donation and H-bonding to $-NH_3$ or by electron pair donation from the N-based, σ(CN) molecular orbital to solvent molecules. The magnitude of the interaction depends on the extent of orbital overlap and energy difference between the interacting orbitals—the usual quantities of importance in a quantum mechanical interaction.

Given the nature of the specific interactions, it is not surprising that the donor number (DN) and acceptor number (AN) introduced by Gutmann are often useful parameters for correlating MLCT solvent shifts.[68,265,290] The donor number is defined as the molar reaction enthalpy for the formation of a 1:1 adduct between $SbCl_5$ and the added solvent in 1,2-dichloroethane. It provides a measure of the ability of individual solvent molecules to donate an electron pair to $SbCl_5$ and, in parallel, to engage in H-bonding to $-NH_3$, **3**.

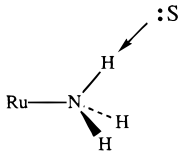

(**3**)

The acceptor number is defined as the magnitude of the chemical shift of the ^{31}P resonance of Et_3PO in a particular solvent relative to the shift in hexane (taken as AN = 0).[23] The shift for $Et_3PO:SbCl_5$ in 1,2-dichloroethane is taken as AN = 100. The acceptor number provides a measure of the ability of individual solvent molecules to act as electron pair acceptors, **4**.

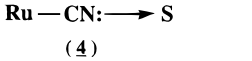

(**4**)

A connection between an NMR measurement and the magnitude of a donor−acceptor interaction is understandable qualitatively, given the relationship between chemical shifts and shielding of nuclei by the surrounding electron clouds. The major theme of the unified solvent model of Drago et al. is the development of a general theory to account for solvent shifts in a variety of probe measurements.[193−195]

Solvent and temperature effects have been studied for $M^{III/II}$ (M = Ru, Fe, Os) couples such as $[Fe(CN)_6]^{3-/4-}$ and $[Ru(NH_3)_5(py)]^{3+/2+}$, where specific interactions dominate, or for $[Ru(bpy)_3]^{3+/2+}$ where they do not.[292,293] $\Delta S°$ was found to increase linearly with $Z_{ox}^2 - Z_{red}^2$ (Z is the ion charge) and the inverse of the ionic radius (a^{-1}) as predicted by the Born equation:

$$\Delta S° = \frac{e^2 N_A}{2 D_s a T}\left(\frac{\mathrm{d} \ln D_s}{\mathrm{d} T}\right)(Z_{ox}^2 - Z_{red}^2) \quad (101)$$

in which e, D_s, N_A, and T have their usual meanings.

It was concluded that specific solvent effects contribute to, but do not dominate $\Delta S°$.[292] The slope of a plot of $\Delta S°$ vs $(Z_{ox}^2 - Z_{red}^2)/a$ was nearly twice as large as the value calculated from eq 101. Acceptable correlations required inclusion of an acceptor number dependence whose origin was attributed to disruption of the surrounding solvent structure by the charged solute. In a later paper the results of this analysis were used to estimate that specific solvent effects contributed $\leq$1−2 kcal/mol to λ_o.[293]

1. Ammine Complexes

E_{abs} for the $d\pi \rightarrow \pi^*$(py) MLCT band in $[Ru(NH_3)_5(py)]^{2+}$ is strongly solvent dependent.[290,294] The charge-transfer character is consistent with substituent effects on the pyridine acceptor, the results of transient absorption and electroabsorption (Stark effect) measurements, and the decrease in E_{abs} with donor number (DN).[229,230,294−299] Consistent with the latter is the fact that E_{abs} increases with DN for ligand-to-metal charge transfer in $[Ru^{III}(NH_3)_5(dmapy)]^{3+}$ (dmapy is 4-(dimethylamino)pyridine) where the direction of charge transfer is reversed:[290]

(102)

For $[Ru(NH_3)_5(L)]^{2+}$ (L = py, *N*-methyl-4,4′-biyridinium cation (MQ^+), 4-cyano-*N*-methylpyridinium (pyd^+)), good correlations were found between E_{abs} and DN ($R^2 \geq 0.94$) in 13 solvents:[290]

$$[Ru^{II}(NH_3)_5(MQ^+)]^{3+} \xrightarrow{h\nu} [Ru^{III}(NH_3)_5(MQ^{\bullet})]^{3+*} \quad (103)$$

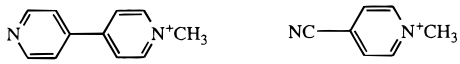

(MQ^+) (pyd^+)

The majority of the solvent effect appears in $\Delta G°$. $\Delta E_{1/2} = E_{1/2}(Ru^{III/II}) - E_{1/2}(pyd^{+/0})$ for $[Ru(NH_3)_5(pyd^+)]^{3+}$ also correlates with DN with comparable slope. The sovent effect in $\Delta E_{1/2}$ is dominated by the $Ru^{III/II}$ couple.

This study was extended to the series $[Ru(NH_3)_5(py)]^{2+}$, $[Ru(bpy)(NH_3)_4]^{2+}$, $[Ru(tpy)(NH_3)_3]^{2+}$, *cis*-$[[Ru(bpy)_2(NH_3)_2]^{2+}$, $[Ru(bpy)(tpy)(NH_3)]^{2+}$, and $[Ru(bpy)_3]^{2+}$ in 13 solvents.[290] Acceptable linear correla-

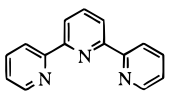

(tpy)

tions between E_{abs} and DN existed for the NH_3-containing complexes. The slopes of E_{abs} vs DN correlations increased with the number of ammine

ligands from $[Ru(tpy)(bpy)(NH_3)]^{2+}$ to $[Ru(NH_3)_5(py)]^{2+}$. This shows that each NH_3 ligand is involved in specific interactions with the solvent.

H-bonding with NH_3 is more important at Ru^{III} than Ru^{II} since N−H acidity is greatly enhanced in the higher oxidation state.[300] $E_{1/2}(Ru^{III/II})$ and MLCT band energies decrease as donor number increases because enhanced electron pair donation to the metal (through H-bonding to individual solvent molecules) stabilizes Ru^{III} over Ru^{II}.

The roles of H-bonding and specific interactions have been investigated quantitatively in $[Ru(NH_3)_5(py)]^{2+}$ by use of the self-consistent reaction field (SCRF) theory of Karelson and Zerner implemented in INDO.[301−306] Application of the SCRF dielectric continuum model to E_{abs} resulted in spectral shifts to the red, but they were too small in magnitude. Addition of a water molecule to each NH_3 with geometry optimization decreased E_{abs} from 40.9×10^3 cm^{-1} to 34.3×10^3 cm^{-1}. Addition of 10 more water molecules with geometry optimization gave excellent agreement with experiment with $E_{abs}(calc) = 24.7 \times 10^3$ and $E_{abs} = 24.\ 6 \times 10^3$ cm^{-1}. The shift between aqueous solution and the gas phase was also successfully reproduced by simple electrostatic models either by placing two −1 charges behind different NH_3 groups on the *x*, *y* and *y*, *z* axes 3.5 Å from Ru, or by placing −0.4 charges behind each NH_3.[301]

Solvent effects in $[Ru(NH_3)_5(py)]^{2+}$ and $[Ru(NH_3)_5(pz)]^{2+}$ were also investigated theoretically by Hush and co-workers.[307−309] They applied ab initio MCSCF and INDO/S-CI methods to estimate gas-phase energies and Monte Carlo simulations to determine solvent structure in the ground-state. E_{abs} was calculated from gas-phase energies and charge distributions and ground state solvent structure. The latter was calculated from an ensemble of configurations generated by using effective pair potentials and rigid Monte Carlo simulations. The intermolecular potential functions were generated by combining Lennard-Jones potentials with intermolecular electrostatic interactions. The first solvation layer was included explicitly and the remaining solvent treated by assuming a dielectric continuum.

E_{abs}(calc) values of 19 000−24 000 cm^{-1} (depending on the assumptions made) were in good agreement with experiment, 21 000 cm^{-1} for $[Ru(NH_3)_5(pz)]^{2+}$.[309] Other features were revealed in the calculations. Complete charge transfer from Ru^{II} to pz would give an excited state with a dipole moment of 17 D while the measured value is 4.8 ± 1.3 D.[229] Inclusion of $d\pi-\pi^*$(pz) back-bonding and polarization of $d\pi$ electron density onto the ligand reduces the value to 8.7 D and additional polarization by the solvent reduces it further to 5.6 D. There is extensive H-bonding with 9−10 water molecules participating in 13−16 H-bonds to the 15 NH_3 hydrogens. A single H-bond exists to the unbound N-atom of pyrazine.

Broo and Larsen investigated electronic structure and electron-transfer barriers or spectra for $[Ru(NH_3)_6]^{2+}$, $[Ru(NH_3)_5(pz)]^{2+}$, $[(NH_3)_5Ru(pz)Ru(NH_3)_5]^{4+/5+/6+}$, $[(NH_3)_5Ru(4,4'\text{-bpy})Ru(NH_3)_5]^{5+}$, and *cis,cis*-$[(bpy)_2ClRu(pz)RuCl(bpy)_2]^{3+}$.[310] They used the ab initio CASSCF method to calculate electronic structure for the ammine complexes and semiempirical CNDO/S and tight-binding methods for the larger systems. The solvent dependence of E_{abs} for $[Ru(NH_3)_5(pz)]^{2+}$ was calculated by a self-consistent reaction field (SCRF).

H-bonding has been probed directly by resonance Raman measurements on $[Ru(bpy)(NH_3)_4]^{2+}$.[294] Resonance enhancements in Raman scattering were observed from an excitation line that fell within the $d\pi(Ru^{II}) \rightarrow \pi^*$(bpy) absorption. A ν(bpy) ring stretching mode shifted from 1548 cm^{-1} in hexamethylphosphoramide (HMPA) to 1558 cm^{-1} in acetonitrile. $Ru-NH_3$ stretching and $H_3N-Ru-NH_3$ bending modes at 456 and 248 cm^{-1} in HMPA (DN = 38.8) shift to 446 and 237 cm^{-1} in acetontrile (DN = 14.1). The shifts to lower energy are consistent with decreased H-bonding and less electron pair donation from the solvent. Low donor number solvents are less able to stabilize the excited state. The increase in ν(bpy) is caused by the increase in $Ru^{III}(bpy^{\bullet-})$ MLCT energy gap in the lower donor number solvents (sections IV and V). This increases the extent of charge transfer, bpy is more highly reduced in the excited state, and ν(bpy) shifts to lower energy.

Linear correlations with donor number have also been found for $Ru^{III/II}$ couples in $[M(NH_3)_5(pzCH_3^+)]^{3+}$ (M = Ru^{II}, Os^{II}) and $[(NH_3)_5Ru^{II}(pz)Ru^{II}(NH_3)_5]^{4+}$.[311,312]

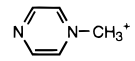

$(pzCH_3^+)$

For the latter, $\Delta E_{1/2}/\Delta DN \approx 0.025 \pm 0.002$ V/DN unit. There is extensive $d\pi-\pi^*(pzCH_3^+)$ mixing along the $M-pzCH_3^+$ axis in the pyrazinium complexes. Taking this as the *z* axis, $d\pi$ orbitals are split into d_{xy} and a d_{xz},d_{yz} pair. A low-energy band of low intensity was observed for $d\pi_{xy} \rightarrow \pi^*(pzCH_3^+)$ which correlates with DN as does $\Delta E_{1/2}$. d_{xz},$d_{yz} \rightarrow \pi^*(pzCH_3^+)$ is observed as an intense band at higher energies. E_{abs} for this band is solvent independent for M = Ru and *increases* slightly with DN for M = Os. There is extensive d_{xz},d_{yz} mixing with $\pi^*(pzCH_3^+)$ and minimal charge-transfer character for M = Ru. Calculations by Hush et al., which show that $d\pi$ and π^* orbitals in $[Ru^{II}(NH_3)_3(pzH^+)]^{3+}$ are accidentally degenerate, are in agreement with this conclusion.[309] For M = Os, the HOMO has more π^* character than $d\pi$ and the transition assumes some ligand-to-metal charge-transfer character. A related scheme was invoked to explain the absence of a solvent dependence for the IT band(s) in the Creutz-Taube ion, section III.A.1.[312]

For *cis,trans*-$[(bpy)_2ClRu^{II}(pz)Ru^{III}(NH_3)_4(L)]^{4+}$ (L = NH_3, py) in 12 solvents, E_{abs} for the IT band and $\Delta E_{1/2}$ (= $E_{1/2}(Ru_b^{III/II}) - E_{1/2}(Ru_a^{III/II})$ with a and b referring to ammine and bpy ends of the complex) correlate with DN ($R^2 > 0.96$).[234] Although the effect is largely in the $Ru_a^{III/II}$ couple, as expected, there is a smaller, but significant, effect on the $Ru_b^{III/II}$ couple. It was attributed to electronic delocalization across the bridge. According to eq 72, the ratio $(\Delta E_{abs}/\Delta\Delta G°)$ should be unity. Any deviation from unity reflects the dependence of λ_o on specific solvent effects.

Experimentally, $\Delta E_{abs}/\Delta(\Delta E_{1/2}) = 1.23 \pm 0.08$ eV/V for L = NH_3 and 1.26 ± 0.07 eV/V for L = py. This points to a DN dependence in λ_o and $E_{abs} - \Delta E_{1/2}$ ($\propto \lambda_o$) was found to correlate with DN with slopes of 0.0095 ± 0.0017 eV/DN (L = NH_3, $R^2 = 0.74$) and 0.0060 ± 0.0017 eV/DN (L = py; $R^2 = 0.83$). The correlations were not improved noticeably by multiparameter fits which included the dielectric function $1/D_{op} - 1/D_s$ and specific solvent effects appear to dominate.

The relative contributions from dielectric continuum solvation and specific solvation have been explored in 14 solvents for nine $Ru^{II}-Ru^{III}$ mixed-valence complexes based on $-Ru(NH_3)_5$, $-trans$-$Ru(NH_3)_4(py)$, and $-Ru(bpy)(NH_3)_3$ with pz, 4-cyanopyridine, and 4,4′-bpy as the bridging ligands.[248] E_{abs} was fit to a dual parameter equation including both $1/D_{op} - 1/D_s$ and DN. Specific-solvent effects dominated except for $[(NH_3)_5Ru^{III}(4,4'\text{-bpy})Ru^{II}(NH_3)_5]^{5+}$.

E_{abs} for the IT band in $[(NH_3)_5Ru^{III}(4,4'\text{-bpy})Ru^{II}(NH_3)_5]^{5+}$ correlates with $1/D_{op} - 1/D_s$.[221,224] Specific-solvent interactions are clearly important for the $Ru^{II}(NH_3)_5]^{3+/2+}$ couple but they may be dominant in $\Delta G°$ and not in λ_o. For the 4,4′-bpy case, $\Delta G° = 0$ and the total effect is in λ_o. In polar solvents, $1/D_{op} \gg 1/D_s$, and λ_o is dominated by the optical part of the dielectric polarization. Even with H-bonding, D_{op} may be nearly the same in the first solvation shell as in the bulk explaining the success of the continuum result. H-bonding may also contribute to the lower than expected sensitivity of E_{abs} to $1/D_{op} - 1/D_s$ (section III.A.1). H-bonding could "freeze" the first solvation shell, increasing the effective radius, decreasing the sensitivity of E_{abs} to solvent changes.

2. Cyano Complexes

A parallel study to the one with ammines has been conducted for both absorption and emission in $[Ru(CN)_5(MQ^+)]^{2-}$, $[Ru(CN)_4(bpy)]^{2-}$, $[Ru(CN)_3(tpy)]^-$, *cis*-$[Ru(bpy)_2(CN)_2]$, and $[Ru(tpy)(bpy)](CN)]^+$.[265] Electron pair, donor−acceptor interactions between cyanide and solvent are significant.[313−322] For $[Ru(tpy)(bpy)](CN)]^+$, E_{abs} increases ~1600 cm^{-1} from pyridine to H_2O while for $[Ru(bpy)_3]^{2+}$ the shift is only ~260 cm^{-1}.

E_{abs} was found to correlate with Gutmann's acceptor number (AN) in 12 solvents for all five complexes ($R^2 \geq 0.79$).[265] The sensitivity of E_{abs} increases with the number of CN^- ligands showing that there are specific interactions between each cyanide and individual solvent molecules and that the effect is additive. E_{em} also varies with AN but is less sensitive than E_{abs} by ~70%.[265,317,318] The difference between the two is given by eq 96, from which,

$$(\Delta E_{abs}/\Delta AN) - (\Delta E_{em}/\Delta AN) = 2(\Delta\lambda_o/\Delta AN) \quad (104)$$

The effect of specific cyano-solvent interactions was explained by invoking electron pair donation from CN^- to low-lying acceptor orbitals on individual solvent molecules.[265] This stabilizes $d\pi(Ru^{II})$ by enhanced $d\pi(Ru^{II})-\pi^*(CN)$ mixing, increases $E_{1/2}$ for the $Ru^{III/II}$ couple, and with it, the $d\pi-\pi^*$(bpy) energy gap.

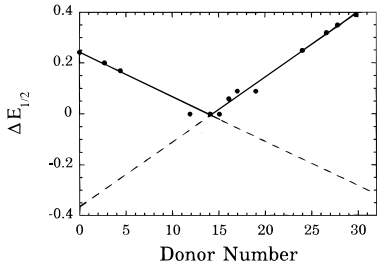

Figure 2. Plots of the potential difference between the first and second oxidation waves for *cis*-$[(bpy)_2ClOs(4,4'\text{-bpy})Ru(NH_3)_5]^{3+}$, $\Delta E_{1/2}$, vs the donor number (DN) of a series of solvents ranging from nitromethane (DN = 2.7) to dimethyl sulfoxide (DN = 29.8). For the mixed-valence complex, *cis*-$[(bpy)_2ClOs(4,4'\text{-bpy})Ru(NH_3)_5]^{4+}$, the thermodynamically stable isomer is $Os^{III}-Ru^{II}$ in solvents of DN < 14 and $Os^{II}-Ru^{III}$ in solvents of DN > 15. The change in slope at DN ≈ 14 (CH_3CN) occurs because of the change from $Os^{III}-Ru^{II}$ to $Os^{II}-Ru^{III}$. The two isomers coexist in solvent mixtures of CH_3CN and propylene carbonate (DN = 15.1). The dotted lines are extrapolations of $\Delta E_{1/2}$ for the two isomers to solvents where they are not stable. The difference between the solid and dotted lines gives $\Delta G°$ for the equilibrium in eq 105. (This graph is reprinted from ref 325. Copyright 1996 American Chemical Society.)

D. Influence of Specific Solvent Effects

1. Solvent-Induced Electron Transfer

The energies involved in specific interactions are sufficient that chemical reactions can be induced by making solvent changes. Intramolecular electron transfer in *cis*-$[(bpy)_2ClOs(4,4'\text{-bpy})Ru(NH_3)_5]^{4+}$ (eq 105) was induced by exploiting the difference in solvent dependences for the $-Ru(NH_3)_5]^{3+/2+}$ and $-Os(bpy)_2Cl]^{2+/+}$ couples.[323−326]

$$cis\text{-}[(bpy)_2ClOs^{III}(4,4'\text{-bpy})Ru^{II}(NH_3)_5]^{4+} \rightleftharpoons cis\text{-}[(bpy)_2ClOs^{II}(4,4'\text{-bpy})Ru^{III}(NH_3)_5]^{4+} \quad (105)$$

$\Delta G°$ for this equilibrium is highly solvent dependent (Figure 2).[325] In nitromethane (DN = 2.7) oxidation to $Os^{III}-Ru^{II}$ is favored by 0.20 eV relative to $Os^{II}-Ru^{III}$. In DMSO (DN = 27.8) specific-solvent effects highly stabilize $-Ru^{III}(NH_3)_5]^{3+}$ and oxidation to $Os^{II}-Ru^{III}$ is favored by 0.39 V. The isomers coexist in mixtures of CH_3CN (DN = 14.1) and propylene carbonate (DN = 15.5) where $\Delta G° \approx 0$, and intramolecular electron transfer can be induced by changing the volume fraction of propylene carbonate in solvent mixtures.[326]

In solvents of DN < 14, the distribution is $Os^{III}-Ru^{II}$. $E_{1/2}$ for the $Os^{III/II}$ couple is relatively independent of solvent and $E_{1/2}$ for the $-Ru^{III/II}(NH_3)_5]^{3+/2+}$ couple decreases with DN. This is reversed for DN > 15. The switch between two isomers is obvious in the plot of $\Delta E_{1/2}$ ($= E_{1/2}(2) - E_{1/2}(1)$) vs DN in Figure 2.[325] Extrapolation of these data allow $\Delta G°$ to be estimated for the mixed-valence equilibrium in eq 105.

The two $Ru^{III/II}$ couples also fall within the same potential range in *trans*,*cis*-$[(py)(NH_3)_4Ru_a(4\text{-NCpy})Ru_bCl(bpy)_2]^{4+}$ (4-NCpy is 4-cyanopyridine).[327]

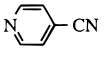

(4-NCpy)

Oxidation occurs first at Ru_b^{II} in low DN solvents and at Ru_a^{II} in high DN solvents. The isomers, $Ru_a^{II}-Ru_b^{III}$ and $Ru_a^{III}-Ru_b^{II}$, coexist at DN $\approx$ 13 and changes in donor number above or below this induce intramolecular electron transfer. Oxidation states were assigned by resonance Raman and thermodynamic half-reaction entropy measurements.

In a somewhat related result it was shown that interconversion from *trans,cis*-$[(py)(NH_3)_4Ru^{II}(4\text{-NCpy})Ru^{III}Cl(bpy)_2]^{4+}$ to *trans,cis*-$[(py)(NH_3)_4Ru^{III}(4\text{-NCpy})Ru^{II}Cl(bpy)_2]^{4+}$ in nitromethane could be induced by outer-sphere complexation of the NH_3 ligands at Ru_a^{III} by low molecular weight poly(ethylene glycol) ($H-(O-CH_2CH_2)_n$-OH) or by dibenzo-36-crown-12 (**5**).[327]

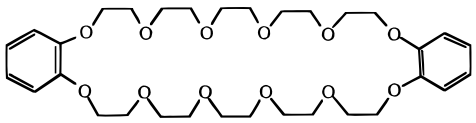

(**5**, dibenzo-36-crown-12)

2. Selective Solvation

Specific interactions can dictate the composition of the first (few) solvation layer(s) in mixed solvents.[290] For $[Ru(NH_3)_5(pyd^+)]^{3+}$ (pyd^+ is 4-cyano-*N*-methylpyridinium, section III.C.1), $E_{abs} = 18.9 \times 10^3$ cm^{-1} (529 nm) in nitromethane (DN = 2.7) and 17.1×10^3 cm^{-1} (584 nm) in DMSO (DN = 29.8). Starting with pure nitromethane, addition of increasing amounts of DMSO results in large incremental changes in E_{abs}. A mixture with $\chi_{DMSO} \approx 0.10$ gave 85−90% of the spectral shift between pure solvents, pointing to preferential solvation by DMSO.

This conclusion was reinforced by electrochemical studies on $[Ru(NH_3)_6]^{2+}$, $[Ru(NH_3)_5(py)]^{2+}$, $[Ru(bpy)(NH_3)_4]^{2+}$, *cis*-$[Ru(bpy)_2(NH_3)_2]^{2+}$, and $[Ru(bpy)_3]^{2+}$ in mixtures of CH_3CN and DMSO.[328] Variations in $E_{1/2}$ with χ_{DMSO} were consistent with preferential DMSO solvation with the effect decreasing in the order: $[Ru(NH_3)_6]^{3+/2+} > [Ru(NH_3)_5(py)]^{3+/2+} > [Ru(bpy)(NH_3)_4]^{3+/2+} > [Ru(bpy)_2(NH_3)_2]^{3+/2+} > [Ru(bpy)_3]^{3+/2+}$. Variations in the $[Ru(bpy)_3]^{3+/2+}$ couple were negligible. Incrementally added DMSO resulted in large initial increases in reaction entropies ($\Delta S°$) followed by gradual decreases and a leveling off as more DMSO was added. The effect of selective solvation on $\Delta S°$ was explained qualitatively by considering both thermodynamic and statistical effects.

Variations in E_{abs} and $E_{1/2}$ with χ_{DMSO} for *trans,cis*-$[(py)(NH_3)_4Ru_a^{III}(pz)Ru_b^{II}Cl(bpy)_2]^{4+}$ in mixtures of CH_3CN and DMSO are also consistent with selective solvation of Ru_a^{III} by DMSO.[329] Equisolvation points (where the molar composition of the first solvent shell is 50−50) occurred at $\chi_{DMSO} = 0.104$ for $Ru_a^{II}-Ru_b^{II}$ and $\chi_{DMSO} = 0.003$ for $Ru_a^{III}-Ru_b^{II}$.

In *trans,cis*-$[(py)(NH_3)_4Ru_a^{II}(L)Ru_b^{II}Cl(bpy)_2]^{3+}$ (L = 4,4′-bpy, bpe; section III.A), $E_{1/2}(Ru_a^{III/II})$ decreases with χ_{DMSO} and $E_{1/2}(Ru_b^{III/II})$ is nearly constant.[330] For L = pz the two couples have nearly the same solvent dependence, suggesting delocalized oxidation states in the mixed-valence form. A sharp, positive "spike" in plots of $\Delta S°$ vs χ_{DMSO} was accounted for by invoking a statistical model.

Addition of DMSO to CH_3CN leads to large changes in E_{abs} for the IT band in $[(NH_3)_5Ru^{II}(4,4'\text{-bpy})Ru^{III}(NH_3)_5]^{5+}$. E_{abs} peaks at $\chi_{DMSO} = 0.035 \pm 0.005$ ($\Delta E_{abs} \approx 1300$ cm^{-1}) and decreases gradually to the value in pure DMSO.[225,226] The E_{abs} vs. χ_{DMSO} curve could be constructed by combining the solvent dependence for $d\pi(Ru^{II}) \rightarrow \pi^*(4,4'\text{-bpy})$ metal-to-ligand charge transfer in $[(NH_3)_5Ru^{II}(4,4'\text{-bpy})Ru^{III}(NH_3)_5]^{5+}$ with $n(dmab) \rightarrow d\pi(Ru^{III})$ ligand-to-metal charge transfer in $[Ru^{III}(NH_3)_5(dmapy)]^{3+}$ (eq 102). It was concluded that $-Ru^{III}(NH_3)_5]^{3+}$ is selectively solvated by DMSO at low χ_{DMSO}. E_{abs} increases because of the mismatch between solvation and oxidation state:

$$\underset{(DMSO)\quad(CH_3CN)}{[(NH_3)_5Ru_a^{III}(4,4'\text{-bpy})Ru_b^{II}(NH_3)_5]^{5+}} \xrightarrow{h\nu} \underset{(DMSO)\quad(CH_3CN)}{[(NH_3)_5Ru_a^{II}(4,4'\text{-bpy})Ru_b^{III}(NH_3)_5]^{5+}} \quad (106)$$

This adds an increment to the solvent reorganizational energy much as in the ion-pairing effect in section III.A.3.

A binding site model was derived to account for these results.[331] Terms were included for electronic delocalization, solute−solvent interactions in the first and outer solvation shells, and an entropic term for solvent partitioning between local solvation shells and the bulk. The energetics of solvent−ligand, solvent−solvent, and intermolecular interactions were included as parameters. Minimization of the resulting free-energy expression led to an equilibrium condition from which domains for symmetrical or unsymmetrical solvation as a function of solvent composition and temperature were deduced. It was concluded that below a certain critical temperature, symmetrical solvation is unstable relative to unsymmetrical solvation. At higher temperatures with k_BT comparable to the magnitude of the specific-solvent interactions, symmetrical solvation is favored on entropic grounds.

Phenomena closely related to selective solvation have been observed in the presence of crown ethers such as **5** and related macrocycles.[327,332−342] They interact with NH_3 ligands and displace solvent molecules from the first solvation shell. In the most favorable cases, complete complexation with the macrocycle occurs and the complex is the dominant form even in dilute solutions. For $[Ru(NH_3)_5(isonicotinamide)]^{2+}$, complexation decreases $E_{1/2}(Ru^{III/II})$ and E_{abs} for MLCT absorption. For the LMCT band in $[Ru^{III}(NH_3)_5(dmapy)]^{3+}$ (eq 102), E_{abs} is increased. These results were explained by invoking H-bonding interactions between the NH_3 ligands and the oxygen atoms of the polyethers.

Binding is enhanced at Ru^{III}. On the basis of ^1H NMR studies, complexation with 18-crown-6 occurs to *trans*-ammines at Ru^{II} and *cis*-ammines at Ru^{III}.[335] With limited crown ether, selective binding to Ru^{III} occurs in $[(NH_3)_5Ru^{III}(4,4'\text{-bpy})Ru^{II}(NH_3)_5]^{5+}$, causing a substantial increase in E_{abs}.[333] This crown ether has been used to trap valences (oxidation states) in $[(NH_3)_5Ru^{III}(pz)Ru^{II}(NH_3)_5]^{5+}$ by stabilizing Ru^{III} and

increasing the reorganizational energy.[336,339] In the doubly complexed form, an increase in E_{abs} for the IT band and a decrease for Ru → pz MLCT have been interpreted by invoking a three-site model with extensive d_π(Ru)−π,π^*(pz)−dπ(Ru) mixing.[339,343−348]

3. Solvent-Induced Delocalization

In the pyrazine-bridged analogue of *cis*-[(bpy)$_2$ClOs(4,4′-bpy)Ru(NH$_3$)$_5$]$^{4+}$, there is an oxidation state switch from *cis*-[(bpy)$_2$ClOs^{III}(pz)Ru^{II}(NH$_3$)$_5$]$^{4+}$ to *cis*-[(bpy)$_2$ClOs^{II}(pz)Ru^{III}(NH$_3$)$_5$]$^{4+}$, but it occurs at DN > 24 rather than at DN > 15.[325,326] There is good evidence for strong electronic coupling in isomer Os^{III}−Ru^{II}. Both the Os$^{III/II}$ and Ru$^{III/II}$ couples vary with DN and a narrow, structured IT band at 8100 cm^{-1} is observed in solvents ranging from acetone to D_2O. Even so, there is spectroscopic evidence that the oxidation states in *cis*-[(bpy)$_2$ClOs^{III}(L)Ru^{II}(NH$_3$)$_5$]$^{4+}$ are localized by the appearance of dπ → dπ bands at Os^{III} in the NIR, and in the pattern of ν(bpy) bands in the mid-IR.[326] The existence of both strong coupling and localization was explained as a consequence of electronic symmetry. There is extensive dπ(Os^{III})−π,π^*(pz)−dπ(Ru^{II}) mixing across the bridge but for only two of the three dπ orbitals at Ru^{II}. The highest dπ level, which contains the exchanging electron, dπ_3, is largely orthogonal to the bridge and only weakly coupled to Os^{III} which causes localization. The IT band can be assigned to dπ_1, dπ_2(Ru^{II}) → dπ_3(Os^{III}) with the transition split by spin−orbit coupling. There is little, if any, charge-transfer character because of extensive mixing with the bridge, and no information about intramolecular electron transfer through the lowest energy pathway, dπ_3(Ru^{II}) → dπ(Os^{III}). In the low DN solvents nitromethane and nitrobenzene, the IT band broadens and shifts to higher energy, consistent with increased charge-transfer character.

In *cis*-[(bpy)$_2$ClOs^{II}(pz)Ru^{III}(NH$_3$)$_5$]$^{4+}$, there is weak electronic coupling and broad, solvent-dependent IT bands appear in the NIR.[326] The two isomers coexist in formamide (DN = 24) and in trimethyl phosphate (DN = 23.0) in which $\Delta H° = -8.2 \pm 2$ kcal/mol and $\Delta S° = 27 \pm 6$ eu for the equilibrium:

$$cis\text{-}[(bpy)_2ClOs^{II}(pz)Ru^{III}(NH_3)_5]^{4+} \rightleftharpoons cis\text{-}[(bpy)_2ClOs^{III}(pz)Ru^{II}(NH_3)_5]^{4+} \quad (107)$$

A positive $\Delta S°$ value is expected because of decreased NH$_3$−solvent interactions in Os^{III}−Ru^{II}.

Instantaneous Ru^{II} → Os^{III} excitation of *cis*-[(bpy)$_2$ClOs^{II}(pz)Ru^{III}(NH$_3$)$_5$]$^{4+}$ by light absorption gives "[(bpy)$_2$ClOs^{III}(pz)Ru^{II}(NH$_3$)$_5$]$^{4+}$" with solvation appropriate to the initial state and weak electronic coupling. Subsequent solvent relaxation is accompanied by increased through-bridge electronic coupling. Conversely, instantaneous Ru^{II} → Os^{III} excitation in *cis*-[(bpy)$_2$ClOs^{III}(pz)Ru^{II}(NH$_3$)$_5$]$^{4+}$ gives "[(bpy)$_2$ClO$_s$^{II}(pz)Ru^{III}(NH$_3$)$_5$]$^{4+}$" with enhanced electronic coupling which decreases as the solvent relaxes. The solvent is strongly coupled to internal electronic structure and the Hush relationship between optical and thermal electron transfer in eq 72 does not apply nor does the time-dependent formulation in eq 14. They assume the Condon approximation and separation of electronic and nuclear coordinates.

The IT band in *trans,trans*-[(py)(NH$_3$)$_4$Ru(pz)Ru(NH$_3$)$_4$(py)]$^{5+}$ is also narrow and structured.[349] There are two components and their relative intensities vary with the mole fraction of DMSO in DMSO−CH$_3$CN mixtures and with the concentration of added PF_6^-. It was suggested that the two components may arise from different forms, one having specific interactions with DMSO and the other not. Another possibility is that the changes are due to changes in rotational orientation of the pyrazine bridge and the effect that it has on the relative intensities of two close lying IT bands. A related effect has been observed in *cis*-[(bpy)$_2$ClOs^{III}(pz)Ru^{II}(NH$_3$)$_5$]$^{4+}$.[326]

These two ions and the Creutz-Taube ion [(NH$_3$)$_5$Ru(pz)Ru(NH$_3$)$_5$]$^{5+}$ all have narrow, structured IT bands and moderate to strong electronic coupling. Hupp et al. investigated [(NH$_3$)$_5$Ru(pz)Ru(NH$_3$)$_5$]$^{5+}$ by resonance Raman with excitation into the IT band at 1320 nm.[182] Eight to nine vibrations were resonantly enhanced including a series of pyrazine stretches consistent with extensive mixing of ligand character in the IT transition. Metal−pyrazine stretches were also enhanced, consistent with residual localization.

These three ions have properties that place them at the borderline between class II (localized, but with strong electronic coupling) and III (delocalized) in the Robin and Day classification scheme.[347−352] There are other examples as well.[353,354] For [(fulvalenyl)Mn$_2$(CO)$_4$(μ-dppm)]$^+$ (**6**), a narrow, intense IT band appears at 6940 cm^{-1} in CH_2Cl_2 (ϵ = 5130 M^{-1} cm^{-1}), but the oxidation states are localized (Mn^I−Mn^0) as shown by the appearance of two separate sets of two ν(CO) bands.[353] In *trans,mer*-[(P(*i*-Pr)$_3$)$_2$(CO)$_3$M(pz)M(CO)$_3$(P(*i*-Pr)$_3$)$_2$]$^+$ (M = Mo, W; P(*i*-Pr)$_3$ = triisopropylphosphane); narrow, solvent-independent IT bands appear (E_{abs} = 4990 cm^{-1}, ϵ = 4600 M^{-1}cm^{-1}, $\Delta\bar{\nu}_{1/2}$ = 730 cm^{-1} for M = W in CH_2Cl_2) but only three ν(CO) bands, consistent with oxidation-state delocalization on the IR time scale.[354]

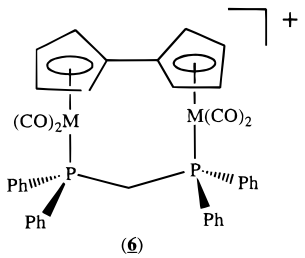

(**6**)

E. Temperature Dependence

The temperature dependence of E_{abs}(IT) for *cis*-[(bpy)$_2$ClRu$_b$^{II}(pz)Ru$_a$^{III}(NH$_3$)$_5$]$^{4+}$:

$$cis\text{-}[(bpy)_2ClRu_b{}^{II}(pz)Ru_a{}^{III}(NH_3)_5]^{4+} \xrightarrow{h\nu} cis\text{-}[(bpy)_2ClRu_b{}^{III}(pz)Ru_a{}^{II}(NH_3)_5]^{4+}$$

has been studied in both CH_3OD and a 42:58 (v:v) mixture of *n*-propionitrile/*n*-butyronitrile.[123] In CH_3OD (μ = 0.035 M), $(\Delta E_{abs}/\Delta T) = -8 \pm 2$ cm^{-1} deg^{-1} from which $\Delta S° = 24 \pm 6$ eu (eq 58). This is the entropy difference between the mixed-valence isomers. From electrochemical measurements, $(\Delta(\Delta E_{1/2})/\Delta T) \approx \Delta S° = +21 \pm 5$ eu with $(\Delta E_{1/2} = E_{1/2}(Ru_b^{III/II}) - E_{1/2}(Ru_a^{III/II})$.

The agreement between the two measurements is of fundamental significance, consistent with the use of $\Delta G°$ in the energy relationship in eq 57 and the results of section II.G.2. Temperature-dependent studies on $[(NH_3)_5Ru^{III}(NC)Fe^{II}(CN)_5]^-$ by Dong and Hupp have led to similar observations and essentially the same conclusion.[355]

The temperature dependences of E_{abs} for IT bands in *cis*-$[(bpy)_2ClRu^{II}(pz)Ru^{III}(NH_3)_5]^{4+}$ and *cis,trans*-$[(4,4'\text{-}(CH_3)_2bpy)_2ClRu^{II}(pz)Ru^{III}(NH_3)_4((4\text{-}Mepy)]^{4+}$ have been measured in nitromethane. For the former, there is a broad IT band at 1350 nm for which $(\Delta E_{abs}/\Delta T) = -18$ cm^{-1} deg^{-1}. For the latter, E_{abs} appears at 1643 nm. It is narrow and structured with $(\Delta E_{abs}/\Delta T) = +2 \pm 1$ cm^{-1} deg^{-1}. The difference between the temperature dependences was used as an argument for localization in the former and delocalization in the latter.[356]

For *cis,cis*-$[(bpy)_2ClRu^{III}(pz)Ru^{II}Cl(bpy)_2]^{3+}$ or $[(NH_3)_5Ru^{III}(4,4'\text{-}bpy)Ru^{II}(NH_3)_5]^{5+}$, $\Delta G° = 0$ and $(\Delta E_{abs}/\Delta T) = (\Delta\lambda_o/\Delta T) = -3$ ($\pm$3) eu and +5 ($\pm$3) eu, respectively, in 42:58 (v:v) *n*-proprionitrile/*n*-butyronitrile.[123] These are entropic differences if λ is a free energy change or heat capacities if λ is an internal energy change (section II.G.2). Matyushov and Schmid accounted for these variations by using their molecular treatment of solvent effects.[240−242] The temperature dependence of λ_o enters both through reorientation of solvent dipoles (D_s and D_{op}) and density fluctuations (solvent density). They partly offset and $(\Delta\lambda_o/\Delta T)$ is small.

The temperature dependence of E_{abs} has been measured for intramolecular charge transfer in betaine-1 (2,4,6-triphenyl-*N*-(4-hydroxyphenyl)pyridinium ion, **1** and in the ion pair:[288]

$$[Fe^{II}(CN)_6]^{4-},MV^{2+} \xrightarrow{h\nu} [Fe^{III}(CN)_6]^{3-},MV^{\bullet+} \quad (108)$$

MV^{2+} is *N,N*′-dimethyl-4,4′-bipyridinium dication, methyl viologen. The CT band for the betaine in 14 solvents was nearly Gaussian with $(\Delta\bar{\nu}_{1/2})^2$ varying linearly with $1/D_{op} - 1/D_s$. The intercept was near zero, suggesting that inhomogeneous broadening and contributions to $(\Delta\bar{\nu}_{1/2})^2$ from low frequency, intramolecular vibrations are negligible. λ_o was calculated to vary from 0.4 eV in chloroform to 1.23 eV in water.

In 4:1 (v:v) ethanol/methanol, $(\Delta\bar{\nu}_{1/2})^2$ varied linearly with T (77−294 K) as predicted by eq 62. From the slope, λ_o = 1.05 eV. The intercept was ∼0. Similar observations were made in a 3:1 (v:v) diethyl ether/ethanol mixture over the same temperature range. In 2:1 ethylene glycol/water, $(\Delta\bar{\nu}_{1/2})^2$ varied linearly with T in the fluid but was nearly independent of T below the glass-to-fluid transition, consistent with a large inhomogeneous broadening. Over the same temperature range, E_{abs} shifted to higher energy by 1600 cm^{-1} consistent with a decrease in entropy content in the excited state, eq 58.

For the ion pair, E_{abs} shifted 1600 cm^{-1} to the blue from 294 to 77 K with $(\Delta E_{abs}/\Delta T)$ comparable to $-(\Delta(\Delta E_{1/2})/\Delta T) = \Delta S° \approx 82$ J K^{-1} mol^{-1} by electrochemical measurements.[288] In 2:1 (v:v) ethylene glycol/H_2O, the variation of $(\Delta\bar{\nu}_{1/2})^2$ with T was linear in fluid solution from 294 to 150 K with λ_o = 2.1 eV. This value is inconsistent with λ_o = 1.45 eV calculated from, $\lambda_o = E_{abs} - \Delta G°$, with E_{abs} = 2.31 eV and $\Delta G°$ = 0.86 eV. The reason for the discrepancy is not clear. The intercept of $(\Delta\bar{\nu}_{1/2})^2$ vs T from 294 to 150 K was near zero, but $\Delta\bar{\nu}_{1/2}$ was temperature-independent below the fluid-to-glass transition.

IV. Emission

Emission is the microscopic reverse of absorption and solvent effects have the same origin although, in general, the reorganizational energies are different for the two, $\lambda \neq \lambda'$ (section II.G.2). For MLCT transitions E_{em} is typically less solvent dependent than E_{abs} (section III.C.2).

Implementation of band-shape analysis for emission is simpler than for absorption because, typically, there is a single emission band while absorption spectra tend to be superpositions of overlapping bands which must first be deconvoluted.

A. Solvent Effects

MLCT emission from polypyridyl complexes is typically broad and featureless in fluid solution at room temperature. For $[Ru^{III}(bpy^{\bullet-})(bpy)_2]^{2+*}$ an apparent vibronic progression of spacing ∼1300 cm^{-1} appears in low-temperature fluids or glasses.[170,269,314,357−359] These features are actually a superposition of vibronic components arising from a series of coupled ν(bpy) vibrations with band energies from 1000 to 1600 cm^{-1}. They can be resolved at low temperatures in single crystals[360−363] and appear in resonance Raman spectra.[364−371] Because of the coupled ν(bpy) vibrations, E_{abs} or E_{em} are not the simple functions of λ and $\Delta G°$ in eqs 57 and 63. These equations are applicable to the lowest energy vibronic component $v = 0 \rightarrow v' = 0$ with $\lambda = \lambda_o$.

A modified version of the single mode fitting result in eq 47 was applied to emission from $[Ru(bpy)_3]^{2+*}$ in seven solvents ranging in polarity from dichloromethane to *N,N*-dimethylformamide.[170] E_o (= $|\Delta G°| - \lambda_o$) varied from 16.8 × 10^3 cm^{-1} (CH_2Cl_2) to 16.2 × 10^3 cm^{-1} (DMF) and was systematically higher than E_{em} by 200−300 cm^{-1}. E_o is the energy of the lowest energy vibronic component ($v' = 0 \rightarrow v = 0$). $\Delta\bar{\nu}_{1/2}$ varied from 2750 cm^{-1} in CH_2Cl_2 to 3030 cm^{-1} in H_2O. No attempt was made to correlate the energy gap or solvent reorganizational energies with solvent dielectric functions.

It follows from eq 91 that $|\Delta G°|$ (= $E_o + \lambda_o$) should vary with the dielectric function $(D_s - 1)/(2D_s + 1)$. In a study in 12 solvents, a marginal correlation (R^2 = 0.59) was found.[372] The slope of the correlation (3340 cm^{-1}) was comparable in magnitude to the

slope of the correlation between ΔE_{abs} and $(1 - D_{op})/(2D_{op} + 1)$ (eq 98, 3670 cm^{-1}) from the solvent-dependent absorption study mentioned in section III.B. The slopes are expected to be comparable since they equal $\vec{\mu}_e^2/a^3$ in either case. Even so, the slope of a plot of ΔE_{em} ($\approx \Delta w(D_s) - \lambda_o$, eq 95) vs the dielectric function in eq 95 (with $\vec{\mu}_g = 0$) is only 2550 cm^{-1}. It should equal $\vec{\mu}_e^2/a^3$ as well.

An even better correlation was obtained between $E_0 + \lambda_o$ and donor number (DN), suggesting the importance of specific solvent effects, sections III.3 and IV.C.[372] Specific-solvent effects play an important role in λ_o. There is essentially no correlation between λ_o and the dielectric function in eq 92. A marginal correlation was observed with DN ($\chi^2 = 0.57$).

Specific-solvent effects in $[Ru(bpy^{\bullet-})(bpy)_2]^{2+*}$ emission may arise from electron donor−acceptor interactions between individual solvent molecules and the partially formed radical anion in π^*(bpy) in the equilibrated excited state. Dielectric continuum theory works well for absorption in $[Ru(bpy)_3]^{2+}$. There is no particular orbital basis for specific interactions in the ground state and the excited state is formed instantaneously in the solvent environment of the ground state.

A Franck−Condon analysis was applied to charge-transfer emission from a series of barrelene-bridged, donor−acceptor compounds.[373] Analysis of spectra in six solvents gave $\hbar\omega = 1300$ cm^{-1} and $\lambda = S\hbar\omega = 0.36-0.45$ eV. $|\Delta G°|$ was calculated from the energy gaps. λ_o, calculated from the bandwidths, varied with $1/D_{op} - 1/D_s$. The intercept of 0.32 eV was consistent with a considerable contribution from coupled low-frequency vibrations, $\lambda_{i,L}$ (eqs 26 and 27).

B. Temperature Dependence

Emission spectra for *fac*-$[Re(bpy)(CO)_3Cl]^*$ in 4:1 ethanol/methanol from 160 to 295 K and in 2-MeTHF from 135 to 295 K were fit by using a two-mode version of eq 47.[166] From the slopes of plots of $(\Delta\bar{\nu}_{1/2})^2$ vs T, $\lambda_o = 1100 \pm 120$ cm^{-1} in 4:1 (v:v) ethanol/methanol and 650 ± 40 cm^{-1} in 2-methyltetrahydrofuran. Extrapolation to $T = 0$ gave $\lambda_{i,L} \approx 3000$ cm^{-1}. The values of λ_o were larger than for $[Ru(bpy)_3]^{2+*}$ in the same solvents. The increase was attributed to the smaller molecular radius, the dipole-in-a-sphere result in eq 92 predicts that λ_o should vary as a^{-3}. $\lambda_{i,L}$ was also larger, suggesting a larger change in metal−ligand skeletal structure in the excited state.

Emission spectra for *fac*-$[Re(bpy)(CO)_3(4\text{-}Etpy)](PF_6)$ in 4:1 (v:v) EtOH/MeOH from 170 to 260 K and for *cis*-$[Os(bpy)_2(CO)(py)](PF_6)_2$ (py is pyridine) from 160 to 220 K were analyzed to give $\lambda_o(Re^I) = 1767 \pm 84$ cm^{-1} and $\lambda_o(Os^{II}) = 1762 \pm 93$ cm^{-1}. Also, from this analysis $\Delta S° = 6.9$ cal mol^{-1} K^{-1} (Re^I) and 4.6 cal mol^{-1} K^{-1} (Os^{II}) based on $(\Delta E_o/\Delta T) = -\Delta S°$ and eq 64. $\Delta S°$ is the entropic change accompanying excited-state decay. It arises mainly from changes in quantum spacings and the associated change in density of states in the coupled solvent modes, section II.G.2. $\Delta S°$ is positive because of the loss of the excited-state dipole in the ground state, eq 109. This decreases solvent interactions, decreasing $\hbar\omega$ for the solvent modes, and increasing the density of states.

$$[Re^{II}(bpy^{\bullet-})(CO)_3(4\text{-}Etpy)]^{+*} \rightarrow [Re^{I}(bpy)(CO)_3(4\text{-}Etpy)]^{+} \quad (109)$$

C. Specific Solvent Effects in Cyano Complexes

E_{em} for *cis*-$[Ru(bpy)_2(CN)_2]^*$ and *cis*-$[Ru(phen)_2(CN)_2]^*$ varies linearly with acceptor number (AN, section III.C.2) with $(\Delta E_{em}/\Delta AN) = 45 \pm 3$ cm^{-1}/AN unit for the bpy complex.[265,317] The quality of the correlations was improved by using a dual parameter fit which included both AN and $1/D_{op} - 1/D_s$.[317] The microscopic origin of the acceptor number dependence was modeled as arising from changes in electron pair donation from the lone pair on the cyanide groups to individual solvent molecules. The inclusion of the dielectric term incorporates continuum effects and the contribution from the remaining solvent molecules in the vicinity of the complex.

E_{em} also varies with acceptor number in 12 solvents for mixed polypyridyl−cyano complexes in the series from $[Ru(tpy)(bpy)(CN)]^+$ to $[Ru(bpy)(CN)_4]^{2-}$ mentioned in section III.C.2.[265] The sensitivity to acceptor number increased linearly with the number of CN^- ligands. For $[Ru(bpy)_2(CN)_2]^*$ in seven solvents, ranging from acetone to water, *both* $(\Delta\bar{\nu}_{1/2})^2$ and E_o vary with acceptor number, with $(\Delta\lambda_o/\Delta AN) = 21 \pm 3$ and $(\Delta E_o/\Delta AN) = 44 \pm 2$ cm^{-1}/AN unit. This shows that the energy gap is far more sensitive to AN than λ_o. Variations in E_o and E_{em} with AN (45 ± 3 cm^{-1}/AN unit) were the same within experimental error showing that simple emission measurements can give accurate information about E_o even though the emission is a convolution of overlapping vibronic components.

From the solvent dependences of the *cis*-$[Ru^{III}(bpy)_2(CN)_2]^+/[Ru^{II}(bpy)_2(CN)_2]$ and *cis*-$[Ru^{II}(bpy)_2(CN)_2]/[Ru^{II}(bpy^{\bullet-})(bpy)(CN)_2]^-$ couples, $(\Delta E_{1/2}/\Delta AN) = 70 \pm 7$ cm^{-1}/AN unit. Taking this as a measure of the solvent dependence of $\Delta G°_{ES}$, the free energy of the excited state above the ground state, provides a second method of evaluating the solvent dependence of λ_o. From eq 63, $\Delta G°_{ES} = |\Delta G°|$ with $(\Delta\lambda_i/\Delta AN) = 0$, $(\Delta\lambda_o/\Delta AN) \sim (\Delta\Delta G°_{ES}/\Delta AN) - (\Delta E_o/\Delta AN) = 26 \pm 7$ cm^{-1}/AN unit.

For λ_o', the solvent reorganizational energy of the excited state above the ground state (section II.G.2 and Figure 1), it follows from eq 57, with $(\Delta\lambda_i/\Delta AN) \sim 0$, that $(\Delta\lambda_o'/\Delta AN) = (\Delta E_{abs}/\Delta AN) - (\Delta\Delta G°_{ES}/\Delta AN) = 12$ cm^{-1}/AN unit. With either method, the variation of λ_o with AN is greater than for λ_o' and by inference, $\lambda_o > \lambda_o'$. The solvent reorganizational energy for the ground state below the excited state is greater than for the excited state above the ground state (λ').

The acceptor number dependence of $\Delta G°_{ES}$ is mainly a ground-state effect with the ground-state stabilized by enhanced donor−acceptor interactions at CN^- as AN is increased. These interactions are greatly attenuated in the $[Ru^{III}(bpy^{\bullet-})(bpy)(CN)_2]^*$ excited state because partial oxidation shifts electron density from cyanide to Ru^{III}.

The acceptor number dependence of λ_o arises from changes in $-CN\cdots$solvent interactions with the $-CN\cdots$solvent displacement coordinate Q increasing in the excited states and $\Delta Q_e > 0$. If these motions are treated as harmonic oscillators with force constants f and f', $\lambda_o = {}^1/_2 f(\Delta Q_e)^2$ and $\lambda_o' = {}^1/_2 f'(\Delta Q_e)^2$. $f > f'$ because $CN\cdots$solvent interactions are decreased in the excited state. λ_o is more sensitive to AN than λ_o' because $\Delta\lambda_o = \lambda_o - \lambda_o' = {}^1/_2(\Delta Q_e)^2(f - f') > 0$.

Specific-solvent effects perturb the internal electronic structure of the solute and couple electronic and solvent coordinates. In general, the extent and even the nature of these interactions differ between the ground and excited states because of the change in electronic structure. In such cases, $\lambda_o \neq \lambda_o'$ and the simple band-shape analyses that relate absorption and emission (eqs 57 and 63) are still valid. The solvent can be modeled as a dielectric continuum with $\lambda_o = \lambda_o'$ only in the absence of specific interactions. Although the $-CN$ groups provide an orbital basis for strong interactions, this may be a general phenomenon. The difference between the solvent dependence of absorption and emission in $[Ru(bpy)_3]^{2+}$ is another example(sections IV.A and III.B).[372]

There is a more fundamental complication, one raised for mixed-valence complexes in section III.C.3. Because solvent motions are coupled to internal electronic structure, application of the Condon approximation and the usual band-shape equations is incorrect. Emission from *cis*-$[Ru(bpy)_2(CN)_2]$* leads to the ground electronic state "$[Ru(bpy)_2(CN)_2]$" with the solvent coordinates of the excited state. Subsequent relaxation is accompanied by an increase in $-CN\cdots$solvent interactions which modifies internal electronic structure by increasing $d\pi(Ru)-CN$ backbonding. Similarly, light absorption by *cis*-$[Ru(bpy)_2(CN)_2]$ leads to "$[Ru^{III}(bpy^{\bullet-})(bpy)(CN)_2]$*" and subsequent relaxation to decreased $CN^- -$solvent interactions which change internal electronic structure.

D. Ion-Pairing

Salts of $[Os(phen)_3]^{2+}$ are completely ion paired in CH_2Cl_2.[169] Slight but systematic shifts occur in E_{em} as the volume of the counteranion is decreased from BPh_4^- (696 nm) to Cl^- (714 nm). This effect was modeled by invoking anion−dipole stabilization of the excited state (eq 110). This interaction increases with the charge density of the anion and is lost in the D_3 symmetry of the ground state.

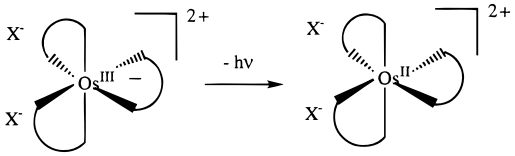

(110)

E. Rigid Media

In rigid media (glasses, frozen solutions, plastics, solids, etc.) MLCT emission occurs at higher energy than in solution, a phenomenon termed "fluorescence rigidochromism" by Wrighton et al.[139−141, 375,376] The shifts can be large. For *cis*-$[Ru(bpy)_2(CN)_2]$*, E_{em} = 588 nm in a 4:1 EtOH/MeOH glass just below the glass-to-fluid transition at ~100 K and decreases to 641 nm in the fluid at 135 K.[377]

This phenomenon occurs because the dipole orientational part of the solvent polarization (section II.A) is frozen in rigid media.[139−141,377−381] Following excitation, the translational part relaxes but the orientational part is frozen. Emission occurs from excited states surrounded by the orientational polarization of the ground-state rather than the equilibrium polarization of the excited state.

Marcus treated this problem by partitioning λ_o into λ_{oo} (the part of λ_o that is frozen in the glass or solid) and λ_{oi} (the part of λ_o that relaxes):[381]

$$\lambda_o = \lambda_{oo} + \lambda_{oi} \tag{111}$$

Large amplitude dipole reorientations (collective rotations) are the major contributor to λ_{oo} and small amplitude translations (phonon-like modes) to λ_{oi} although the model proposed by Marcus is independent of the origin of the λ's.

In a frozen medium λ_{oo} becomes part of the energy gap and is no longer part of the reorganizational energy. In the classical limit, E_{abs} and E_{em} are given by[381]

$$E_{abs}(T,P) = \lambda_{oo}(T_e,P_e) + \lambda_{oi}(T,P) + \lambda_i(T,P) + \Delta G°(T,P) \tag{112a}$$

and

$$E_{em}(T,P) = \lambda_{oo}(T_e,P_e) - \lambda_{oi}(T,P) + \lambda_i(T,P) + \Delta G°(T,P) \tag{112b}$$

The energy gap becomes, $\Delta G°(T,P) + \lambda_{oo}(T_e,P_e)$, and the reorganizational energy, $\lambda_{oi}(T,P) + \lambda_i(T,P)$. The quantities in these equations are, in general, functions of temperature (T) and pressure (P). It is assumed that $\lambda = \lambda'$. Dipole orientations in the frozen medium are adapted to the electronic distribution of the ground state at a pressure (P_e) just below the pressure required for freezing and/or temperature (T_e) just above the glass transition temperature T_g (T_e and P_e depend on the speed of cooling). $\lambda_{oo}(T_e,P_e)$ is determined by the dielectric properties of the solvent at T_e and P_e where the dipole orientations can adapt to the electronic distribution of the ground state. It presumably remains nearly the same in the glass, unless there are significant changes in structure in the surrounding medium.

If λ and $\Delta G°$ remain relatively constant over the small changes in temperature and pressure in the glass-to-fluid transition, the difference in E_{abs} between the rigid and fluid states is given by[139,378,381]

$$E_{abs}(\text{rigid}) - E_{abs}(\text{fluid}) \approx 0 \tag{113a}$$

and in E_{em} by

$$E_{em}(\text{rigid}) - E_{em}(\text{fluid}) \approx 2\lambda_{oo} \tag{113b}$$

From the two-sphere model in eq 9, λ_{oo} and λ_{oi} are given by

$$\lambda_{oo} = e^2\left(\frac{1}{2a_1} + \frac{1}{2a_2} - \frac{1}{d}\right)\left(\frac{1}{D_{s,fr}} - \frac{1}{D_s}\right) \quad (114a)$$

$$\lambda_{oi} = e^2\left(\frac{1}{2a_1} + \frac{1}{2a_2} - \frac{1}{d}\right)\left(\frac{1}{D_{op}} - \frac{1}{D_{s,fr}}\right) \quad (114b)$$

$D_{s,fr}$ is the static dielectric constant in the frozen medium. For polar solvents it is far less than D_s (see below). For the dipole-in-a-sphere model in eq 79, λ_{oo} and λ_{oi} are given by

$$\lambda_{oo} = \frac{(\vec{\mu}_e - \vec{\mu}_g)^2}{a^3}\left[\frac{1 - D_{s,fr}}{2D_{s,fr} + 1} - \frac{1 - D_s}{2D_g + 1}\right] \quad (115a)$$

$$\lambda_{oi} = \frac{(\vec{\mu}_e - \vec{\mu}_g)^2}{a^3}\left[\frac{1 - D_{op}}{2D_{op} + 1} - \frac{1 - D_{s,fr}}{2D_{s,fr} + 1}\right] \quad (115b)$$

The theoretical work by Marcus was inspired by two seemingly conflicting sets of experimental results.[378,382,383] Changes in E_{abs} for the IT bands in biferrocene cation $[(C_5H_5)Fe^{III}(C_5H_5{-}C_5H_5)Fe^{II}(C_5H_5)]^+$ and *cis,cis*-$[(bpy)_2ClRu^{II}(pz)Ru^{III}Cl(bpy)_2]^{3+}$ were measured by Hammack et al. through the fluid-to-glass transitions in nitromethane, nitrobenzene, and acetonitrile by increasing pressure at room temperature. Band energies and band shapes varied only slightly even though D_s decreases from 33.7 at 25° at 1 atm to 3.4 in frozen nitromethane. This led the authors to conclude that eq 79 is not valid and that dielectric continuum theory had been misapplied in experimental studies on mixed-valence complexes.

In a following paper by Worl and Meyer it was pointed out that the interpretation given by Hammack et al. of their data was incorrect.[378] Light absorption is instantaneous on the time scale for nuclear motions in either frozen or fluid solutions. There are only slight difference between the two in local structure and E_{abs} is expected to be nearly the same in both. This was demonstrated experimentally by measuring E_{abs} and E_{em} for MLCT absorption and emission in $[Re(bpy)(CO)_3Cl]$ in 4:1 (v:v) EtOH/MeOH through the glass-to-fluid transition from 120 to 140 K. As expected, E_{abs} *did not* shift appreciably while E_{em} did (18 500 to 16 000 cm^{-1}), as predicted by eq 113.[378]

According to eqs 113−115, E_{em}(rigid) − E_{em}(fluid) is a function of λ_{oo} which varies as $\Delta\vec{\mu} = \vec{\mu} - \vec{\mu}_g$. If $\Delta\vec{\mu}$ is small, shifts are small and so is the rigidochromism. This is the case for ligand-localized, $\pi\pi^*$ emissions from $[Ir(bpy)_3]^{3+}$, $[Re(dppz)(CO)_3(4\text{-}Etpy)]^+$, or $[Ru(bi\text{-}isoquinoline)_3]^{2+}$.[377,384,385]

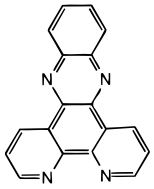

(dppz)

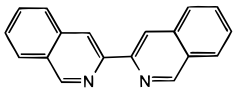

(bi-isoquinoline)

The effect of pressure-induced transitions on E_{em} and lifetimes for $[Re(phen)(CO)_3Cl]$ and $[Re(4,7\text{-}(phenyl)_2phen)(CO)_3Cl]$ were investigated in solvents ranging from *m*-xylene to DMF at room temperature.[386] In nonpolar solvents such as *m*-xylene, E_{em} shifted continuously with pressure. In polar solvents, E_{em} increased dramatically upon freezing. This is predicted by eq 113 and 115 since $D_s > D_{s,fr}$. In nonpolar solvents, where $D_{s,fr} \approx D_s$, E_{em}(rigid) − E_{em}(fluid) ≈ 0, and the effect is slight.

For $[Ru(bpy)_3]^{2+*}$ in 4:1 (v:v) EtOH/MeOH at room temperature, E_{em} varies with P, $(\Delta E_{em}/\Delta P) = -390$ cm^{-1}/GPa, from 16 410 cm^{-1} at 10^{-4} GPa (1 atm) to 15 680 cm^{-1} at 1.8 GPa.[387] The energy gap decreases with P because D_s increases with pressure. Spectral changes in the fluid-to-glass transition caused by increasing the pressure at constant temperature were similar to those induced by decreasing the temperature at constant pressure. In a frozen solution at 100 K, changes in pressure had negligible effect, as expected, because the solvent dipoles are already frozen in the rigid lattice.

F. Solvent Effects on Excited State Ordering and Interconversion

If two or more excited states of different orbital origin and comparable energies coexist, changes in solvent or temperature can cause dramatic changes in photophysical properties and the appearance of dual emission. There are many examples in the literature.[388−410] Only selected examples involving charge-transfer excited states will be mentioned here.

One of the first observations of this kind was made by Wrighton and co-workers on *fac*-$[Re(3\text{-}bp)_2(CO)_3X]$ and *fac*-$[Re(4\text{-}bp)_2(CO)_3X]$ (X = Cl^-, Br^-, I^-) in EPA (5:5:2 (v:v:v) diethyl ether/isopentane/ethanol).[394] In

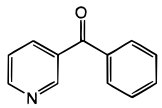

(3-benzoylpyridine; 3-bp)

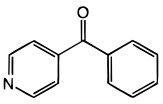

(4-benzoylpyridine; 4-bp)

a glass at 77 K both nπ^* (τ = 1400 μs for X = Cl^-) and MLCT emissions (τ = 18 μs) are observed, but only MLCT emission in the fluid. In the fluid, interconversion between nπ^* and MLCT

$$[Re^{I}(3\text{-}bp^*)(3\text{-}bp)(CO)_3Cl] \rightarrow [Re^{II}(3\text{-}bp^{\bullet-})(3\text{-}bp)(CO)_3Cl]^* \quad (116)$$
$$n^1(d\pi)^6\pi^{*1} \qquad n^2(d\pi)^5\pi^{*1}$$

is rapid but there is an increased barrier in the glass, section VI.C.

Closely related phenomena have been observed for *fac*-$[Re(phen)(CO)_3(CH_3CN)]^+$ and related complexes in EPA at 77 K.[395] They display an excitation-dependent mix of long ($\pi\pi^*$) and short-lived (MLCT) emissions. Interconversion between states is inefficient in the glass. The MLCT state is the only emitter in solution at room temperature.

In these cases, the lowest state is presumably MLCT with a kinetic inhibition to $n\pi^*$or $\pi\pi^* \rightarrow$ MLCT interconversion in the glass. In others the

Scheme 1

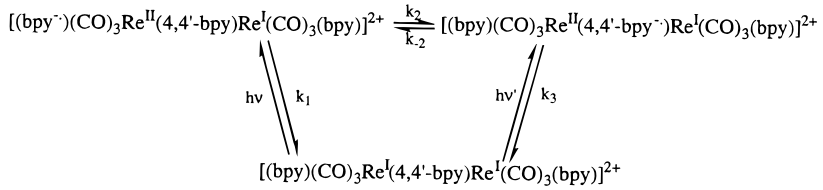

actual ordering of states may change. The MLCT state is favored in the fluid. In the transition from glass to fluid, excited-state energies change from $\Delta G° + \lambda_{oo}$ to $\Delta G°$. The stabilization by λ_{oo} in the fluid favors the MLCT state since, from eq 115, $\Delta\lambda_{oo} = \lambda_{oo}$(MLCT) $- \lambda_{oo}(\pi\pi^*) \propto (\Delta\vec{\mu}_{MLCT})^2 - (\Delta\vec{\mu}_{\pi\pi^*})^2$, and $\Delta\vec{\mu}$(MLCT) $> \Delta\vec{\mu}(\pi\pi^*)$. A change in relative ordering of states may occur for *fac*-[Re(4-phenylpyridine)$_2$(CO)$_3$Cl] in 2-propanol and EPA where only $\pi\pi^*$ emission is observed at 77 K and MLCT emission appears in the fluid.[376]

In 4:1 (v:v) EtOH/MeOH or 2-MeTHF, *fac*-[Re(dppz)(CO)$_3$Cl] is a $\pi\pi^*$ emitter at 77 K, a dual, $\pi\pi^*$-MLCT emitter in the fluid below 200 K, and a MLCT emitter at 298 K.[385] The lowest state at 298 K is $\pi\pi^*$ as shown by transient resonance Raman and UV−visible measurements.[396] This is a case where $\pi\pi^*$ is the lower state, but MLCT is shorter-lived. By 298 K, it is sufficiently populated to dominate excited-state decay.

For [Zn(PhS)$_2$(phen)] at 77 K in a series of solvent glasses, there is evidence for emission from both phen-localized, $^3\pi\pi^*$, and ligand-to-ligand (thiol to phen) charge transfer (LLCT) states.[390] Their relative intensities vary with glass composition. They are comparable in 1:9 (v:v) $CHCl_3$/EtOH but the LLCT emission increases in intensity and shifts to lower energy as the alcohol content is increased. The appearance of dual emission shows that $\pi\pi^*$ and LLCT do not interconvert efficiently and that LLCT is lower (section VI.C).

Evidence supporting "intramolecular solvation" by the hydrocarbon "tail" in the nitrile series [Re(bpy)(CO)$_3$(NC(CH$_2$)$_n$CH$_3$)]$^+$ (n = 0, 2, 5, 7, 9, 10, 13, 17) and their phenanthroline analogues was flawed because of highly emitting isonitrile impurities in the samples.[397,398] In a more recent study, the salt [Re(bpy)(CO)$_3$(CN-*t*-Bu)]$^+$ was shown to be a dual emitter at 77 K in a 9:2 (v:v) DMF/CH_2Cl_2 glass.[398]

In 4:1 (v:v) EtOH/MeOH at room temperature, Re$^I \rightarrow$ bpy, Re$^I \rightarrow$ 4,4′-bpy excitation of *fac*,*fac*-[(bpy)(CO)$_3$Re^I(4,4′-bpy)Re^I(CO)$_3$(bpy)]$^{2+}$ gives an equilibrium mixture of Re^{II}(bpy$^{\bullet-}$) and Re^{II}(4,4′-bpy$^{\bullet-}$) MLCT states within 5 ns. Their interconversion by intramolecular electron transfer (k_2, k_{-2} in Scheme 1) is rapid at room temperature but competitive with decay from the excited states (k_1, k_3) below 180 K.[411]

At room temperature, the equilibrium favors Re^{II}(4,4′-bpy$^{\bullet-}$) as solvent polarity is increased from dichloroethane (D_s = 10.4), CH_3CN (D_s = 36.2), to propylene carbonate (D_s = 65.1) and the mole fraction of Re^{II}(4,4′-bpy$^{\bullet-}$) increases from ≤ 0.10 to 0.55. Polar solvents stabilize Re^{II}(4,4′-bpy$^{\bullet-}$) over Re^{II}(bpy$^{\bullet-}$) because of the greater dipole moment (∼5.5 Å vs 2.3 Å). From eq 90, the difference in solvation energies (Δw_s) between excited states of dipole moments $\vec{\mu}_{e,1}$ and $\vec{\mu}_{e,2}$ is given by

$$\Delta w_s = \frac{1}{a^3}(\vec{\mu}_{e,1}{}^2 - \vec{\mu}_{e,2}{}^2)\frac{1 - D_s}{2D_s + 1} \qquad (117)$$

The ordering of MLCT and ligand field (dd) states in [Fe(bpy)(CN)$_4$]$^{2-}$ can be inverted by solvent variations at room temperature.[412] MLCT is highly solvent dependent due to specific interactions with the CN^- ligands (sections III.C.2 and IV.C) with E_{abs} shifting from 482 nm in H_2O to 725 nm in acetone. There is an inversion between MLCT and dd states in these two solvents. A related effect has been reported by Hupp et al. for [Ru(bpy)(NH$_3$)$_4$]$^{2+}$ which is photolabile toward NH_3 loss in nitromethane (DN = 2.7) but stable in DMSO (DN = 29.8).

V. Excited State Decay. Solvent and Temperature Effects

Excited states decay by a combination of radiative and nonradiative processes. Nonradiative processes include pathways in which excited states undergo chemical reactions such as electron transfer, energy transfer, or bond breaking, and nonradiative decay in which excited to ground-state conversion occurs without emission of light. Each process has an associated solvent and temperature dependence and each influences emission quantum yields (Φ_{em}), lifetimes (τ), and nonradiative rate constants (k_{nr}) (section II.F.2).

A. Radiative Decay

Strickler and Berg showed that k_r for organic fluorescence could be calculated from integrated absorption spectra by using eq 34. Values were obtained that were within 20−30% of the experimental values.[144] Belletête and Durocher measured radiative rate constants and average emission energies for a series of 3*H*-indole derivatives in five solvents.[413] A correlation was found to exist between $\ln(k_r/n^3)$ (n is the index of refraction) and $\ln \bar{\nu}$ ($\bar{\nu}$ is the average fluorescence energy, E_{em}) with a slope of ∼11 which is larger than the predicted slope of 3 based on eq 34. This was taken as evidence that the transition moments, $\vec{M}$, increased with the excited-state energy gap. It was also found that k_r was viscosity-dependent.

For 44 organic exciplexes, Gould, Farid, and coworkers found that a linear correlation existed between $\log(k_r/n^3)$ and $\log(\bar{\nu})$ with the expected slope of 3 for low energy emitters.[414] Exciplexes that emitted at higher energies deviated from the correlation due to changes in the extent of charge transfer.

This increased the extent of mixing with local excited states on the donors or acceptors and increased transition moments.

B. Nonradiative Decay

The single mode energy gap law result in eq 37 has been tested quantitatively for Os^{II}, Ru^{II}, and Re^{I} polypyridyl complexes in the form:[134,166]

$$\ln(k_{nr}) = \ln(\beta_o) + \ln(F) \tag{118}$$

with the vibrational overlap term, ln*(F),* given by

$$\ln(F) = -{}^1/_2 \ln(\hbar\omega E_0) - S - \frac{\gamma E_0}{\hbar\omega} + \left(\frac{\gamma+1}{\hbar\omega}\right)^2\left(\frac{(\Delta\bar{\nu}_{1/2})^2}{16\ln 2}\right) \tag{119}$$

and

$$\beta_o = C_k{}^2\omega_k(\pi/2)^{1/2} \tag{120}$$

with, $E_o = |\Delta G°| - \lambda_o$ and

$$(\Delta\bar{\nu}_{1/2})^2/16\ln 2 = \lambda_o k_B T \tag{121}$$

The complexes studied were $[Os(bpy)(L)_4]^{2+}$ and $[Os(phen)(L)_4]^{2+}$, *cis*-$[Ru(bpy)_2(L)_2]^{2+}$, and *fac*-[Re(4,4′-$(X)_2$bpy)$(CO)_3$Cl] (X = NH_2, NEt_2, $NHCOCH_3$, OCH_3, CH_3, Cl, H, C_6H_5).[134,166,416] The L were a variety of

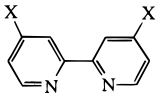

(4,4'-$(X)_2$bpy)

phosphine, pyridine, arsine, and other coordinated ligands. ln(*F*) was calculated from E_o, $\hbar\omega_M$, S_M, and $\Delta\bar{\nu}_{1/2}$ obtained by Franck−Condon analysis of the emission spectra (section II.G.1). There was a correlation between ln(k_{nr}) and ln(F) with a slope of 1 as predicted by eq 118. Both bpy and phen complexes fall on the same correlation. From the intercept and eq 120, ln(β_o) = 34. On the basis of this value and assuming $\hbar\omega_k = 300$ cm^{-1}, $V_k \sim 1300$ cm^{-1} for Os^{II}, 600 cm^{-1} for Re^{I}.

1. Solvent Effects

The effect of the solvent on k_{nr} for $[Ru(bpy)_3]^{2+}$* was investigated in six polar solvents from CH_2Cl_2 to DMF.[170] ln(k_{nr}) varied linearly with E_o (and E_{em}) from E_o = 16 150 to 16 750 cm^{-1}. The slope of the correlation (-7.4 ± 0.7 eV^{-1}) was the same, to within experimental error, as for k_{nr} in the series *cis*-[Ru-$(bpy)_2(L)_2]^{2+}$ in CH_2Cl_2 at 200 K and $[Os^{II}(bpy)(L)_4]^{2+}$* (7.5 ± 0.7 eV^{-1}) where the energy gap was varied by varying L.[415,416] The agreement between the two shows that the important factor is the energy gap, not how it is varied. The solvent correlations work because γ is solvent-independent and variations in λ_o are relatively small.

There are other nonradiative decay channels for $[Ru(bpy)_3]^{2+}$* and related Ru^{II} complexes.[170,388,415−422] In one, thermal activation and decay occur through a low-lying dd state or states of electronic configuration $d\pi^5 d\sigma^{*1}$. The $d\sigma$*orbitals (e_g in octahedral symmetry) are antibonding with regard to the metal−ligand bonds leading to metal−ligand bond lengthening, rapid nonradiative decay, and ligand loss photochemistry. This introduces a temperature dependence in τ of the form,[389]

$$\tau^{-1} = \frac{k + k'\exp[-(\Delta E'/RT)]}{1 + \exp[-(\Delta E'/RT)]} \tag{122}$$

or if $\Delta E' \gg RT$,

$$\tau^{-1} = k + k'\exp[-(\Delta E'/RT)] \tag{123}$$

with $k = k_r + k_{nr}$ for the lowest, emitting MLCT state or states. In $[Ru(bpy)_3]^{2+}$* there are three low-lying MLCT states all with the $d\pi^5\pi^{*1}$ configuration.[388,417] Kinetically, they behave as a single state above 100 K. The interpretation of $\Delta E'$ and k' in eq 123 depends on the kinetic limit assumed. In one, $\Delta E'$ is the energy of activation for an irreversible MLCT → dd surface crossing and k' the associated frequency factor. There are additional decay channels arising from thermal population and decay through other low-lying MLCT states which also influence the kinetics and temperature dependence of τ.[389]

In the solvent-dependent study on $[Ru(bpy)_3]^{2+}$* mentioned above, τ and ϕ_{em} were measured as a function of temperature. The kinetic parameters varied from $k' = 4.5 \times 10^{13}$ s^{-1}, $\Delta E' = 3560$ cm^{-1} in CH_2Cl_2 to $k' = 4.0 \times 10^{13}$ s^{-1}, $\Delta E' = 3820$ cm^{-1} in DMF. From these data the fraction of nonradiative events that occur through the MLCT → dd decay channel varies from 0.37 in DMF to 0.80 in CH_2Cl_2. These results were discussed in terms of an irreversible MLCT → dd surface crossing with the associated changes in electronic configuration, $d\pi^5\pi^{*1} \rightarrow d\pi^5 d\sigma^{*1}$. A linear correlation was found to exist between ln(k') and $\Delta E'$ (Barclay−Butler plot) of slope 4.7×10^{-3} cm^{-1} and intercept 13.7.

For $[Os(phen)_3]^{2+}$* in 10 nonhydroxylic solvents, ln(k_{nr}) was found to decrease linearly with E_{em} with the slope of the correlation (−8.6 eV^{-1}) comparable to that for $[Os(phen)(L)_4]^{2+}$* with L varied.[168,415] On the basis of eq 119, with low-frequency modes treated classically, a solvent dependence in k_{nr} is predicted with contributions from both E_o and $(\Delta\bar{\nu}_{1/2})^2$:

$$\ln k_{nr} \propto -\frac{\gamma E_o}{\hbar\omega_M} + \left(\frac{\gamma+1}{\hbar\omega_M}\right)^2\lambda_{o,L}k_B T = -\frac{\gamma(E_{em} + \lambda_{i,L})}{\hbar\omega_M} + \left(\frac{\gamma+1}{\hbar\omega_M}\right)^2\lambda_{o,L}k_B T \tag{124}$$

In this analysis, low-frequency modes are included in $\lambda_{o,L}$ (eq 26). The importance of $\lambda_{o,L}$ can be seen in the deviation of alcohols and H_2O from the ln(k_{nr}) vs E_{em} plot for $[Os(phen)_3]^{2+}$* in Figure 3A. It is predicted by eq 124 that there should be separate ln(k_{nr}) -E_{em} correlations for each solvent for a family of complexes. ln(k_{nr}) should decrease linearly with E_{em}, but the correlations should be offset by the difference in solvent reorganizational energy, $\Delta\lambda_o$. There is

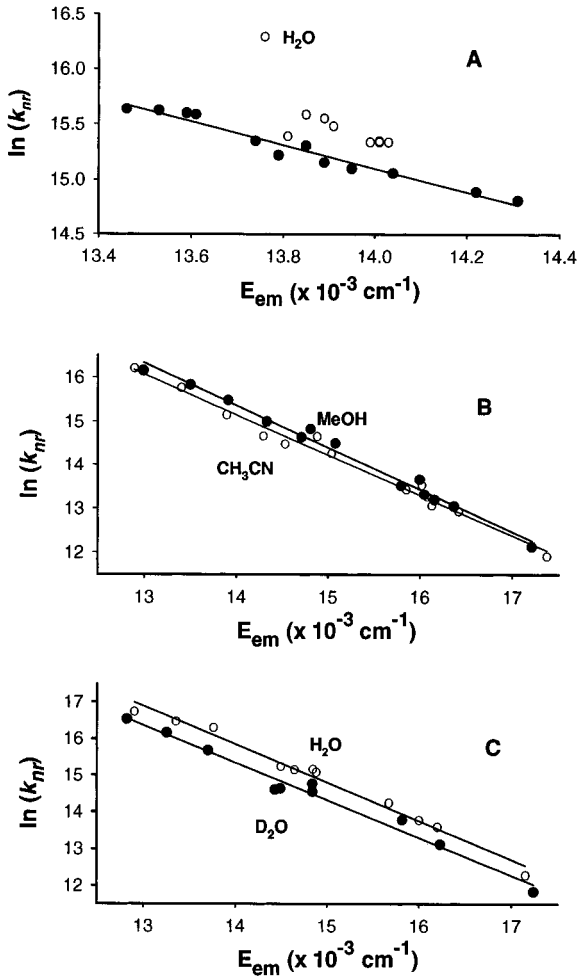

Figure 3. Plots of $\ln(k_{nr})$ vs E_{em} for (A) $[Os(phen)_3]^{2+*}$ in hydroxylic (○) and nonhydroxylic (●) solvents, and for *cis*-$[Os(phen)_2(L)_2]^{2+*}$ (L = $^1/_2$ phen, CH_3CN, etc.) in (B) CH_3CN (○) and CH_3OH (●), and (C) H_2O (○) and D_2O (●). These data were taken from refs 168 and 358.

evidence for this in the $\ln(k_{nr})$ vs E_{em} plots in CH_3CN and CH_3OH in Figure 3B. For the family of complexes *cis*-$[Os(phen)_2(L)_2]^{2+*}$ the slopes of the individual correlations are -7.4 eV^{-1} (CH_3CN) and -7.8 eV^{-1} (CH_3OH).

Even with the apparent agreement with eq 124, the underlying analysis is not sufficient to explain the H_2O/D_2O kinetic isotope effect of ~2 in Figure 3C. The data in D_2O fall on the correlation line for the nonhydroxylic solvents. The H_2O/D_2O kinetic isotope effect for nonradiative decay of $[Ru(bpy)_3]^{2+*}$ is ~2 as well.[237] This is necessarily a quantum effect. There is no significant difference in dielectric properties between H_2O and D_2O until the water librations at 450−775 cm^{-1} (section III.A.2).[20] The quantum effect may arise through coupling with ν(OH) at ~3500 cm^{-1} as an acceptor. The coupling mechanism would be through an electrostatic interaction between the excited-state dipole and the asymmetrical charge distribution in the O−H bonds of individual solvent molecules. Even though these modes have small S values, and may be hard to observe in resonance Raman experiments, they could play a significant role in nonradiative decay because of their high frequency (section II.F.2).

2. Temperature Dependence

Nonradiative decay is typically dominated by coupled medium- or high-frequency vibrations as energy acceptors. If $E_o \gg S\hbar\omega$, vibrational overlaps are not increased appreciably for levels above $v = 0$ and they contribute little, if any, to the temperature dependence.

Even so, the energy gap law results in eq 37 and 119 predict a temperature dependence for k_{nr} with

$$\frac{\partial(\ln k_{nr})}{\partial T} = -\frac{\gamma}{\hbar\omega_M}\left(\frac{\partial E_o}{\partial T}\right) + \left(\frac{\gamma+1}{\hbar\omega_M}\right)^2 \lambda_{o,L} k_B$$

$$= \frac{\gamma}{\hbar\omega_M}\Delta S° + \left(\frac{\gamma+1}{\hbar\omega_M}\right)^2 \lambda_{o,L} k_B \qquad (125)$$

This assumes that β_o and γ are independent of T and that $\Delta S^o = -(\partial E_o/\partial T)$ (eq 58).

The temperature dependence arises in the solvent from the entropic difference between states (neglecting electronic entropy) and the temperature-dependent broadening of the solvent distribution. $\Delta S°$ can be positive or negative depending on whether the transition results in an increase or decrease in solvent polarization, λ_o is always positive. k_{nr} could increase, decrease, or be independent of T depending on the signs and relative magnitudes of $\Delta S°$ and λ_o.

Excited state decay in *fac*-$[Re(bpy)(CO)_3(4\text{-}Etpy)]^{+*}$ and *cis*-$[Os(bpy)_2(CO)(py)]^{2+*}$ in 4:1 (v:v) EtOH/MeOH from 170 to 260 K for Re^I and 160−220 K for Os^{II} is free of kinetic complications from higher dd or MLCT states.[374] Spectral fitting was used to evaluate E_o, $\hbar\omega$, S_M, and $\Delta\bar{\nu}_{1/2}$ and $\ln(F)$. k_{nr} was evaluated from lifetime and quantum yield measurements (eq 31). Comparison between experimental values of $(\Delta\ln(k_{nr})/\Delta T)$ and values calculated by eq 125 gave for *fac*-$[Re(bpy)(CO)_3(4\text{-}Etpy)]^{+*}$, 2.1×10^{-3} K^{-1} vs 8.3×10^{-3} K^{-1} and for *cis*-$[Os(bpy)_2(CO)(py)]^{2+*}$, 3.7×10^{-3} K^{-1} vs 2.6×10^{-3} K^{-1}. Given the assumptions involved, the agreement is impressive providing further confirmation of the ability of the energy-gap law to account for nonradiative decay.

C. Time-Dependent Effects

Application of modern, ultrafast lasers has allowed transient measurements to be made on dynamical processes on time scales approaching femtoseconds. This allows dynamics of relaxation processes to be observed directly on short time scales and is providing new insight into early time events in electron transfer and related processes.[28,39,42,80−94,423−427] Typically, solvent dynamics are measured by observing time-dependent absorption or emission spectral shifts as the solvent relaxes and the energy gap decreases. There have been many measurements of this kind, largely, on organic charge-transfer excited states. A distribution of relaxation processes has been observed ranging from tens of femtoseconds to several picoseconds for ordinary solvents at room temperature.

In some cases, time-dependent spectral shifts have been analyzed by using the correlation function in eq 126:[28,80,428,429]

$$C(t) = \frac{\bar{\nu}(t) - \bar{\nu}(\infty)}{\bar{\nu}(0) - \bar{\nu}(\infty)} \quad (126)$$

In this equation $\bar{\nu}(0)$ and $\bar{\nu}(t)$ are the energies of the absorption or emission maximum at time 0 or time t after excitation. $\bar{\nu}(\infty)$ is the energy after relaxation and equilibration. On ultrafast time scales the decay of *C(t)* is biphasic. On longer time scales, *C(t)* decays exponentially for solvents whose dielectric properties can be described by the simple Debye function in eq 1:[427]

$$C(t) = \exp[-(t/\tau_r)] \quad (127)$$

and τ_r is related to the longitudinal relaxation time, τ_l, by

$$\tau_r \approx \tau_1 = (\epsilon_\infty/\epsilon_o)\tau_D \quad (128)$$

ϵ_∞ and ϵ_o are the optical and static dielectric constants and τ_D the Debye relaxation time. For alcohols, $\epsilon(\omega)$ includes multiple regions of Debye-like behavior and *C(t)* is nonexponential. The correlation function in eq 126 has been used to analyze time-dependent shifts in emission energies of polar fluorescent probes in solution following ultrafast laser excitation.[80,81,87]

This technique has been applied to emission from *cis*-$[Ru(bpy)_2(CN)_2]$*.[430,431] Its maximum is time dependent in methanol, ethanol, 1-propanol, or 1-butanol at −20 °C and decay kinetics nonexponential. At early times, E_{em} shifts to the red, but past 2 ns remains constant and decay is exponential since the solvent is equilibrated. The decay data were fit to a biexponential function with τ_r for the slower component coinciding with the longest of the three longitudinal relaxation times in the bulk solvents. The faster component, which accounted for more than half of the decay, was suggested to arise from local heating due to above-threshold excitation or to faster relaxation of solvent molecules in the first few solvation shells around the complex.

Femtosecond pump−probe measurements on the mixed-valence complex in eq 129 reveal the existence of multiple time scales for reaction and relaxation:[432−434]

$$[(NH_3)_5Ru^{III}(NC)Ru^{II}(CN)_5]^- \xrightarrow{h\nu} [(NH_3)_5Ru^{II}(NC)Ru^{III}(CN)_5]^- \quad (129)$$

Electron transfer occurs on the 80 fs time scale which is far shorter than the 500 fs time scale for solvent reorientation and longer than the time scale for inertial (translational) dynamics (20 ∼ 30 fs). Electron transfer precedes solvent reorientation which increases the energy gap and the electron-transfer barrier. Electron transfer is sufficiently rapid that the product is formed in hot, nonequilibrium vibrational levels as shown directly by transient vibrational measurements.[434]

Time dependences also appear on longer time scales in media such as polymeric films and in the glass-to-fluid transition region of solvents where there are slow relaxation processes. If time scales for relaxation and excited state decay are comparable, the two processes are coupled kinetically. As the medium relaxes, the energy gap decreases. This causes spectral shifts to the red and decreasing lifetimes. These phenomena are related to those observed on ultrafast time scales in fluids, but they occur on a slower time scale in these orientationally more restrictive environments. Coupling with excited-state decay is extended in time, and this can result in nonexponential decay kinetics over a significant fraction of the decay.

Balzani et al. measured emission spectra and lifetimes for a series of Ru^{II} polypyridyl complexes in 4:5 (v/v) propionitrile/butyronitrile between 250 and 84 K.[384] Significant changes occurred through the glass-to-fluid transition region with τ fit to, $1/\tau = B/\{1 + \exp[C(1/T - 1/T_B)]\}$ with C, B, and T_B empirical parameters. To explain the temperature dependence, a nonradiative decay pathway was invoked which is "frozen" in the glass but operative in the fluid. It was also suggested that solvent repolarization could play a role within the glass transition region by enhancing nonradiative decay.

For $[Ru(bpy_3)]^{2+}$* in 4:1 (v:v) EtOH/MeOH, Ferguson and Krausz noted that E_{em} shifted to lower energy as the temperature was increased through the glass to fluid transition.[435] The spectrum was time dependent at 130 K. The shifts and time dependence were attributed to a transition from a delocalized state, in which the excited electron was delocalized over all three bpy ligands $[Ru^{III}(bpy^{-1/3})_3]^{2+}$*, to a localized state in which it was localized on one, $[Ru^{III}(bpy^{\bullet -})(bpy)_2]^{2+}$* (section III.B). It was suggested that the delocalized-to-localized transition might be induced by movement of the charge-compensating anions into positions more favorable for charge localization on one ligand.[435] However, time-resolved emission measurements on $[Ru(bpy)_3]X_2$ ($X = Cl^-$, ClO_4^-, PF_6^-), $[Ru(4,4'\text{-}(Ph)_2bpy)_3](PF_6)_2$ (4,4′-$(Ph)_2$bpy is 4,4′-diphenyl-2,2′-bipyridine), and $[Ru(bpy)_2(4,4'\text{-}(CO_2Et)_2bpy)](PF_6)_2$(4,4′-$(CO_2Et)_2$bpy is 4,4′-bis(ethylcarboxylato)-2,2′-bpyridine) revealed that shifts in E_{em} ($\Delta E_{em} \approx 620$ cm^{-1}) were nearly independent of anion and ligand structure.[380,435−437] For *cis*-$[Ru(bpy)_2(CN)_2]$, $\Delta E_{em} = 1030$ cm^{-1} is nearly twice that for the dications, even though the molecule is neutral.

Danielson et al. proposed that the shifts were due to solvent relaxation.[379] Shifts for $[Os(phen)(das)_2]^{2+}$* and $[Os(phen)_2(das)]^{2+}$* (das = 1,2-bis(dimethylarsino)benzene) were comparable even though $[Os(phen)(das)_2]^{2+}$* has only one acceptor ligand, ruling out a delocalized-to-localized transition. For *cis*-$[Os(bpy)_2(CO)(py)]^{2+}$*, just below and just above the glass-to-fluid transition, $\ln(k_{nr})$ varied linearly with E_o consistent with the energy gap law.[141]

In the glass or fluid, the ensemble of excited states is surrounded by a homogeneous or near homogeneous solvent distribution and the energy gap law applies. As the glass softens, partial relaxation of the surrounding orientational polarization occurs during the lifetime of the excited state. Those excited states that decay at later times have a decreased energy gap. The energy gap becomes time-dependent and k_{nr} assumes the form:

$$\ln(k_{nr}(t)) \approx A - \gamma E_o(t)/\hbar\omega_M \quad (130)$$

This creates a continuous or near continuous distribution of lifetimes and nonexponential decays.

These ideas have been pursued in more detail experimentally for a series of Ru^{II} polypyridyl complexes in the glass transition region in 4:1 (v:v) EtOH/MeOH.[387] The correlation functions *C(t)* describing the time dependence of E_{em} were nonexponential but could be fit to the biexponential expression in eq 131 with relaxation times τ_{r1} and τ_{r2}:

$$C(t) = A \exp[-(t/\tau_{r1})] + (1 - A) \exp[-(t/\tau_{r2})] \quad (131)$$

$\ln(\tau_{r1})$ or $\ln(\tau_{r2})$ varied linearly with $1/T$ with the magnitudes of τ_{r1} and τ_{r2} increasing in deuterated alcohols. E_{em} was not time-dependent in aprotic solvents such as DMSO, CH_3CN, or propylene carbonate at their freezing points. From this observation and the appearance of an isotope effect, it was concluded that H-bonding was responsible for the time-dependent shifts, although a related behavior was observed in 2-MeTHF as well.

From emission spectral fitting, E_o and S decrease as the glass softens.[141,438] $(\Delta\bar{\nu}_{1/2})^2$ increases linearly with T, but there is a discontinuity at the glass transition, below which $(\Delta\bar{\nu}_{1/2})^2$ becomes nearly temperature-independent. This is predicted by the analysis in section IV.E since in the glass, λ_{oo} becomes part of the energy gap and only λ_{oi} contributes to the bandwidth, $(\Delta\bar{\nu}_{o,1/2})^2 = 16k_BT\,\lambda_{oi}\ln 2$.

Time-dependent effects have been observed for MLCT emitters in other media including polymeric films. For $[Ru(bpy)_2(5\text{-}NH_2\text{-}1,10\text{-phenanthroline})](PF_6)_2$ bound to chlorosulfonated polystyrene by sulfonamide binding, $-NHSO_2-$, E_{em} is time-dependent and decays nonexponentially with CH_3CN as the external solvent.[439] Emission decays were fit to the biexponential function in eq 131 with, $\tau_1 = 115$ ns and $\tau_2 = 700$ ns with E_{em} shifting from ~ 605 nm at 20 ns to ~620 nm at 100 ns. Lifetimes were nearly exponential with the polymer dissolved in DMSO or in dry films at 77 K. These observations point to a film relaxation process on the tens of nanoseconds time scale which is kinetically coupled to excited-state decay.

In electrochemically polymerized films of $poly[Ru(vbpy)_3](PF_6)_2$ (vbpy is 4-methyl-4′-vinyl-2,2′-bipyridine), E_{em} shifts to lower energy with time, and decays are nonexponential.[440] In copolymeric films of $poly[Ru(vbpy)_3](PF_6)_2$, $poly[Zn(vbpy)_3](PF_6)_2$, E_{em}, and τ approach values observed in polar solvents, and the decays become nearly exponential as the mole fraction of Zn^{II} is increased from 0 to ~0.9. The Zn^{II} complex has no low-lying excited states and acts as an inert diluent of comparable size. Energy transfer to low-energy "trap" sites formed by excited state-ground-state interactions was invoked to explain the time dependence of E_{em}.

The photophysical properties of $[Ru(bpy)_3]^{2+*}$ have been investigated in thin films,[441−447] in zeolites,[448−452] and clays and layered inorganic solids.[453−461] Excited state decay is nearly exponential in the films but nonexponential in the rigid inorganic matrixes. Lifetimes are temperature dependent, consistent with eq 123, but k' and $\Delta E'$ are characteristic of thermal activation and decay through a higher lying MLCT state ($k' = 10^7-10^{10}$ s^{-1}; $\Delta E' = 300-1500$ cm^{-1}) rather than a MLCT → dd surface crossing. For $[Ru(bpy)_2(daf)]^{2+}$ (daf is diazafluorene) in zeolite Y compared to water, the magnitude of $\Delta E'$ is increased by ~1700 cm^{-1} compared to 4:1 (v:v) EtOH/MeOH.

These media are also stabilizing with regard to photochemical ligand loss from complexes such as *cis*-$[Ru(bpy)_2(py)_2]^{2+}$ which lose ligands with high quatum efficiency in solution. Stabilization has been attributed to an inhibition to MLCT → dd surface crossing by increasing the activation barrier. This is a differential effect with dielectric effects destabilizing MLCT relative to dd and an internal pressure effect increasing λ and the classical energy of activation for barrier crossing. Other factors that may contribute are limited translational diffusion of the leaving group and an increased barrier to ligand loss from the dd state.

VI. Solvent Effects on Electron Transfer

The role of solvent on electron transfer has been discussed extensively in the literature.[6,8,43,44−48] It influences $\Delta G°$ and contributes to the reorganizational energy (λ_o) (section II.B). In some cases electron-transfer dynamics are dictated by the solvent.[79−98] For bimolecular reactions involving ions, the dielectric properties of the solvent influence the spatial distribution of the ions by their ability to screen the charges and this contributes to the magnitude of k_{ET} as well (section II.B).

Because the literature is extensive, the emphasis here will be on two areas, electron transfer in the "inverted region" and electron transfer in rigid media. The influence of rigid media on charge-transfer absorption and emission were discussed in section IV.E. In the inverted region, the driving force exceeds the reorganization energy, $-\Delta G° > \lambda$ and there are similarities with nonradiative decay (section II.E).

A. Electron Transfer in the Inverted Region

As illustrated in Figure 4 electron transfer in the inverted region occurs with the reactant energy curve nested within the product curve. $\ln(k_{ET})$ is predicted to decrease quadratically with $-\Delta G°$, by classical barrier crossing as illustrated in Figure 4B (eq 24). If there are coupled medium- or high-frequency vibrations (Figure 4A), transitions from vibrational levels below the intersection between potential curves become important. In the energy gap law limit, $\ln(k_{ET})$ varies linearly with $-\Delta G°$.

1. Solvent and Medium Effects

After being predicted by Marcus,[8,46,62] the inverted region escaped experimental detection for nearly two decades. The first observations were made by pulse radiolysis in glasses between spatially separated molecules by Miller[462,463] and indirectly by electrogenerated chemiluminescence by Bard et al.[464,465] Since then, evidence for the inverted region has been found in a number of systems.[466−489] The first

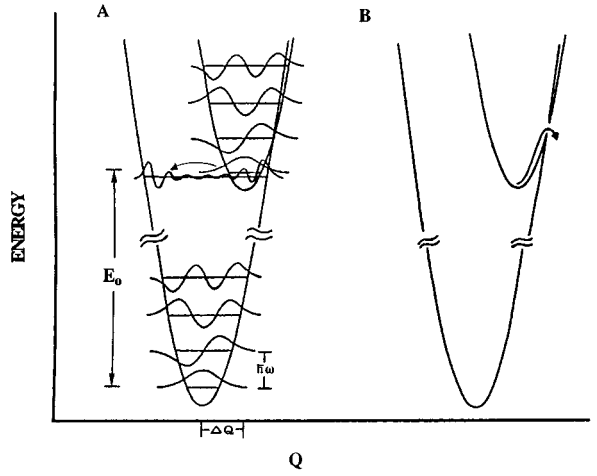

Figure 4. Schematic energy-coordinate diagram illustrating electron transfer in the inverted region (A) by vibrational channels below the intersection between the two free energy surfaces (nuclear tunneling) and (B) by classical barrier crossing.

unambiguous, intramolecular example was the landmark work of Closs and Miller.[466−468] Rate constants for intramolecular electron transfer between a biphenyl radical anion donor and a series of organic acceptors (A) across a steroid spacer were measured by pulse radiolysis:

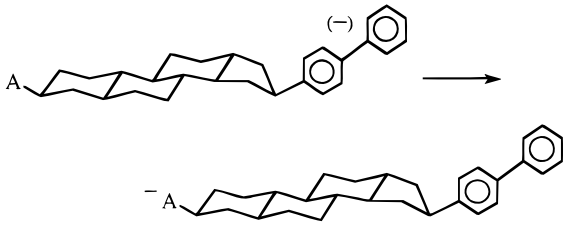

(132)

The dependence of $\ln(k_{ET})$ on $\Delta G°$ could be accounted for by eq 25 with $\hbar\omega_M = 1500$ cm^{-1}, $S_M = 2.4$, $H_{DA} = 6.2$ cm^{-1}, and $\lambda_{o,L} \approx 0.75$ eV in 2-methyltetrahydrofuran, 0.45 eV in di-*n*-butyl ether, and 0.15 eV in isooctane. The variation of λ_o with solvent was qualitatively consistent with dielectric continuum theory (eq 9) but the $\Delta G°$ values used in the correlations were obtained from electrochemical measurements in DMF with an added supporting electrolyte.

Back electron transfer in $[(4,4'\text{-}(X)_2bpy^{\bullet-})Re^{I}(CO)_3(py\text{-}PTZ^{\bullet+})]^+$ (X = CH_3O, CH_3, H, $C(O)NEt_2$, CO_2Et) and $[(bpz^{\bullet-})Re^{I}(CO)_3(py\text{-}PTZ^{\bullet+})]^+$ (bpz is 2,2′-bipyrazine):

$$[(4,4'\text{-}(X)_2bpy^{\bullet-})Re^{I}(CO)_3(py\text{-}PTZ^{\bullet+})]^+ \xrightarrow{k_{ET}} [(4,4'\text{-}(X)_2bpy)Re^{I}(CO)_3(py\text{-}PTZ)]^+ \quad (133)$$

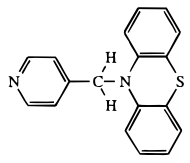

(py-PTZ)

has been studied by laser flash photolysis in 1,2-dichloroethane.[484,485] In the series, the variations in −X cause $\Delta G°$ to vary from −1.5 to −2.3 eV, and k_{ET} decreases by ∼30. $\ln(k_{ET})$ decreased linearly with $|\Delta G°|$ as predicted by eq 29.

k_{ET} for back electron transfer in eq 134 was measured in seven polar solvents with k_{ET}

$$[Re^{I}(CO)_3(bpy^{\bullet-}CH_2PTZ^{\bullet+})Cl] \xrightarrow{k_{ET}} [Re^{I}(CO)_3(bpyCH_2PTZ)Cl] \quad (134)$$

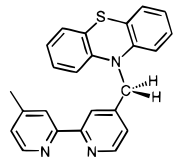

(bpyCH$_2$PTZ)

varying from 4.3×10^6 s^{-1} in benzonitrile to 6.7×10^6 s^{-1} in propylene carbonate.[490] By using eq 29, the two-sphere model in eq 9 for λ_o, neglecting electrostatic interactions between $bpy^{\bullet-}$ and $-PTZ^+$, and assuming $-\Delta G° \gg \lambda_o$, ln k_{ET} is given by

$$\ln k_{ET} \propto -\frac{\gamma|\Delta G°|}{\hbar\omega_M} + \left(\frac{\gamma+1}{\hbar\omega_M}\right)^2 k_B T\lambda_o$$

$$\propto -\frac{\gamma\Delta E_{1/2}}{\hbar\omega_M} + \left(\frac{\gamma+1}{\hbar\omega_M}\right)^2 k_B T e^2\left(\frac{1}{2a_1} + \frac{1}{2a_2} - \frac{1}{d}\right)\left(\frac{1}{D_{op}} - \frac{1}{D_s}\right) \quad (135)$$

In this equation, $\Delta E_{1/2} = E_{1/2}(-PTZ^{+/0}) - E_{1/2}(bpy^{0/-})$. Experimentally, the variation in k_{ET} with solvent was found to fit the equation, $\ln(k_{ET}) = 22.5 + 3.4\ \Delta E_{1/2} + 1.2(1/D_{op} - 1/D_s)$. The coefficient $\gamma/\hbar\omega = -3.4$ eV^{-1} was taken from the correlation of $\ln(k_{ET})$ with $\Delta G°$ for back electron transfer in $[(4,4'\text{-}(X)_2bpy^{\bullet-})Re^{I}(CO)_3(py\text{-}PTZ^+)]^+$ (eq 133).

For back electron transfer in eq 133 with X = H, k_{ET} in CH_2ClCH_2Cl increased from 1.05×10^7 to 1.65×10^7 s^{-1} as the ionic strength was increased from 0.0002 to 0.32 M with added $[N(n\text{-}C_4H_9)_4](PF_6)$.[489] The effect leveled off past $\mu = 0.16$ M. $\Delta G°$ values were obtained by electrochemcial measurements. The results could be explained qualitatively by invoking the energy gap law and the effect of ion pairing in decreasing the energy gap.

A similar observation has been made in contact ion pairs by Thompson and Simon.[425] In nonpolar ethyl acetate, addition of $[N(n\text{-}C_4H_9)_4]ClO_4$ causes a decreases in the driving force and an increase in k_{ET}. In CH_3CN there was no change in k_{ET} with added 1.0 M $[N(n\text{-}C_4H_9)_4]ClO_4$.

The effect of added electrolyte was also investigated for the electron-transfer reaction in the normal region shown in eq 136 which was studied by pulse radiolysis.[491] In tetrahydrofuran (THF) with $\mu = 10-30$ mM, k_{ET} was found to decrease by up to 2−3 orders of magnitude relative to the value in neat THF as the size of the cation in the electrolyte was increased. The magnitude of the effect increased with the size

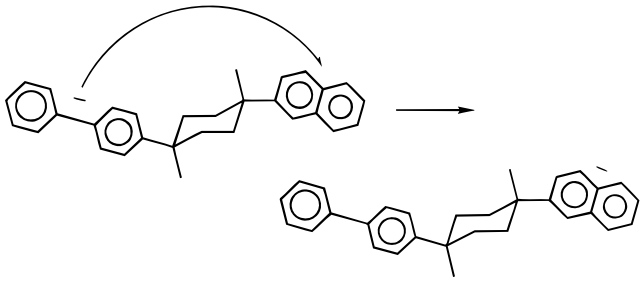

(136)

of the cation in a series of tetraphenylborate salts where the cation was varied from Li^+ to $[N(n\text{-}C_{18}H_{37})_4]^+$. This was an unexpected result since electrostatic interactions decrease with increasing cation size. The energy of the transannular charge-transfer band in the 6,13-dihydropentacene anion, measured under similar conditions, shifts to higher energy as the size of the cation (C^+) decreases, as expected.

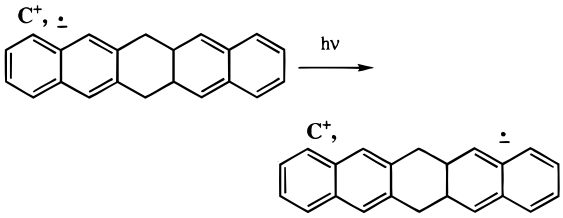

(137)

The discrepancy between the two observations was explained as a dynamical effect. Translational motion of the charge-compensating cation is coupled to thermal electron transfer and this motion may dictate the magnitude of ν_n in eq 2. The dynamics of ion atmosphere relaxation have been studied by time-resolved emission measurements of probe molecules in electrolyte solutions on fast time scales.[492−495] Compared to the neat liquid, an additional component was observed in the decay kinetics that was attributed to the relaxation of the ion atmopshere.

Inverted region electron transfer has been studied in contact radical ion pairs (CRIP) formed by laser flash photolysis of organic donor−acceptor complexes such as hexamethylbenzene−1,2,4,5-tetracyanobenzene (TCB,HMB):[185,496−498]

$$\text{HMB,TCB} \xrightarrow{h\nu} \text{HMB}^+,\text{TCB}^- \xrightarrow{k_{ET}} \text{HMB,TCB} \quad (138)$$

These complexes emit and emission spectral fitting and resonance Raman were used to evaluate the electron-transfer barrier. The solvent dependence of k_{ET} has been measured for the CRIPs formed from phthalic anhydride or pyromellitic dianhydride or other acceptors and aromatic donors. k_{ET} decreased with $-\Delta G°$ as predicted by eq 29. When the effect of solvent on $\Delta G°$ was taken into account, plots of $\ln(k_{ET})$ vs $|\Delta G°|$ fell on separate correlations for data obtained in ethyl acetate, acetone, or acetonitrile, consistent with eq 124 and variations in λ_o between these solvents as for nonradiative decay in Figure 3B.

The difference in distance dependence predicted for normal and inverted electron transfer by Marcus and Sutin [143, 499,500] (section II.E) has been incorporated into an analysis explaining how electrogenerated chemiluminescence (ecl) yields vary with solvent for electron transfer between $Mo_6Cl_{14}^-$ and $Mo_6Cl_{14}^{3-}$ or 4-cyano-*N*-methylpyridinium radical.[501,502] The latter reaction proceeds by two distinct electron-transfer channels. One gives an excited state of the cluster (and emission). The other gives the ground state, eq 139:

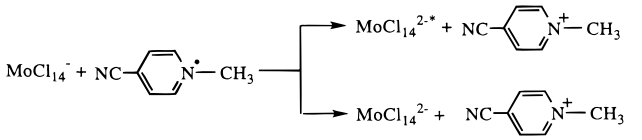

(139)

On the basis of a somewhat convoluted analysis, it was concluded that in polar solvents (acetone and a series of nitriles), electron transfer to the ground state (which is favored by −2.13 to −2.30 eV) occurs across a single intervening solvent molecule. In CH_2Cl_2 and CH_2ClCH_2Cl, which are nonpolar, electron transfer occurs with the reactants in close contact.

The difference in distance dependence has also been investigated for intramolecular electron transfer in a series of Ru^{II} chromophore−quencher complexes.[488] The photoinduced forward electron transfer occurs in the normal region while thermal back electron transfer occurs in the inverted region. The distance dependence of k_{ET} for forward electron transfer ($\beta = 1.38$ Å^{-1}) is twice as great as for back electron transfer ($\beta = 0.66$ Å^{-1}). This difference can be accounted for by including the distance dependence of λ_o.

A solvent dynamical effect has been reported for back electron transfer in a cofacially linked porphyrin.[503] Excitation at 532 nm gives an intramolecular contact radical ion pair followed by back electron transfer to the ground state. In seven solvents—CH_2Cl_2, acetone, dimethylformamide, and a series of alkyl acetates—a nearly linear dependence was found between k_{ET} and τ_l^{-1} as predicted by eq 12. There was no obvious variation in k_{ET} with the energy gap and no attempt was made in the analysis to incorporate the solvent dependence of either $\Delta G°$ or λ_o.

In a more recent paper, k_{ET} was found to vary linearly with τ_l^{-1} in series of nitriles and acetates, but the data in the two types of solvents fell on different correlations with dramatically different slopes.[504,505] The difference was attributed to a difference in activation energies. For a Zn^{II} porphyrin−modified free base chlorin analogue, $\Delta G°$ was less favorable by 0.3 eV, there was a decrease in activation energy, and $k_{ET} \approx \tau_l^{-1}$. k_{ET} fell on the same linear correlation in both sets of solvents.

2. Temperature Dependence

If there are coupled medium- or high-frequency vibrations, the temperature dependence of electron transfer in the inverted region is expected to be different from the normal region and like that for nonradiative decay (eq 125). There is no requirement for barrier crossing but there can be a temperature dependence. It arises from the entropic difference

arising from changes in frequency and densities of states in the coupled solvent modes and from the temperature-dependent solvent distribution function which incorporates λ_o. In the inverted region, k_{ET} could increase, decrease, or even be independent of temperature. If the energy gap law applies, $\ln(k_{ET})$ is predicted to vary with T, and not $1/T$ as in the usual Arrhenius temperature dependence.

Some of these predictions have been borne out experimentally. For the electron-transfer reaction in eq 132 with A = naphthalenyl, $\Delta G° \sim 0$ in 2-MeTHF.[506] A classical temperature dependence was observed with $\ln(k_{ET}T^{-1/2})$ varying linearly with $1/T$. A value of $\Delta H^* = 0.22$ eV was calculated from the slope of the correlation. $\Delta G°$ was calculated from the measured equilibrium constant and λ_o from eq 9 by using D_s and D_{op} values for 2-MeTHF measured at each temperature.

With A = benzoquinone, $\Delta G° = -2.29$ eV at room temperature, electron transfer occurs in the inverted region, and k_{ET} is nearly temperature independent.[507] The data were analyzed by using eq 25 and parameters obtained in previous studies.

The energy gap law result equivalent to eq 125 for nonradiative decay is

$$\frac{\partial \ln k_{ET}}{\partial T} \approx -\frac{\gamma \Delta S°}{\hbar\omega_M} + \left(\frac{\gamma+1}{\hbar\omega_M}\right)^2 \lambda_{o,L} k_B \quad (140)$$

$\Delta S°$ in eq 140 does not include electronic entropy. $\lambda_{o,L}$ includes low-frequency vibrations treated classically.

The dependence of k_{ET} on T has been tested experimentally for the reaction in eq 134.[490] $\ln(k_{ET})$ was found to increase linearly with T from 223 K ($k_{ET} = 6.33 \times 10^6$ s^{-1}) to 303 K ($k_{ET} = 7.11 \times 10^6$ s^{-1}) in propylene carbonate with $\partial(\ln(k_{ET})/\partial T) = 9 \times 10^{-4}$ K^{-1}. From temperature-dependent electrochemical measurements, $\Delta S° = 12$ cal mol^{-1} K^{-1}. The positive value is expected because charge is neutralized in the reaction. From these values and $\gamma/\hbar\omega = 3.4$ eV^{-1}, $\hbar\omega_M \sim 1300$ cm^{-1}, the value $\lambda_{o,L} \sim 0.4$ eV was calculated by using eq 140. This value is in good agreement with an estimate made from self-exchange rate constants for related $-$PTZ$^{+/0}$ and bpy$^{0/-}$ couples.

B. Electron Transfer in Rigid Media

Electron transfer reactions that occur readily in fluid solution are often inhibited or even cease to occur in rigid media.[139,140] This is not always the case. Electron transfer continues to occur in the reaction centers of some photosynthetic bacteria even at 4 K, [508−511] and in glasses between isolated donors and acceptors[463−465,512−516] or molecular assemblies [140,517−520] if the reactions are highly favored.

This apparent rigid medium effect has the same origin as the rigid medium effect on emission (section IV.E) and nonradiative decay (section IV.B). It arises because λ_{oo} becomes part of $\Delta G°$ rather than λ_o.[139,381] The free-energy change in a frozen medium, $\Delta G°_{fr}$ is related to that in the fluid, $\Delta G°_{fl}$, by

$$\Delta G°_{fr} = \Delta G°_{fl} + \lambda_{oo} \quad (141)$$

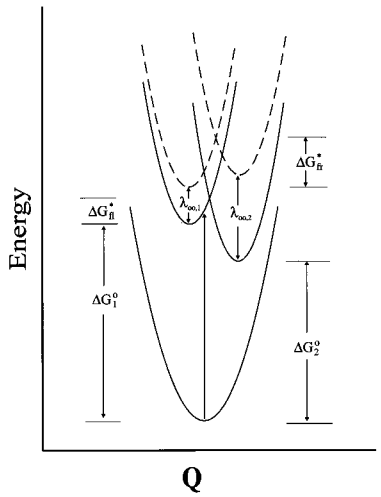

Figure 5. Energy-coordinate diagram for an excited-state electron transfer in fluid (solid curves) and frozen media (dashed curves). The various energy quantities are defined in the text.

The classical barriers to electron transfer in frozen (ΔG^*_{fr}) and fluid (ΔG^*_{fl}) media are related by

$$\Delta G^*_{fr} = \frac{(\lambda_i + \lambda_{oi} + (\Delta G°_{fr} + \lambda_{oo}))^2}{4(\lambda_i + \lambda_{oi})} = \left(1 + \frac{\lambda_{oo}}{\lambda_i + \lambda_{oi}}\right)\Delta G^*_{fl} \quad (142)$$

From the dielectric continuum expressions for λ_{oo} and λ_{oi} in eqs 114 and 115, $\Delta(\Delta G^*) = \Delta G^*_{fr} - \Delta G^*_{fl}$, increases in polar media and with the electron-transfer distance.

The rigid medium effect on photoinduced electron transfer is more complex. An example is illustrated in Figure 5 based on eq 133, in which initial $Re^{I} \rightarrow$ bpy excitation is followed by $-$PTZ $\rightarrow Re^{II}$ electron transfer. The energy of the initial $Re^{II}(bpy^{\bullet -})$ MLCT state is $\Delta G°_{1,fl} + \lambda_{oo,1}$. $\Delta G°_{1,fl}$ is the free energy of the MLCT excited state above the ground state in the fluid and $\lambda_{oo,1}$ is the frozen part of its solvent reorganizational energy. $\Delta G°_{fr}$ for $-$PTZ $\rightarrow Re^{II}$ electron transfer is given by

$$\Delta G°_{fr} = (\Delta G°_{2,fl} - \Delta G°_{1,fl}) + (\lambda_{oo,2} - \lambda_{oo,1}) = \Delta(\Delta G°_{ES,fl}) + \Delta\lambda_{oo} \quad (143)$$

and the classical free energy of activation by

$$\Delta G^*_{fr} = \frac{(\lambda_i + \lambda_{oi} + \Delta G°_{fr})^2}{4(\lambda_i + \lambda_{oi})} \quad (144)$$

In eq 143, $\Delta G°_{2,fl}$ and $\lambda_{oo,2}$ refer to the second state. Electron transfer is spontaneous ($\Delta G°_{2,fr} < 0$) when

$$(\Delta G°_{2,fl} + \lambda_{oo,2}) < (\Delta G°_{1,fl} + \lambda_{oo,1}) \quad (145)$$

The inverted region is reached when

$$-[\Delta(\Delta G°_{ES,fl}) + \Delta\lambda_{oo}] > (\lambda_i + \lambda_{oi}) \quad (146)$$

On the baiss of this analysis, the reorganizational energy is *lower* in a frozen solution than in the fluid. The driving force ($-\Delta G°$) is *either greater or less*, depending on whether $\Delta\lambda_{oo}$ is positive or negative. The sign of $\Delta\lambda_{oo}$ depends on the difference in charge distribution between reactants and products and whether solvent polarization increases or decreases. It is positive for the intramolecular electron transfer in Figure 5 and this increases $\Delta G^{\ddagger}_{fr}$.

The importance of driving force for photoinduced electron transfer in rigid media has been demonstrated experimentally.[140] Emission from $[Re(4,4'\text{-}(X)_2bpy)(CO)_3(MQ^+)]^{2+}$ (MQ^+ is *N*-methyl-4,4′-bipyridinium cation, section III.C.1) for X = H was observed in 4:1 EtOH/MeOH at 77 K with no evidence for significant quenching by intramolecular electron transfer (eq 147). In $[Re(4,4\text{-}(NH_2)_2bpy)(CO)_3(MQ^+)]^{2+}$, electron transfer does occur as shown by the appearance of a $Re^{II}(MQ^{\bullet})$-based emission. At room temperature in CH_3CN, $\Delta G°$ for $4,4\text{-}(X)_2bpy^{\bullet-} \rightarrow MQ^+$ electron transfer decreases from ~ -0.49 eV (X = H) to -1.0 eV ($X = NH_2$). Related observations have been made in 4:1 EtOH/MeOH at 77 K for *cis*-$[Ru(Me_4bpy)_2(MQ^+)_2]^{4+}$ (Me_4bpy is 4,5,4′,5′-tetramethyl-2,2′-bipyridine) compared to *cis*-$[Ru(bpy)_2(MQ^+)_2]^{4+}$.[521]

$$[Re^{II}(4,4'\text{-}(X)_2bpy^{\bullet-})(CO)_3(MQ^+)]^{2+*} \rightarrow [Re^{II}(4,4'\text{-}(X)_2bpy)(CO)_3(MQ^{\bullet})]^{2+*} \quad (147)$$

This is not simply a temperature effect.[517] For $[Re(4,4\text{-}(NH_2)_2bpy)(CO)_3(MQ^+)](PF_6)_2$ in poly(methylmethacralyte) (PMMA) or in a powdered sample of the salt, there is evidence for electron transfer by the appearance of the characteristic red-shifted emission from $Re^{II}(MQ^{\bullet})$. For $[Re(bpy)(CO)_3(MQ^+)](PF_6)_2$ the emission is largely from $Re^{II}(bpy^{\bullet-})$.

The influence of driving force on electron transfer was studied in 2-MeTHF for a family of derivatized porphyrins, having quinone or tetracyanoquinodimethane acceptors (eq 148).[519]

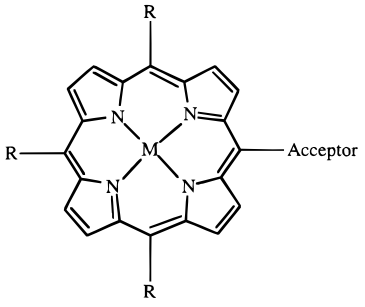

R = phenyl or pentyl
M = Zn or 2H

Acceptors:

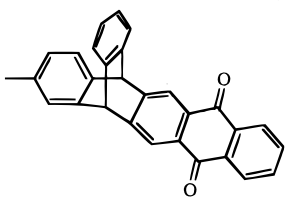

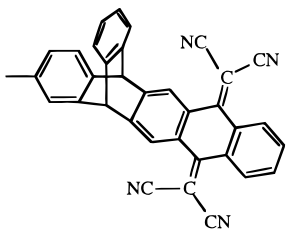

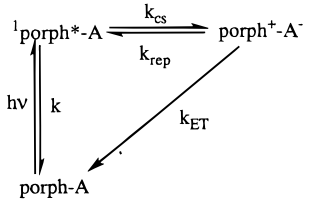

(148)

The free energy change for charge separation to give porph$^+$-A$^-$, $\Delta G°_{CS}$, is

$$\Delta G°_{cs} = \Delta G°_{ip} - E_s \quad (149)$$

$\Delta G°_{ip}$ is the free energy of the charge-separated state, porph$^+$-A$^-$, above the ground state. It was obtained by electrochemical measurements. E_s is the energy of the lowest porphyrin singlet state from fluorescence measurements. The driving force at which $\Delta G°_{CS} \sim 0$ was estimated by the onset of biphasic decay kinetics which gave $\lambda_{oo} \approx 0.80 \pm 0.05$ eV. With this value in hand, it was possible to fit k_{ET} to eq 24. k_{ET} reached a maximum at $\Delta G° = -0.6$ eV from which it was estimated that $\lambda_i + \lambda_{oi} \approx -\Delta G° = 0.6$ eV.

For back electron transfer in the inverted region in a rigid medium, it follows from eq 29 that

$$\ln k_{ET} \propto -\frac{\gamma(|\Delta G°_{fl} + \lambda_{oo})}{\hbar\omega} + \left(\frac{\gamma+1}{\hbar\omega}\right)k_B T(\lambda_{oi} + \lambda_{i,L}) \quad (150)$$

An increase in energy gap is predicted to decrease k_{ET} in frozen solution compared to the fluid. This effect has been observed both for electron transfer in eq 151 and nonradiative decay in eq 152.[517] The

$$[Re^{I}(4,4\text{-}(CO_2Et)_2bpy^{\bullet-})(CO)_3(py\text{-}PTZ^+)]^+ \rightarrow [Re^{I}(4,4\text{-}(CO_2Et)_2bpy)(CO)_3(py\text{-}PTZ)]^+ \quad (151)$$

$$[Re^{II}(4,4\text{-}(NH_2)_2bpy)(CO)_3(MQ^{\bullet})]^{2+*} \rightarrow [Re^{I}(4,4\text{-}(CO_2Et)_2bpy)(CO)_3(MQ^+)]^{2+} \quad (152)$$

rate constants for both are decreased by ~40 in PMMA compared to CH_3CN because of the frozen medium effect. In PMMA the energy gap is increased by $\lambda_{oo,2}$ (eq 141) relative to a fluid with comparable dielectric properties.

C. Interconversion between Excited States

The dynamical rigid medium effect can also inhibit interconversion between different excited states of the same molecule. Examples were cited in section IV.F involving ligand-localized and MLCT excited states in *fac*-$[Re(3\text{-benzoylpyridine})_2(CO)_3X]$ ($X = Cl^-$, Br^-, I^-) and *fac*-$[Re(phen)(CO)_3(CH_3CN)]^+$. In these complexes, emission was observed from both ligand-localized and MLCT states in EPA glasses but only from the MLCT state in the fluid. The MLCT state lies lower in either medium.

As for nonradiative decay to the ground state, section II.F.2, these interconversions involve transitions between different electronic states of the same molecule. Interconversion between them involves a change in electronic distribution rather than electron

transfer. It is induced by "promoting modes" which mix the electronic wave functions of the two states and cause the transition.

As for electron transfer, the medium is coupled to the transition if there is a change in polarization. In a glass or frozen solution, λ_{oo} becomes part of the driving force (eq 143), which increases the free energy of activation (eq 144). The change in solvent polarization between states appears in eq 146 by the difference, $\Delta\lambda_{oo} = \lambda_{oo,2} - \lambda_{oo,1}$. This quantity can either decrease or increase the driving force, ΔG°_{fr}, depending on the relative magnitudes of $\lambda_{oo,1}$ and $\lambda_{oo,2}$.

For a $\pi\pi^* \rightarrow$ MLCT transition, $\pi^1 d\pi^6\pi^{*1} \rightarrow \pi^2 d\pi^5\pi^{*1}$, $\lambda_{oo,2} > \lambda_{oo,1}$, and $\Delta\lambda_{oo} > 0$. There is an increase in reorganizational energy because λ_o varies with the square of the dipole moment (eq 92) and $|\vec{\mu}_{MLCT}| > |\vec{\mu}_{\pi\pi^*}|$. This increases ΔG°_{fr} over ΔG°_{fl} and ΔG^{*}_{fr} over ΔG^{*}_{fl} increasing the barrier in the rigid medium. This explains why both MLCT and $\pi\pi^*$ emissions are observed in the glass for *fac*-[Re(3-benzoylpyridine)$_2$(CO)$_3$X] (X = Cl$^-$, Br$^-$, I$^-$) and *fac*-[Re(phen)(CO)$_3$(CH$_3$CN)]$^+$ even though MLCT is lowest lying. In the fluid ΔG^* is decreased ($\Delta G^{*}_{fr} > \Delta G^{*}_{fl}$) and the interconversion is rapid.

This analysis predicts that if the order of the excited states is reversed, nπ^* or $\pi\pi^* <$ MLCT, the opposite situation should hold. The rate constant for MLCT $\rightarrow \pi\pi^*$ interconversion should *increase* in a rigid medium. There is experimental evidence that this is the case. In *fac*-[Re(dppz)(CO)$_3$Cl] the ordering of excited states is $\pi\pi^* <$ MLCT. This complex is an MLCT emitter in fluid solution, but there is no evidence for MLCT emission in the glass. Similarly, *fac*-[Re(4-phenylpyridine)$_2$(CO)$_3$Cl] in 2-propanol or EPA is an MLCT emitter in solution but a $\pi\pi^*$ emitter in the glass. In these cases MLCT excitation appears to be followed by rapid MLCT $\rightarrow \pi\pi^*$ interconversion, as predicted.

VII. Overview and Conclusions

In this review we have attempted to document a variety of charge-transfer phenomena and how they are influenced by the medium in which they occur. Some unusual effects exist, but there is a general framework for analyzing many of them, often quantitatively. The level of understanding is high, but much remains to be learned before the role of solvent (or the medium) is completely understood. As a way of summarizing the current level of understanding, generalizing our observations, and helping to point to future developments, we offer the following comments.

A general theoretical framework exists for understanding solvent effects (Section II). At the most fundamental level, it is based on time-dependent perturbation theory and the Golden rule (section II.C). It treats solvent effects in absorption, emission, electron transfer, and nonradiative decay in a quantitative manner with a common theoretical framework. The theory is independent of specific models used for the solvent, such as a dielectric continuum, but does rely on application of the Condon approximation and the separation of electron and nuclear coordinates in defining the barriers between states. It is *not* applicable to cases where the solvent is coupled strongly to internal electronic structure which differs between states, section III.D.3 and IV.C.

Parameters for spectral (absorption and emission) and dynamical (electron transfer and nonradiative decay) processes are related when they occur between the same states. The same vibrations and solvent modes are coupled to the transitions. This allows spectral parameters, or combinations of spectral parameters and ΔG°, to be used to calculate relative or absolute rate constants for electron transfer or nonradiative decay and their temperature dependences.

The relationships, $E_{abs} = \Delta G^{\circ} + \lambda$, $E_{em} = \Delta G^{\circ} - \lambda$, are fundamental but accurate only for Gaussian bands in the classical limit. ΔG° is the correct energy quantity in these relationships but only if temperature effects are dominated by the solvent with $\Delta\omega = |\omega - \omega'| \ll \omega,\omega'$ for low-frequency, collective solvent modes (section II.G.2). In general, absorption and emission band shapes are convolutions of overlapping vibronic components and absorption and emission maxima are complex functions of ΔG°, λ_o, S_j and $\hbar\omega_j$ for the coupled vibrations.

ΔG° and λ_o have different microscopic origins and different solvent and temperature dependences. This limits the fundamental insight gained by simple absorption and emission band measurements. It also limits the ability of solvent scales based on these measurements to provide fundamental insight.

There is still an open question as to whether the solvent reorganizational energies that appear in the simple band-shape equations are internal energy or free energy quantities. This is a point of fundamental importance that remains to be resolved.

In the absence of specific solvent effects, dielectric continuum theory does give an adequate accounting of the solvent dependences of ΔG° and λ_o which can be separated by spectral fitting. Application to specific cases relies on adoption of an appropriate dielectric cavity for the solute. A future direction should be implementing new procedures for modeling charge distributions and molecular geometries with more realistic models, perhaps based on procedures used to calculate surface charge distributions in proteins.

Initial results from molecular theories of the solvent are encouraging and calculationally accessible since solvent molecules past the first solvation layer can be modeled as a continuum (section III.A.2). Future developments will lead to further refinement but, hopefully, at not too great a cost in added mathematical complexity and without the loss of physically transparent models.

Specific-solvent effects arising from H-bonding or electron pair, donor−acceptor interactions tend to dominate the solvent dependence when they occur (Section III.C.D). They can shift absorption maxima by thousands of wavenumbers, change ΔG° for electron transfer by tens of kilocalories per mole, induce intramolecular electron transfer, and cause selective solvation. There is no general theory to explain these effects but in ammine or

cyano complexes they do correlate with the Gutmann donor or acceptor numbers. They are additive in the number of NH_3 or CN^- ligands and affect $\Delta G°$ and λ_o differently.

If specific-solvent effects dominate, there are important fundamental consequences. One is that the solvent is coupled to the internal electronic structure of the solute. This complicates the analysis of spectral band shapes because it mixes solvent and electronic coordinates, the Condon approximation is no longer valid, and λ_o is different for absorption and emission.

Continued theoretical work is required, hopefully resulting in physically transparent, parametrized theoretical models. They must incorporate specific interactions and their effects on internal electronic structure and changes that occur in electronic structure between states.

There is a continuing need for the development of models for collective solvent orientational modes and translational phonon-like modes and how they couple to electron transfer. Invoking collective harmonic motions and treating them quantum mechanically provides physically transparent models which are more intuitive than continuum models and introduces temperature effects and entropy in a satisfying way.

Medium dynamics play various roles in charge transfer depending on their time scales relative to charge transfer (section V.C). For electron transfer in the normal region, solvent reorganization is required, is an important part of the barrier, and can be limiting dynamically in the adiabatic limit. On ultrafast time scales, the medium relaxes to adjust to the charge distribution of the state that is newly formed causing time-dependent spectral shifts and nonexponential decays. In polymeric films or glass-to-fluid transitions, relaxation times are slower and, when coupled to excited-state decay, cause time-dependent shifts in emission spectra and nonexponential kinetics.

There are special effects in rigid media. In rigid media, the orientational part of λ_o becomes part of the driving force increasing $\Delta G°$, the electron-transfer barrier, and emission energies. In photoinduced electron transfer, the classical electron-transfer barrier can be increased or decreased compared to the fluid depending on the relative magnitudes of solvent reorganizational energies with the ground state. A related effect exists for excited-state interconversion.

For the experimentalist, all of this is satisfying. There is a useful theoretical framework which can explain a variety of phenomena and account for solvent and temperature effects. For the theoretician, much remains to be done. Continued advances and a close interplay between theory and experiment are required. More sophisticated models are needed and new formalisms which include coupling between solvent and electronic coordinates. The goal is to achieve a higher level of quantification based on physically transparent models which are quantitative without the loss of intuitive insight.

Acknowledgments are made to Department of Energy under grant DE-FG02-96ER14607 and the National Science Foundation under grant CHE-9321413 for support in the writing of this review.

VIII. References

(1) Dogonadze, R. R., Kalman, E., Kornyshev, A. A., Ulstrup, J., Eds. *The Chemical Physics of Solvation, Pt. A;* Elsevier Science Publishers B.V.: Amsterdam, 1985.
(2) Reichardt, C. *Solvent Effects in Organic Chemistry*, 2nd ed.; VCH Publisher: Weinheim, 1988.
(3) Ulstrup, J. *Charge-Transfer Processes in Condensed Media, Lecture Notes in Chemistry;* Springer-Verlag: New York, 1979; Vol. 10.
(4) Canon, R. D. *Electron-Transfer Reactions;* Butterworth: London, 1980.
(5) Taube, H. *Electron-Transfer Reactions in Solution;* Academic: New York, 1970.
(6) Marcus, R. A. *Annu. Rev. Phys. Chem.* **1966**, *15*, 155.
(7) Marcus, R. A. Commemorative Issue. *J. Phys. Chem.* **1986**, *90*, no.
(8) Marcus, R. A.; Sutin, N. *Biochim. Biophys. Acta* **1985**, *811*, 265.
(9) Hush, N. S. *Prog. Inorg. Chem.* **1967**, *8*, 391.
(10) Creutz, C. *Prog. Inorg. Chem.* **1983**, *30*, 1.
(11) Meyer, T. J.; Taube, H. In *Comprehensive Coordination Chemistry*; Wilkinson, G., Gillard, R. D., McCleverty, J. A., Eds.; Pergomman Press: London, 1987; Vol. 1, p 331.
(12) Sutin, N.; Brunschwig, B. S.; Creutz, C.; Winkler, J. R. *Pure Appl. Chem.* **1988**, *60*, 1817.
(13) Sutin, N. Creutz, C. *Pure Appl. Chem.* **1980**, *52*, 2717.
(14) Juri, A.; Barigelletti, F.; Campagna, S.; Balzani, V.; Belser, P.; von Zelewski, A. *Coord. Chem. Rev.* **1988**, *84*, 85.
(15) Libby, W. F. *J. Phys. Chem.* **1952**, *56*, 863.
(16) Basolo, F.; Pearson, R. G. *Mechanisms of Inorganic Reactions; a Study of Metal Complexes in Solution*; Wiley: New York, 1958.
(17) Lees, A. J. *Chem. Rev.* **1987**, *87*, 711.
(18) Balzani, V.; Juris, A.; Venturu, M.; Campagna, S.; Serroni, S. *Chem. Rev.* **1996**, *96*, 759.
(19) Geoffroy, G. L.; Wrighton, M. S. *Organometallic Photochemistry*; Academic Press: New York, 1979.
(20) Eisenberg, D.; Kauzmann, W. *The Structure and Properties of Water*; Oxford University Press: London, 1969; pp 242−245.
(21) Böttcher, C. J. F. *Theory of Electric Polarization*; Elsevier Publishing Co.: New York, 1952.
(22) Fröhlich, H. *Theory of Dielectrics*; Oxford University Press: Oxford, 1949.
(23) Cole, R. H. In *Molecular Liquids − Dynamics and Interactions*; Barnes, A. J., et al., Eds.; D. Reidel Publishing Co.: New York, 1984; pp 59−110.
(24) Marcus, R. A. *J. Chem. Phys.* **1956**, *24*, 979
(25) Gerschel, A. In *Molecular Liquids − Dynamics and Interactions*; Barnes, A. J. et al. eds; D. Reidel Publishing Co.: New York, 1984; p 163.
(26) Levich, V. *Adv. Electrochem. Electrochem. Eng.* **1966**, *4*, 249.
(27) Stratt, R. M. *Acc. Chem. Res.* **1995**, *28*, 201.
(28) Simon, J. D. *Acc. Chem. Res.* **1988**, *21*, 128.
(29) Davies, M. In *Dielectric Properties and Molecular Behavior*; Hill, N. E.; Vaughan, W. E., Price, A. H., Eds.; Van Nostrand Reinhold Co.: London, 1969.
(30) Garg, S. K.; Smyth, C. P. *J. Phys. Chem.* **1965**, *69*, 1294.
(31) Dogonadze, R. R.; Kuznetsov, A. M. *Prog. Surf. Sci.* **1975**, *6*, 1.
(32) Born, M.; Huang, K. *Dynamical Theory of Crystal Lattices*; Oxford University Press: London, 1954.
(33) Holstein, T. *Ann. Phys.* **1959**, *8*, 325; 343.
(34) Frohlich, H. *Adv. Phys.* **1954**, *3*, 325.
(35) For solvents that can form H-bonded clusters there are also higher frequency librations (section III.A.2).
(36) Zwanzig, R. *J. Stat. Phys.* **1973**, *9*, 215
(37) Stillinger, F. H.; Weber, T. A. *Science* **1984**, *225*, 983.
(38) Fried, L. E.; Mukamel, S. *Adv. Chem. Phys.* **1993**, *84*, 435.
(39) Voth, G. A.; Hochstrasser, R. M. *J. Phys. Chem.* **1996**, *100*, 13034.
(40) Tomasi, J.; Persico, M. *Chem. Rev.* **1994**, *94*, 2027.
(41) Billing, G. D.; Mikkelsen, K. V. *Advanced Molecular Dynamics and Chemical Kinetics*; Wiley: New York, 1997.
(42) Stratt, R. M.; Maroncelli, M. *J. Phys. Chem.* **1996**, *100*, 12981.
(43) Sutin, N. *Prog. Inorg. Chem.* **1983**, *30*, 441.
(44) Newton, M. D.; Sutin, N. *Annu. Rev. Phys. Chem.* **1984**, *35*, 437.
(45) Sutin, N. *Acc. Chem. Res.* **1982**, *15*, 275.
(46) Marcus, R. A. *Rev. Mod. Phys.* **1993**, *65*, 599.
(47) Hush, N. S. *Coord. Chem. Rev.* **1985**, *64*, 135.
(48) Barbara, P. F.; Meyer, T. J.; Ratner, M. A. *J. Phys. Chem.* **1996**, *100*, 13148.
(49) Marcus, R. A. *Discuss. Faraday Soc.* **1960**, *29*, 129.
(50) Noyes, R. M. *Prog. React. Kinet.* **1961**, *1*, 129.

(51) Meyer, T. J. *Prog. Inorg. Chem*. **1983**, *30*, 389.
(52) Eigen, M. *Z. Physik. Chem. [N.F.]* **1954**, *1*, 176.
(53) Eigen, M.; Maeyer, L. de In *Techniques of Organic Chemistry* 2nd ed.; Fries, S. L., Lewis, E. S., Weissberger, A., Eds., Wiley: New York, 1963; Vol. 8, Part 2, p 895.
(54) Fuoss, R. M. *J. Am. Chem. Soc.* **1958**, *80*, 5059.
(55) Petrucci, S. In *Ionic Interactions*; Petrucci, S., Ed.; Academic: New York, 1970; Vols I and II.
(56) Eigen, M.; Kruse, W.; Mauss, G.; Maeyer, D. L. *Prog. React. Kinet.* **1964**, *2*, 287.
(57) Debye, P. *Trans. Electrochem. Soc.* **1942**, *82*, 265
(58) Marcus, R. A. *J. Chem. Phys.* **1956**, *24*, 966.
(59) Marcus, R. A. *J. Chem. Phys.* **1957**, *26*, 867.
(60) Marcus, R. A. *J. Chem. Phys.* **1957**, *26*, 872.
(61) Marcus, R. A. *J. Chem. Phys.* **1965**, *43*, 679.
(62) Marcus, R. A. *Discuss. Faraday Soc.* **1960**, *29*, 21.
(63) Marcus, R. A. *Faraday Discuss. Chem Soc.* **1982**, *74*, 7.
(64) Hush, N. *Trans. Faraday Soc.* **1961**, *57*, 557.
(65) Hush, N. *Electrochim. Acta* **1968**, *13*, 1005.
(66) German, E. D.; Kuznetsov, A. M. *Electrochim. Acta* **1981**, *26*, 1595.
(67) Dogonadze, R. R.; Kuznetsov, A. M. In *Comprehensive Treatise of Electrochemistry*; Conway, B. E., Bockris. J. O. M., Yeager, E., Eds.; Plenum Press: New York, 1983; Vol. 7, p 1.
(68) Gutmann, V. *The Donor−Acceptor Approach to Molecular Interactions*, Plenum Press: New York, 1978.
(69) Tachiya, M. *J. Phys. Chem*. **1989**, *93*, 7050.
(70) Tachiya, M. *Chem. Phys. Lett.* **1989**, *159*, 505.
(71) Kakitani, T. *Trends Photochem. Photobiol.* **1991**, *2*, 349.
(72) Carter, E. A.; Hynes, J. T. *J. Phys. Chem*. **1989**, *93*, 2184.
(73) Marcus, R. A. *J. Phys. Chem*. **1989**, *93*, 3078.
(74) Alexander, M. K. *J. Phys. Chem*. **1992**, *96*, 3337.
(75) Brunschwig, B. S.; Creutz, C.; Macartney, D. H.; Sham, T.-K.; Sutin, N. *Faraday Discuss. Chem. Soc.* **1982**, *74*, 113.
(76) Newton, M. D. *Chem. Rev.* **1991**, *91*, 767.
(77) Sutin, N.; Brunschwig, B. S. In *Mechanistic Aspects of Inorganic Reactions*; Rorabacher, D. B., Endicott, J. F., Eds.; ACS Symp. Ser. 198, 1982; American Chemical Society: Washington, D.C., p 105.
(78) Dogonadze, R. R. In *Reaction of Molecules at Electrodes*; Hush, N. S., Ed.; Wiley: New York; Chapter 3.
(79) Weaver, M. J. *Chem. Rev.* **1992**, *92*, 463.
(80) Barbara, P. F.; Jarzeba, W. *Adv. Photochem*. **1990**, *15*, 1.
(81) Maroncelli, M. *J. Mol. Liquids* **1993**, *57*, 1.
(82) Calef, D. F.; Wolynes, P. G. *J. Phys. Chem*. **1983**, *87*, 3387.
(83) Heitele, H. *Angew. Chem., Int. Ed. Engl.* **1993**, *32*, 359.
(84) Jortner, J.; Bixon, M. *J. Chem. Phys.* **1988**, *88*, 167.
(85) Sumi, H.; Marcus, R. A. *J. Chem. Phys.* **1986**, *84*, 4894.
(86) Bagchi, B. *Annu. Rev. Phys. Chem*. **1989**, *40*, 115.
(87) Fleming, G. R.; Cho, M. *Annu. Rev. Phys. Chem*. **1996**, *47*, 109.
(88) Zusman, L D. *Chem. Phys.* **1988**, *119*, 51.
(89) Kosower, E. M.; Huppert, D. *Annu. Rev. Phys. Chem*. **1986**, *37*, 127.
(90) Morillo, M.; Cukier, R. I. *J. Chem. Phys.* **1988**, *89*, 6736.
(91) Carter, E. A.; Hynes, J. T. *J. Phys. Chem*. **1991**, *94*, 5961.
(92) Bixon, M.; Jortner, J. *Chem. Phys.* **1993**, *176*, 467.
(93) Huppert, D.; Ittah, V.; Masad, A.; Kosower, E. M. *Chem. Phys. Lett*. **1988**, *150*, 349.
(94) Simon, J. D.; Rossky, P. J. *Nature*, **1994**, *370*, 263.
(95) Weaver, M. J.; Phelps, D. K.; Nielson, R. M.; Golovin, M. N.; McManis, G. E. *J. Phys. Chem*. **1990**, *94*, 2949.
(96) Jimenez, R.; Fleming, G. R.; Kumar, P. V.; Maroncelli, M. *Nature* **1994**, *369*, 471.
(97) Yoshihara, K.; Tomonaga, K.; Nagasawa, Y. *Bull. Chem. Soc. Jpn*. **1995**, *68*, 696.
(98) Maroncelli, M.; MacInnis, J.; Fleming, G. R. *Science* **1989**, *243*, 1674.
(99) Ballhausen, C. J. *Molecular Electronic Structures of Transition Metal Complexes*; McGraw-Hill: New York, 1979.
(100) Steinfeld, J. I. *Molecules and Radiation*; The MIT Press: Cambridge, 1985.
(101) Jortner, J. *Philos. Mag*. **1979**, *B40*, 317.
(102) Jortner, J.; Bixon, M. *Ber. Bunsen-Ges. Phys. Chem*. **1995**, *99*, 296.
(103) Myers, A. B. *Chem. Phys.* **1994**, *180*, 215.
(104) Mataga, N.; Kubota, T. *Molecular Interactions and Electronic Spectra*; Marcel Dekker: New York, 1970; Chapter 3, p 107.
(105) Huang, K.; Rhys, A. *Proc. R. Soc*. **1950**, *A204*, 406.
(106) Kubo, R.; Toyozawa, Y. *Prog. Theor. Phys.* **1955**, *13*, 160.
(107) Lax, M. *J. Chem. Phys.* **1952**, *20*, 1752.
(108) DeVault, D. *Q. Rev. Biophys*. **1980**, *13*, 387.
(109) Wilson, E. B., Jr.; Decius, J. C.; Cross, P. C. *Molecular Vibrations*; Dover Publications, Inc.: New York, 1980.
(110) Cotton, F. A. *Chemical Applications of Group Theory*, 2nd ed.; Wiley: New York; 1971.
(111) Kestner, N. R.; Logan, J.; Jortner, J. *J. Phys. Chem*. **1974**, *78*, 2148.
(112) Jortner, J. *J. Chem. Phys*. **1976**, *64*, 4860.
(113) Bixon, M.; Jortner, J. *Faraday Discuss. Chem. Soc.* **1982**, *74*, 17.
(114) Siders, P.; Marcus, R. A. *J. Am. Chem. Soc.* **1981**, *103*, 741; 748.
(115) Marcus, R. A. *J. Chem. Phys*. **1984**, *81*, 4494.
(116) Islampour, R.; Lin. S. H. *J. Phys. Chem*. **1991**, *95*, 10261.
(117) Islampour, R.; Alden, R. G.; Wu, G. Y. C.; Lin. S. H. *J. Phys. Chem*. **1993**, *97*, 6793.
(118) De Vault, D. *Quantum Mechanical Tunneling in Biological Systems;* Cambridge University Press: Cambridge, 1984.
(119) Efrima, S.; Bixon, M. *Chem. Phys.* **1976**, *13*, 447.
(120) Ulstrup, J.; Jortner, J. *J. Chem. Phys.* **1975**, *63*, 4358.
(121) Weinstraub, O.; Bixon, M. *J. Phys. Chem*. **1994**, *98*, 3407.
(122) Marcus, R. A.; Sutin, N. *Comments Inorg. Chem*. **1986**, *5*, 119.
(123) Hupp, J.; Neyhart, G.; Meyer, T. J.; Kober, E. K. *J. Phys. Chem*. **1992**, *96*, 10820.
(124) Zasukha, V. A.; Volkov, S. V. *Int. J. Quantum Chem*. **1985**, *28*, 17.
(125) Chandler, D.; Kuharski, R. *Faraday Discuss. Chem. Soc.* **1988**, *85*, 329.
(126) Bader, J. S.; Kuharski, R. A.; Chandler, D. *J. Chem. Phys.* **1990**, *93*, 230.
(127) Kuharski, R. A.; Bader, J. S.; Chandler, D. Sprik, M.; Klein, M. L.; Impey, R. W. *J. Chem. Phys.* **1988**, *89*, 3248.
(128) Brunschwig, B. S.; Logan, J.; Newton, M. D.; Sutin, J. *J. Am. Chem. Soc.* **1980**, *102*, 5798.
(129) Temble, B. L.; Friedman, H. L.; Newton, M. D. *J. Chem. Phys.* **1982**, *76*, 1490.
(130) Friedman, H. L.; Newton, M. D. *Faraday Discuss. Chem. Soc.* **1982**, *74*, 73.
(131) Brunschwig, B. S.; Sutin, N. *Comments Inorg. Chem* **1987**, *6*, 209.
(132) Burshtein, A. I.; Frantsuzov, P. A.; Zharikov, A. A. *J. Chem. Phys.* **1992**, *96*, 4261.
(133) Gehlen, J. N.; Chandler, D. *J. Chem. Phys.* **1992**, *97*, 4958.
(134) Kober, E. M.; Caspar, J. V.; Lumpkin, R. S.; Meyer, T. J. *J. Phys. Chem*. **1986**, *90*, 3722.
(135) Freed, K. M.; Jortner, J. *J. Chem. Phys.* **1970**, *52*, 6272.
(136) Zharikov, A. A.; Sherer, P. O. J.; Fisher, S. F. *J. Phys. Chem*. **1994**, *98*, 3424.
(137) Nadler, W.; Marcus, R. A. *J. Chem. Phys.* **1987**, *86*, 3906.
(138) Walker, G. C.; Akesson, E.; Jonhson, A. E.; Levinger, N. E.; Barbara, P. F. *J. Phys. Chem*. **1992**, *96*, 3728.
(139) Chen, P.; Meyer, T. J. *Inorg. Chem*. **1996**, *35*, 5520.
(140) Chen, P.; Danielson, E.; Meyer, T. J. *J. Phys. Chem*. **1988**, *92*, 3708.
(141) Lumpkin, R. S.; Meyer, T. J. *J. Phys. Chem*. **1986**, *90*, 5307.
(142) Brunschwig, B. S.; Ehrenson, S.; Sutin, N. *J. Am. Chem. Soc.* **1984**, *106*, 6858.
(143) Marcus, R. A.; Siders, P. *J. Phys. Chem*. **1982**, *86*, 622.
(144) Strickler, S. J.; Berg, R. A. *J. Chem. Phys*. **1962**, *37*, 814.
(145) Birks, J. B.; Dyson, D. J. *Proc. R. Soc. London, A* **1963**, *275*, 135.
(146) Lin, S, H. *Radiationless Transitions*; Academic: New York, 1980.
(147) Bixon, M.; Jortner, J.; Cortes, J.; Heitele, H.; Michel-Beyerle, M. E. *J. Phys. Chem*. **1994**, *98*, 7298.
(148) Avouris, P.; Gelbart, W. M.; El-Sayed, M. A. *Chem. Rev*. **1977**, *77*, 793.
(149) Heller, E. J.; Brown, R. C. *J. Chem. Phys*. **1983**, *79*, 3336.
(150) Freed, K. F. *Acc. Chem. Res.* **1978**, *11*, 74.
(151) Robinson, G. W.; Frosch, R. P. *J. Chem. Phys*. **1962**, *37*, 1962.
(152) Robinson, G. W.; Frosch, R. P. *J. Chem. Phys*. **1963**, *38*, 1187.
(153) Bixon, M.; Jortner, J. *J. Chem. Phys*. **1968**, *48*, 715.
(154) Englman, R.; Jortner, J. *Mol. Phys*. **1970**, *18*, 145.
(155) Freed, K. F. *Top. Curr. Chem*. **1972**, *31*, 65.
(156) Lin, S, H. *J. Chem. Phys*. **1966**, *44*, 3759.
(157) Siebrand, W. *J. Chem. Phys*. **1967**, *46*, 440.
(158) Siebrand, W. *J. Chem. Phys*. **1971**, *55*, 5843.
(159) Gillipsie, G. P.; Lim, E. C. *Chem. Phys. Lett*. **1979**, *63*, 193.
(160) Griesser, H. J.; Wild, U. P. *Chem. Phys*. **1980**, *52*, 117.
(161) Dinur, U.; Scharf, B. *J. Chem. Phys*. **1983**, *79*, 2600.
(162) Macierjewski, A.; Safarzadeh-Amiri, A.; Verrall, R. E.; Steer, R. P. *Chem. Phys*. **1984**, *87*, 295.
(163) Horrocks, Jr. W. D.; Albin, M. *Prog. Inorg. Chem*. **1984**, *31*, 1.
(164) Haas, Y.; Stein, G. *J. Phys. Chem*. **1972**, *76*, 1093.
(165) Stein, G.; Wurzberg, E. *J. Chem. Phys*. **1975**, *62*, 208.
(166) Worl, L. A.; Duesing, R.; Chen, P.; Ciana, L. D.; Meyer, T. J. *J. Chem. Dalton Trans*. **1991**, 849.
(167) Caspar. J. V.; Meyer, T. J. *J. Phys. Chem*. **1983**, *87*, 952.
(168) Caspar, J. V.; Sullivan, B. P.; Kober, E. M.; Meyer, T. J. *Chem. Phys. Lett*. **1982**, *91*, 91.
(169) Vining, W. J.; Caspar, J. V.; Meyer, T. J. *J. Phys. Chem*. **1985**, *89*, 1095.
(170) Caspar, J. V.; Meyer, T. J. *J. Am. Chem. Soc.* **1983**, *105*, 5583.
(171) Yoon, D. I.; Berg-Brennan, C. A.; Lu, H.; Hupp, J. T. *Inorg. Chem*. **1992**, *31*, 3192.
(172) Paulson, S.; Sullivan, B. P.; Caspar, J. V. *J. Am. Chem. Soc.* **1992**, *114*, 6905.
(173) Brunschwig, B. S.; Ehrenson, S.; Sutin, N. *J. Phys. Chem*. **1987**, *91*, 4714.

(174) Tutt, L.; Tannor, D.; Schindler, J.; Heller, E. J. *J. Phys. Chem.* **1983**, *87*, 3017.
(175) Heller, E. J. *Acc. Chem. Res.* **1981**, *14*, 368.
(176) Tannor, D.; Heller, E. J. *J. Chem. Phys.* **1982**, *77*, 202.
(177) Heller, E. J.; Sundberg, R. L.; Tannor, D. *J. Phys. Chem.* **1982**, *86*, 1822.
(178) Zink, J. I.; Shin, K.-C. K. *Adv. Photochem.* **1991**, *16*, 119.
(179) Spears, K. G. *J. Phys. Chem.* **1995**, *99*, 2469.
(180) Coalson, R. D.; Evans, D. G.; Nitzan, A. *J. Phys. Chem.* **1994**, *101*, 436.
(181) Todd. M. D.; Nitzan, A.; Ratner, M. A.; Hupp, J. T. *J. Photochem. Photobiol. A* **1994**, *82*, 87.
(182) Lu, H.; Petrov, V.; Hupp, J. T. *Chem. Phys. Lett.* **1995**, *235*, 521.
(183) Doorn, S. K.; Blackbourn, R. L.; Johnson, C. S.; Hupp, J. T. *Electrochim. Acta* **1991**, *36*, 1775.
(184) Shin, K. S.; Zink, J. I. *J. Am. Chem. Soc.* **1990**, *112*, 7148.
(185) Kulinowski, K.; Gould, I. R.; Myers, A. B. *J. Phys. Chem.* **1995**, *99*, 9017.
(186) Reichardt, C. *Angew. Chem., Int. Ed. Engl.* **1979**, *18*, 98
(187) Reichardt, C. *Chem. Soc. Rev.* **1992**, 148.
(188) Buncel, E.; Rajagopal, S. *Acc. Chem. Res.* **1990**, *23*, 226.
(189) Rettig, W. *Ber. Bunsen-Ges. Phys. Chem.* **1991**, *95*, 259
(190) Sone, K.; Fukuda, Y. *Rev. Inorg. Chem.* **1991**, *11*, 123.
(191) Schmid. R. *Rev. Inorg. Chem.* **1991**, *11*, 255.
(192) Marcus, Y. *Chem. Soc. Rev.* **1993**, 409.
(193) Drago, R. S.; Kovala-Demertzi, D.; Ferris, D. C. *J. Coord. Chem.* **1994**, *32*, 145.
(194) Drago, R. S.; Hirsh, M. S.; Ferris, D. C. Chronister, C. W. *J. Chem. Soc., Perkin Trans* 2, **1994**, 219.
(195) Drago, R. S.; Ferris, D. C. *J. Phys. Chem.* **1995**, *99*, 6563.
(196) Kosower, E. M. *J. Am. Chem. Soc.* **1958**, *80*, 3253.
(197) Kosower, E. M.; Mohammad, M. *J. Am. Chem. Soc.* **1971**, *93*, 2713.
(198) Brown, D. B., ed. *Mixed Valence Compounds;* D. Reidel Publishing Co.: Dordrecht, 1980.
(199) Prassides, K., ed. *Mixed Valence Systems: Applications in Chemistry, Physics and Biology;* Kluwer Academic Publisher: Dordrecht, The Netherlands, 1990.
(200) Creutz, C.; Taube, H. *J. Am. Chem. Soc.* **1969**, *91*, 3988.
(201) Taube, H. *Pure Appl. Chem.* **1976**, *44*, 25.
(202) Richardson, D. E.; Taube, H. *J. Am. Chem. Soc.* **1983**, *105*, 40.
(203) Richardson, D. E.; Taube, H. *Coord. Chem. Rev.* **1984**, *60*, 107.
(204) Powers, M. J.; Salmon, D. J.; Callahan, R. W.; Meyer, T. J. *J. Am. Chem. Soc.* **1976**, *98*, 6731.
(205) Callahan, R. W.; Meyer, T. J. *Chem. Phys. Lett.* **1976**, *39*, 82.
(206) Callahan, R. W.; Keene, R. F.; Meyer, T. J.; Salmon, D. J. *J. Am. Chem. Soc.* **1977**, *99*, 1064.
(207) Powers, M. J.; Meyer, T. J. *J. Am. Chem. Soc.* **1980**, *102*, 1289.
(208) Meyer, T. J. *Acc. Chem. Res.* **1978**, *11*, 94.
(209) Creutz, C.; Newton, M. D.; Sutin, N. *J. Photochem. Photobiol. A: Chem.* **1994**, *82*, 47.
(210) Doorn, S. K.; Hupp, J. T. *J. Am. Chem. Soc.* **1989**, *111*, 1142.
(211) Doorn, S. K.; Hupp, J. T. *J. Am. Chem. Soc.* **1989**, *111*, 4704.
(212) Creutz, C.; Taube, H. *J. Am. Chem. Soc.* **1973**, *95*, 1086.
(213) Eggleston, D. S.; Goldsby, K. A.; Hodgson, D. J.; Meyer, T. J. *Inorg. Chem.* **1985**, *24*, 4573.
(214) Kober, E. M.; Goldsby, K. A.; Narayana, D. N. S.; Meyer, T. J. *J. Am. Chem. Soc.* **1983**, *105*, 4303.
(215) Schoonover, J. R.; Timpson, C. J.; Meyer, T. J.; Bignozzi, C. A. *Inorg. Chem.* **1992**, *31*, 3185.
(216) Goodman. B. A.; Raynor, J. B. *Adv. Inorg. Radiochem.* **1970**, *13*, 192.
(217) Powers, M. J.; Meyer, T. J. *J. Am. Chem. Soc.* **1978**, *100*, 4393.
(218) Lowery, M. D.; Hammack, W. S.; Drickamer, H. G.; Hendrickson, D. N. *J. Am. Chem. Soc.* **1987**, *109*, 8019.
(219) Dong, T.; Kanbara, T.; Hendrickson, D. N. *J. Am. Chem. Soc.* **1986**, *108*, 4423.
(220) McManis, G. E.; Gochev, A.; Nielson, R. M.; Weaver, M. J. *J. Phys. Chem.* **1989**, *93*, 7733.
(221) Brunschwig, B. S.; Ehrenson, S.; Sutin, N. *J. Phys. Chem.* **1986**, *90*, 3657.
(222) Tom, G. M.; Creutz, C.; Taube, H. *J. Am. Chem. Soc.* **1974**, *96*, 7828.
(223) Creutz, C. *Inorg. Chem.* **1978**, *17*, 3723.
(224) Hupp, J. T.; Meyer, T. J. *Inorg. Chem.* **1987**, *26*, 2332.
(225) Hupp, J. T.; Weydert, J. *Inorg. Chem.* **1987**, *26*, 2657.
(226) Blackbourn, R. L.; Hupp, J. T. *J. Phys. Chem.* **1988**, *92*, 2817.
(227) Hupp, J. T.; Dong, Y.; Blackbourn, R. L.; Lu, H. *J. Phys. Chem.* **1993**, *97*, 3278.
(228) Oh, O.; Boxer, S. G. *J. Am. Chem. Soc.* **1990**, *112*, 8161.
(229) Oh, D. H.; Sano, M.; Boxer, S. G. *J. Am. Chem. Soc.* **1991**, *113*, 6880.
(230) Reimers, J. R.; Hush, N. S. *J. Phys. Chem.* **1991**, *95*, 9773.
(231) In equivalent coordination environments, the $Ru^{III/II}$ couples are more positive than $Os^{III/II}$ by ~0.4 V.
(232) Goldsby, K. A.; Meyer, T. J. *Inorg. Chem.* **1984**, *23*, 3002.
(233) Sullivan, B. P.; Curtis, J. C.; Kober, E. M.; Meyer, T. J. *Nouv. J. Chim.* **1980**, *4*, 643.
(234) Chang, J. P.; Fung, E. Y.; Curtis, J. C. *Inorg. Chem.* **1986**, *25*, 4233.
(235) Hudis, J.; Dodson, R. W. *J. Am. Chem. Soc.* **1956**, *78*, 911.
(236) Guarr, T.; Buhks, E.; McLendon, G. *J. Am. Chem. Soc.* **1983**, *105*, 3763.
(237) Van Houten, J.; Watts, R. J. *J. Am. Chem. Soc.* **1975**, *97*, 3843.
(238) Hupp, J. T.; Meyer, T. J. *J. Phys. Chem.* **1987**, *91*, 1001.
(239) Ulstrup, J. *J. Phys. Chem.* **1987**, *91*, 5153.
(240) Matyushov, D.; Schmid, R. *J. Phys. Chem.* **1994**, *98*, 5152.
(241) Matyushov, D. *Mol. Phys.* **1993**, *79*, 795.
(242) Matyushov, D. *Chem. Phys.* **1993**, *174*, 199.
(243) Blackbourn, R. L.; Hupp, J. T. *Chem. Phys. Lett.* **1988**, *150*, 399.
(244) Hupp, J. T. *Inorg. Chem.* **1990**, *29*, 5010.
(245) Blackbourn, R. L.; Hupp, J. T. *J. Phys. Chem.* **1990**, *94*, 1788.
(246) Lewis, N. A.; Obeng, Y. S. *J. Am. Chem. Soc.* **1988**, *110*, 2306.
(247) Kuznetsov. A. M.; Phelps, D. K.; Weaver, M. J. *Int. J. Kinet.* **1990**, *22*, 815.
(248) Lau, K. W.; Hu, A. M.; Yen, M. H.; Fung, E. Y.; Grzybicki, S.; Matamoros, R.; Curtis, J. C. *Inorg. Chim. Acta* **1994**, *226*, 137.
(249) Liptay, W. *Angew. Chem., Intl. Ed.* **1969**, *8*, 177.
(250) Mataga, N.; Kaifu, Y.; Koizumi, *Bull. Chem. Soc. Jpn.* **1956**, *29*, 465.
(251) Marcus, R. A. *J. Chem. Phys.* **1965**, *43*, 1261.
(252) Ooshika, Y. *J. Phys. Soc. Jpn.* **1954**, *9*, 594.
(253) Lippert, E. *Z. Naturforsch., A.* **1955**, *10A*, 541.
(254) Lippert, E. *Z. Elektrochem.* **1957**, *61*, 962.
(255) Bayliss, N. S.; McRae, E. G. *J. Chem. Phys.* **1954**, *58*, 1002.
(256) McRae, E. G. *J. Phys. Chem.* **1957**, *61*, 562.
(257) Rettig, W. *Ber. Bunsen-Ges. Phys. Chem.* **1991**, *95*, 259.
(258) Liptay, W.; Walz, G. *Z. Naturforsch.* **1971**, *26A*, 2007.
(259) Nicol, M. F. *Appl. Spectrosc. Rev.* **1974**, *8*, 183.
(260) Suppan, P. *J. Photochem. Photobiol, A: Chemistry*, **1990**, *50*, 293.
(261) Lutskii, A. E.; Prezhdo, V. V.; Degtereva, L. I.; Gordienko, V. G. *Russ. Chem. Rev.* **1982**, *51*, 802.
(262) Kirkwood, J. G.; Westheimer, F. H. *J. Chem. Phys.* **1938**, *6*, 506.
(263) Kober, E. M.; Sullivan, B. P. Meyer, T. J. *Inorg. Chem.* **1984**, *23*, 2098.
(264) Milder, S. J. *Inorg. Chem.* **1989**, *28*, 868.
(265) Timpson, C. J.; Bignozzi, C. A.; Sullivan, B. P.; Kober, E. M.; Meyer, T. J. *J. Phys. Chem.* **1996**, *100*, 2915.
(266) Oh, D. H.; Boxer, S. G. *J. Am. Chem. Soc.* **1990**, *111*, 1130.
(267) Dallinger, R. F.; Woodruff, W. H. *J. Am. Chem. Soc.* **1979**, *101*, 4391.
(268) Bradley, P. G.; Kress, N.; Hornberger, B. A.; Dallinger, R. F.; Woodruff, W. H. *J. Am. Chem. Soc.* **1981**, *103*, 7441.
(269) For a review on $[Ru(bpy)_3]^{2+}$, see: Krausz. E.; Ferguson, J. *Prog. Inorg. Chem.* **1989**, *37*, 293.
(270) Omberg, K. M.; Schoonover, J. R.; Treadway, J. A.; Leasure, R. M.; Dyer, R. B.; Meyer, T. J. *J. Am. Chem. Soc.* **1997**, *119*, 7013.
(271) Nicol, M.; Swain, J.; Shum, Y. Y.; Merin, R.; Chen, R. H. H. *J. Chem. Phys*, **1968**, *48*, 3587.
(272) Nicol, M.; Wild, S. M.; Yancey, J. *J. Chem. Phys.* **1973**, *58*, 4350.
(273) Sullivan, B. P. *J. Phys. Chem.* **1989**, *93*, 24
(274) Ali, R.; B.; Banerjee, P.; Burgess, J. Smith, A. E. *Transition Met. Chem.* **1988**, *13*, 107.
(275) Ali, R.; B.; Banerjee, P.; Burgess, J. Smith, A. E. *Transition Met. Chem.* **1981**, *6*, 145.
(276) Manuta, D. M.; Lees, A., Jr. *Inorg. Chem.* **1983**, *22*, 3825.
(277) Manuta, D. M.; Lees, A., Jr. *Inorg. Chem.* **1986**, 25, 3212.
(278) Zulu, M. M.; Lees, A., Jr. *Inorg. Chem.* **1988**, *27*, 1139.
(279) Lever, A. B. P. *Inorganic Electronic Spectroscopy;* Elsivier: Amsterdam, 1984; p 208.
(280) Kaim, W.; Kohlmann, S.; Ernst, S.; Olbrich-Deussner, B.; Bessenbacher, C.; Schulz, A. *J. Organometallic Chem.* **1987**, *321*, 215.
(281) Kaim, W.; Kohlmann, S. *Inorg. Chem.* **1986**, *25*, 3306.
(282) Daamen, H.; Stufkens, D. J.; Oskam, A. *Inorg. Chim. Acta* **1980**, *39*, 25.
(283) Haga, M.; Koizumi, K. *Inorg. Chim. Acta* **1985**, *104*, 47.
(284) Dodsworth, E. S.; Lever, A. B. P. *Coord. Chem. Rev.* **1990**, *97*, 271.
(285) Dodsworth, E. S.; Lever, A. B. P. *Inorg. Chem.* **1990**, *29*, 499.
(286) Perng, B.-C.; Newton, M. D.; Raineri, F. O.; Friedman, H. L. *J. Chem. Phys.* **1996**, *104*, 7153.
(287) Perng, B.-C.; Newton, M. D.; Raineri, F. O.; Friedman, H. L. *J. Chem. Phys.* **1996**, *104*, 7177.
(288) Kjær, A. M.; Kristjansson, I.; Ulstrup, J. *J. Electroanal. Chem.* **1986,** *204*, 45.
(289) Kjær, A. M.; Ulstrup, J. *J. Am. Chem. Soc.* **1987,** *109*, 1934.
(290) Curtis, J. C.; Sullivan, B. P.; Meyer, T. J. *Inorg. Chem.* **1983**, *22*, 224.
(291) Lay, P. A. *J. Phys. Chem.* **1986**, *90*, 878.
(292) Hupp, J. T.; Weaver, M. J. *Inorg. Chem.* **1984**, *23*, 3639.
(293) Hupp, J. T.; Weaver, M. J. *J. Phys. Chem.* **1985**, *89*, 1601.
(294) Doorn, S. K.; Hupp, J. T. *J. Am. Chem. Soc.* **1989**, *111*, 4704.
(295) Ford, P. C.; Rudd, D. P.; Gaunder, R.; Taube, H. *J. Am. Chem. Soc.* **1968**, *90*, 1187.
(296) Malouf, G.; Ford, P. C. *J. Am. Chem. Soc.* **1977**, *99*, 7213.

(297) Winkler, J. R.; Netzel, T. L.; Creutz, C.; Sutin, N. *J. Am. Chem. Soc.* **1987**, *109*, 2381.
(298) Ford, P. C.; Wink, D.; DiBenedetto, T. *Prog. Inorg. Chem.* **1983**, *30*, 213.
(299) Crosby, G. A.; Watts, R. J.; Carstens, D. H. W. *Science* **1970**, *170*, 1195.
(300) Meyer, T. J. Ph.D. Dissertation, Stanford University, 1966.
(301) Stravrev, K. K.; Zerner, M. C.; Meyer, T. J. *J. Am. Chem. Soc.* **1995**, *117*, 8684.
(302) Karelson, M. M.; Zerner, M. C. *J. Phys. Chem.* **1992**, *96*, 6949.
(303) Zerner, M. C. *ZINDO-95 program*; Quantum Theory Project, University of Florida: Gainsville, FL.
(304) Zerner, M. C.; Loew, G. H.; Kirshner, R. F.; Muller-Westerhoff, U. T. *J. Am. Chem. Soc.* **1980**, *102*, 589.
(305) Ridler, J. E.; Zerner, M. C. *Theor. Chim. Acta* **1973**, *32*, 111.
(306) Bacon, A. D.; Zerner, M. C. *Theor. Chim. Acta* **1979**, *53*, 21.
(307) Zeng, J.; Hush, N. S.; Reimers, J. R. *J. Phys. Chem.* **1995**, *99*, 10459.
(308) Zeng, J.; Hush, N. S.; Reimers, J. R. *J. Phys. Chem.* **1996**, *100*, 19292.
(309) Zeng, J.; Hush, N. S.; Reimers, J. R. *J. Am. Chem. Soc.* **1996**, *118*, 2059.
(310) Broo, A.; Larsson, S. *Chem. Phys.* **1992**, *161*, 363.
(311) Creutz, C.; Chou, M. H. *Inorg. Chem.* **1987**, *26*, 2995.
(312) Chou, M. H.; Creutz, C.; Sutin, N. *Inorg. Chem.* **1992**, *31*, 2318.
(313) Balzani, V.; Sabbatini, N.; Scadola, F. *Chem. Rev.* **1986**, *86*, 319.
(314) Klassen, D. M.; Crosby, G. A. *J. Chem. Phys.* **1968**, *48*, 1853.
(315) Bignozzi, C. A.; Chioboli, C.; Indelli, M. T.; Rampi Scandola, M. A.; Scandola, F. *J. Am. Chem. Soc.* **1986**, *108*, 7872.
(316) Belser, P.; von Zelewsky, A.; Juris, A.; Barigelletti, F.; Balzani, V. *Gazz. Chim. Ital.* **1985**, *115*, 723.
(317) Fung, E. Y.; Chua, A. C. M.; Curtis, J. C. *Inorg. Chem.* **1988**, *27*, 1294.
(318) Kitamura, N.; Sato, M.; Kim, H.-B. Obata, R.; Tazuke, S. *Inorg. Chem.* **1988**, *27*, 651.
(319) Winkler, J. R.; Sutin, N. *Inorg. Chem.* **1987**, *26*, 220.
(320) Bignozzi, C. A.; Scandola, F. *Inorg. Chem.* **1984**, *23*, 1540.
(321) Demas, J. N.; Peterson, S. H.; Harris, E. W. *J. Phys. Chem.* **1977**, *81*, 1039.
(322) Leasure, R. M.; Sacksteder, L.; Nesselrodt, D.; Reitz, G. A.; Demas, J. N.; DeGraff, B. A. *Inorg. Chem.* **1991**, *30*, 3722.
(323) Hupp, T. J.; Neyhart, G. A.; Meyer, T. J. *J. Am. Chem. Soc.* **1986**, *108*, 5349.
(324) Hupp, T. J.; Kober, E. M.; Heyhart, G. A.; Meyer, T. J. In *Mixed-Valence Systems: Applications in Chemistry, Physics and Biology*; Kluwer Acadamic Publishers: Netherlands; p 51.
(325) Neyhart, G. A.; Hupp, J. T.; Curtis, J. C.; Timpson, C. J.; Meyer, T. J. *J. Am. Chem. Soc.* **1996**, *118*, 3724.
(326) Neyhart, G. A.; Timpson, C. J.; Bates, W. D.; Meyer, T. J. *J. Am. Chem. Soc.* **1996**, *118*, 8, 3730.
(327) Curtis, J. C.; Roberts, J. A.; Blackbourn, R. L.; Dong, Y.; Massum, M.; Johoson, C. S.; Hupp, J. T. *Inorg. Chem.* **1991**, *30*, 3856.
(328) Blackbourn, R. L.; Hupp, J. T. *Inorg. Chem.* **1989**, *28*, 3786.
(329) Ennix, K. S.; McMahon, P. T.; Rosa, R.; Curtis, J. C. *Inorg. Chem.* **1987**, *26*, 2660.
(330) Curtis, J. C.; Blackbourn, R. L.; Ennix, K. S.; Hu, S.; Roberts, J. A.; Hupp, J. T. *Inorg. Chem.* **1989**, *28*, 3791.
(331) Katriel, J.; Ratner, M. A. *J. Phys. Chem.* **1989**, *93*, 5065.
(332) Todd, M. D.; Dong, Y.; Hupp, T. J. *Inorg. Chem.* **1991**, *30*, 4685.
(333) Todd, M. D.; Dong, Y.; Horney, J.; Yoon, D. I.; Hupp, T. J. *Inorg. Chem.* **1993**, *32*, 2001.
(334) Ando, I.; Ishimura, D.; Mitrumi, M.; Ujimoto, K.; Kurihara, H. *Polyhedron*, **1992**, *11*, 2335.
(335) Ando, I.; Ishimura, D.; Ujimoto, K.; Kurihara, H. *Inorg. Chem.* **1994**, *33*, 5010.
(336) Dong, Y.; Hupp, T. J. Yoon, D. I. *J. Am. Chem. Soc.* **1993**, *115*, 4379.
(337) Colquhoun, H. M.; Stoddart, J. F.; Williams, D. J. *Angew. Chem., Int. Ed. Engl.* **1986**, *25*, 487.
(338) Zhang, X. L.; Kankel, C. R.; Hupp, J. T. *Inorg. Chem.* **1994**, *33*, 4738.
(339) Hupp, J. T.; Dong, Y. *Inorg. Chem.* **1994**, *33*, 4421.
(340) Nielson, R. M.; Hupp, J. T. *Inorg. Chem.* **1996**, *35*, 1402.
(341) Nielson, R. M.; Hupp, J. T. *J. Am. Chem. Soc.* **1995**, *117*, 9085.
(342) Nielson, R. M.; Lyon, L. A.; Hupp, J. T. *Inorg. Chem.* **1996**, *35*, 970.
(343) Zhang, L. T.; Ko, J.; Ondrechen, M. J. *J. Am. Chem. Soc.* **1987**, *109*, 1666.
(344) Ko, J.; Ondrechen, M. J. *J. Am. Chem. Soc.* **1985**, *107*, 6161.
(345) Root, L. J.; Ondrechen, M. J. *Chem. Phys. Lett.* **1982** *93*, 421.
(346) Ondrechen, M. J.; Gozashoti, S.; Zheng, L. T.; Zhou, F. *Adv. Chem. Ser.* **1990**, *226*, 225.
(347) Piepho, S. B. *J. Am. Chem. Soc.* **1988**, *110*, 6319
(348) Piepho, S. B. *J. Am. Chem. Soc.* **1990**, *112*, 4197
(349) Roberts, J. A.; Hupp, J. T. *Inorg. Chem.* **1992**, *31*, 157.
(350) Wong, K. Y.; Schatz, P. N. *Prog. Inorg. Chem.* **1981**, *28*, 369.
(351) Robin, M. B.; Day, P. *Adv. Inorg. Chem. Radiochem.* **1967**, *10*, 247.
(352) Day, P. *Int. Rev. Phys. Chem.* **1981**, *1*, 149.
(353) Atwood, C. G.; Geiger, W. E. *J. Am. Chem. Soc.* **1993**, *115*, 5310.
(354) Brum, W.; Kaim, W.; Waldor, E.; Krycik, M. *Inorg. Chem.* **1995**, *34*, 663.
(355) Dong, Y.; Hupp, J. T. *Inorg. Chem.* **1992**, *31*, 3322.
(356) Hupp, J. T.; Dong, Y. *J. Am. Chem. Soc.* **1993**, *115*, 6428.
(357) Crosby, G. A. *Acc. Chem. Res.* **1975**, *8*, 231.
(358) Caspar, J. V. Ph.D. Thesis, University of North Carolina, Chapel Hill, 1982.
(359) Lumpkin, R. D. Ph.D. Thesis, University of North Carolina, Chapel Hill, 1987.
(360) Yersin, H.; Braun, D. *Chem. Phys. Lett.* **1991**, *179*, 85.
(361) Huber, P.; Yersin, H. *J. Phys. Chem.* **1993**, *97*, 12705.
(362) Riesen, H.; Krausz, E.; Puza, M. *Chem. Phys. Lett.* **1988**, *151*, 65
(363) Kato, M.; Yamaguchi, S.; Hirota, *J. Phys. Chem.* **1988**, *92*, 6511.
(364) Caspar, J. V.; Westmoreland, T. D.; Allen, G. H.; Bradley, P. G.; Meyer, T. J.; Woodruff, W. H. *J. Am. Chem. Soc.* **1984**, *106*, 3492.
(365) Mabrouk, P. A.; Wrighton, M. S. *Inorg. Chem.* **1986**, *25*, 526.
(366) Mallick, P. K.; Strommen, D. P.; Kincaid, J. R. *J. Am. Chem. Soc.* **1990**, *112*, 1686.
(367) Mallick, P. K.; Danzer, G. D.; Strommen, D. P.; Kincaid, J. R. *J. Phys. Chem.* **1988**, *92*, 5628.
(368) Strommen, D. P.; Mallick, P. K.; Danzer, G. D.; Lumpkin, R. S.; Kincaid, J. R. *J. Phys. Chem.* **1990**, *94*, 1357.
(369) Maruszewski, K.; Bajdor, K.; Strommen, D. P.; Kincaid, J. R. *J. Phys. Chem.* **1995**, *99*, 6286.
(370) Chang, Y. S.; Xu, X.; Yabe, T.; You, S.-C.; Anderson, D. R.; Orman, L. K.; Hopkins, J. B. *J. Phys. Chem.* **1990**, *94*, 729.
(371) Yabe, T.; Orman, L. K.; Anderson, D. R.; You, S.-C.; Xu, X.; Hopkins, J. B. *J. Phys. Chem.* **1990**, *94*, 7128.
(372) Striplin, D.; Meyer, T. J. Manuscript in preparation.
(373) Cortes, J.; Heitele, H.; Jortner, J. *J. Phys. Chem.* **1994**, *98*, 2527.
(374) Claude, J. D.; Meyer, T. J. *J. Phys. Chem.* **1995**, *99*, 51.
(375) Wrighton, M.; Morse, D. L. *J. Am. Chem. Soc.* **1974**, *96*, 998.
(376) Giordano, P. J.; Wrighton, M. S. *J. Am. Chem. Soc.* **1979**, *101*, 2888.
(377) Worl, L. A. Ph.D. Dissertation, University of North Carolina, Chapel Hill, 1989.
(378) Worl, L. A.; Meyer, T. J. *Chem. Phys. Lett.* **1988**, *143*, 541.
(379) Danielson, E.; Lumpkin, R. S.; Meyer, T. J. *Chem. Phys. Lett.* **1987**, *91*, 1305.
(380) Kitamura, N.; Kim, H.-B.; Kawanishi, Y.; Obata, R.; Tazuke, S. *J. Phys. Chem.* **1986**, *90*, 1488.
(381) Marcus, R. A. *J. Phys. Chem.* **1990**, *94*, 4963.
(382) Hammack, W. S.; Drickamer, H. G.; Lowery, M. D.; Hendrickson, D. N. *Chem. Phys. Lett.* **1988**, *132*, 231.
(383) Hammack, W. S.; Drickamer, H. G.; Lowery, M. D.; Hendrickson, D. N. *Inorg. Chem.* **1988**, *27*, 1307.
(384) Barigelletti, F.; Belser, P.; Von Zelewsky, A.; Juris, A.; Balzani, V. *J. Phys. Chem.* **1985**, *89*, 3680.
(385) Bates, W. D.; Chen, P.; Meyer, T. J. Unpublished results.
(386) Salman, O. A.; Drickamer, H. G. *J. Chem. Phys.* **1982**, *77*, 3337.
(387) Hiraga, T.; Kitamura, N.; Kim, H.-B.; Tazuke, S.; Mori, N. *J. Phys. Chem.* **1989**, *93*, 2940.
(388) Hager, G. D.; Crosby, G. A. *J. Am. Chem. Soc.* **1975**, *97*, 7031.
(389) Lumpkin, R. S.; Kober, E. M.; Worl, L. A.; Murtaza, Z.; Meyer, T. J. *J. Phys. Chem.* **1990**, *94*, 239.
(390) Crosby, G. A.; Highland, R. G.; Truesdell, K. A. *Coord. Chem. Rev.* **1985**, *64*, 41.
(391) Burt, J. A.; Crosby, G. A. *Chem. Phys. Lett.* **1994**, *220*, 493.
(392) Striplin, D. R.; Crosby, G. A. *J. Phys. Chem.* **1995**, *99*, 7977.
(393) Jordan, K. J.; Wacholtz, W. F.; Crosby, G. A. *Inorg. Chem.* **1991**, *30*, 4588.
(394) Giordano, P. J.; Fredericks, S. M.; Wrighton, M. S.; Morse, D. L. *J. Am. Chem. Soc.* **1978**, *100*, 2257.
(395) Fredericks, S. M.; Luong, J. C.; Wrighton, M. S. *J. Am. Chem. Soc.* **1979**, *101*, 7415.
(396) Schoonover, J. R.; Bates, W. D.; Meyer, T. J. *Inorg. Chem.* **1995**, *34*, 6421.
(397) Reitz, G. A.; Demas, J. N.; Degraff, B. A.; Stephens, E. M. *J. Am. Chem. Soc.* **1988**, *110*, 0, 5051.
(398) Sacksteder, L.; Lee, M.; Demas, J. N.; DeGraff, B. A. *J. Am. Chem. Soc.* **1993**, *115*, 8230.
(399) Watts, R. J.; White, T. P.; Griffith, B. G. *J. Am. Chem. Soc.* **1975**, *97*, 6914.
(400) Spellane, P.; Watts, R. J. *Inorg. Chem.* **1993**, *32*, 5633.
(401) Wallace, L.; Heath, G. A.; Krausz, E.; Moran, G. *Inorg. Chem.* **1991**, *30*, 347.
(402) Krausz, E.; Higgins, J.; Riesen, E.; Moran, G. *Inorg. Chem.* **1993**, *32*, 2, 4053.
(403) Shaw, J. R.; Schmel, R. H. *J. Am. Chem. Soc.* **1991**, *113*, 389.
(404) DeArmond, M. K.; Carlin, C. M. *Coord. Chem. Rev.* **1981**, *36*, 325.
(405) Kutal, C. *Coord. Chem. Rev.* **1990**, *99*, 213.
(406) Endicott, J. F.; Lessard, R. B.; Lynch, D.; Perkovic, M. W.; Ryu, C. K. *Coord. Chem. Rev.* **1990**, *97*, 65.
(407) Zuleta, J. A.; Burberry, M. S.; Eisenberg, R. *Coord. Chem. Rev.* **1990**, *97*, 47.

(408) Rawlins, K. A.; Lees, A. J.; Adamson, A. W. *Inorg. Chem.* **1990**, *29*, 3866.
(409) Glezen, M. M.; Lees, A. J. *J. Am. Chem. Soc.* **1989**, *111*, 6602.
(410) Casadonte, D. J.; McMillan, D. R. *J. Am. Chem. Soc.* **1987**, *109*, 331.
(411) Tapolsky, G.; Duesing, R.; Meyer, T. J. *J. Phys. Chem.* **1991**, *95*, 1105.
(412) Winkler, J. R.; Creutz, C.; Sutin, N. *J. Am. Chem. Soc.* **1987**, *109*, 3740.
(413) Belletête, M.; Durocher, G. *J. Phys. Chem.* **1992**, *96*, 9183.
(414) Gould, I. R.; Mueller, L. J.; Farid, S. *Z. Phys. Chem.* **1991**, *170*, 143.
(415) Caspar, J. V.; Kober, E. M.; Sullivan, B. P.; Meyer, T. J. *J. Am. Chem. Soc.* **1982**, *104*, 630.
(416) Caspar, J. V.; Meyer, T. J. *Inorg. Chem.* **1983**, *22*, 2444.
(417) Kober, E. M.; Meyer, T. J. *Inorg. Chem.* **1984**, *23*, 3877.
(418) Van Houten, J.; Watts, R. J. *J. Am. Chem. Soc.* **1976**, *98*, 4853.
(419) Durham, B.; Caspar, J. V.; Nagle, J. K.; Meyer, T. J. *J. Am. Chem. Soc.* **1982**, *104*, 4803.
(420) Hoggard, P. E.; Porter, G. B. *J. Am. Chem. Soc.* **1978**, *100*, 1457.
(421) Wallace, W. M.; Hoggard, P. E. *Inorg. Chem.* **1980**, *19*, 2141.
(422) Van Houten, J.; Watts, R. J. *Inorg. Chem.* **1978**, *17*, 3381.
(423) Wynne, K.; Galli, C.; Hochstrasser, R. M. *J. Chem. Phys.* **1994**, *100*, 4797.
(424) Miyasaka, H.; Tabata, A.; Kamada, K.; Mataga, N. *J. Am. Chem. Soc.* **1993**, *115*, 7335.
(425) Thompson, P. A.; Simon, J. D. *J. Am. Chem. Soc.* **1993**, *115*, 5657.
(426) Reid, P. J.; Barbara, P. F. *J. Phys. Chem.* **1995**, *99*, 2546.
(427) Lian, T.; Kholodenko, Y.; Hochstrasser, R. M. *J. Phys. Chem.* **1995**, *99*, 3554.
(428) Bagchi, B.; Oxtoby, D. W.; Fleming, G. R. *Chem. Phys.* **1984**, *86*, 257
(429) van Der Zwan, G.; Hynes, J. T. *J. Phys. Chem.* **1985**, *89*, 4181.
(430) Kozik, M.; Sutin, N.; Winkler, J. R. *Coord. Chem. Rev.* **1990**, *97*, 23.
(431) Zhang, X.; Kozik, M.; Sutin, N.; Winkler, J. R. In *Electron Transfer in Inorganic, Organic and Biological Systems*; Bolton, J. R., Mataga, N., McLendon, G., Eds.; Advances in Chemistry No. 228; American Chemical Society: Washington, DC, 1991; p 247.
(432) Tominaga, K.; Kliner, D. A. V.; Johnson, A. E.; Levinger, N. E.; Barbara, P. F. *J. Chem. Phys.* **1995**, *99*, 2609.
(433) Reid, P. J.; Silva, C.; Barbara, P. F.; Karki, L.; Hupp, J. T. *J. Phys. Chem.* **1995**, *99*, 2609.
(434) Doorn, S. K.; Dyer, R. B.; Stoutland, P. O.; Woodruff, W. H. *J. Am. Chem. Soc.* **1993**, *115*, 6398.
(435) Ferguson, J.; Krausz, E. R.; Maeder, M. *J. Phys. Chem.* **1985**, *89*, 1852.
(436) Kim, H.-B.; Kitamura, N.; Tazuke, S. *Chem. Phys. Lett.* **1988**, *143*, 77.
(437) Kim, H.-B.; Kitamura, N.; Tazuke, S. *J. Phys. Chem.* **1990**, *94*, 1414.
(438) Kim, H.-B.; Kitamura, N.; Tazuke, S. *J. Phys. Chem.* **1990**, *94*, 7401.
(439) Surridge, N. A.; McClanahan, S. F.; Hupp, J. T.; Danielson, E.; Gould, S.; Meyer, T. J. *J. Phys. Chem.* **1989**, *93*, 294.
(440) Devenney, M.; Gould, S.; Guadalupe, A.; Sullivan, B. P.; Caspar, J. V.; Meyer, T. J. *J. Phys. Chem.* **1997**, *101*, 4535.
(441) Sabatani, E.; Nikol, H. D.; Gray, H. B.; Anson, F. C. *J. Am. Chem. Soc.* **1996**, *118*, 1158.
(442) Colón, J. L. Martin, C. R. *Langmuir* **1993**, *9*, 1066.
(443) Nagai, K.; Ueno, Y.; Takayami, N.; Kaneko, M. *Macromol. Chem. Phys.* **1995**, *196*, 1241.
(444) Majda, M.; Faulkner, L. R. *J. Electroanal. Chem.* **1984**, *169*, 97.
(445) Weynig, X.; McDonough, R. C., III; Langsdorf, B.; Demas, J. N.; DeGraff, B. A. *Anal. Chem.* **1994**, *66*, 4133.
(446) Milosavijevic, B. H.; Thomas, J. K. *J. Phys. Chem.* **1983**, *87*, 616.
(447) Allsopp, S. R.; Cox, A.; Kemp, T. J.; Reed, W. J. *J. Chem. Soc., Faraday Trans.* 1 **1978**, *74*, 1275.
(448) Maruszewski, K.; Kincaid, J. R. *Inorg. Chem.* **1995**, *34*, 2002.
(449) Turbeville, W.; Robins, D. S.; Dutta, P. K. *J. Phys. Chem.* **1992**, *96*, 5024.
(450) Maruszewski, K.; Strommen, D. P.; Kincaid, J. R. *J. Am. Chem. Soc.* **1993**, *115*, 8345.
(451) Incavo, J. A.; Dutta, P. K. *J. Phys. Chem.* **1990**, *94*, 3075.
(452) Yonemoto, E. H.; Kim, Y. I.; Schmehl, R. H.; Wallin, J. O.; Shoulders, B. A.; Richardson, B. R.; Haw, J. F.; Mallouk, T. E. *J. Am. Chem. Soc.* **1994**, *116*, 10557.
(453) Colón, J. L.; Yang, C.-Y.; Clearfield, A.; Martin, C. R. *J. Phys. Chem.* **1990**, *94*, 874.
(454) Colón, J. L.; Yang, C-.Y.; Clearfield, A.; Martin, C. R. *J. Phys. Chem.* **1988**, *92*, 5777.
(455) Kuykendall, V. G.; Thomas, J. K. *J. Phys. Chem.* **1990**, *94*, 4224.
(456) Thomas, J. K. *Acc. Chem. Res.* **1988**, *21*, 275.
(457) Turro, N. J.; Kumar, C. V.; Grauer, Z.; Barton, J. K. *Langmuir* **1987**, *3*, 1056.
(458) Kumar, C. V.; Williams, Z. J. *J. Phys. Chem.* **1995**, *99*, 17632.
(459) Vliers, D. P.; Collin, D.; Schoonheydt, R. A.; De Schryver, F. C. *Langmuir* **1986**, *2*, 165.
(460) Fan, J.; Tysoe, S.; Strekas, T. C.; Gafney, H. D.; Serpone, N.; Lawless, D. *J. Am. Chem. Soc.* **1994**, *116*, 5343.
(461) Castellano, F. N.; Heimer, T. A.; Tandhasetti, M. T.; Meyer, G. J. *Chem. Mater.* **1994**, *6*, 1041
(462) Beitz, J. V.; Miller, J. R. *J. Chem. Phys.* **1979**, *71*, 4579.
(463) Miller, J. R.; Beitz, J. V.; Huddleson, R. K. *J. Am. Chem. Soc.* **1984**, *106*, 5057.
(464) Wallace, W. L.; Bard, A. J. *J. Phys. Chem.* **1979**, *83*, 1350.
(465) Marcus, R. A. *J. Chem. Phys.* **1965**, *43*, 2654.
(466) Closs, G. L.; Miller, J. R. *Science* **1988**, *240*, 440.
(467) Miller, J. R.; Calcaterra, L. T.; Closs, G. L. *J. Am. Chem. Soc.* **1984**, *106*, 3047.
(468) Closs, G. L.; Calcaterra, L. T.; Green, N. J.; Penfield, K. W.; Miller, J. V. *J. Phys. Chem.* **1986**, *90*, 3673.
(469) Farid, R. S.; Chang, I.; Winkler, J. R.; Gray, H. B. *J. Phys. Chem.* **1994**, *98*, 5176.
(470) Fox, L. S.; Kozik, M.; Winkler, J. R.; Gray, H. B. *Science* **1990**, *247*, 1069.
(471) McCleskey, T. M.; Winkler, J. R.; Gray, H. B. *J. Am. Chem. Soc.* **1992**, *114*, 6935.
(472) Wasielewski, M. R.; Niewczyk, M. P.; Svec, W. A.; Pewitt, E. B. *J. Am. Chem. Soc.* **1985**, *107*, 1080.
(473) McLendon, G.; Miller, J. R. *J. Am. Chem. Soc.* **1985**, *107*, 7781.
(474) McLendon, G. *Acc. Chem. Res.* **1988**, *21*, 160.
(475) Ohno, T.; Yoshimura, A.; Mataga, N. *J. Phys. Chem.* **1986**, *90*, 3295.
(476) Asahi, T.; Mataga, N. *J. Phys. Chem.* **1989**, *93*, 6575.
(477) Asahi, T.; Ohkohchi, M.; Mataga, N. *J. Phys. Chem.* **1993**, *97*, 13132.
(478) Gould, I. R.; Ege, D.; Mattes, S. L.; Farid, S. *J. Am. Chem. Soc.* **1987**, *109*, 3794.
(479) Gould, I. R.; Moser, J. E.; Armitage, B.; Farid, S. *J. Am. Chem. Soc.* **1989**, *111*, 1917.
(480) Gould, I. R.; Moody, R.; Farid, S. *J. Am. Chem. Soc.* **1988**, *110*, 7242.
(481) Irvine, M. D.; Harrison, R. J.; Beddard, G. S.; Leighton, P.; Sanders, J. K. M. *Chem. Phys.* **1986**, *104*, 315.
(482) Archer, M. P.; Gadzekpo, V. P. Y.; Bolton, J. R.; Schmidt, J. A.; Weedon, A. C. *J. Chem. Soc., Faraday Trans.* 2, **1986**, *82*, 2305.
(483) Zou, C.; Miers, J. B.; Ballew, R. M.; Dlott, D. D.; Schuster, G. B. *J. Am. Chem. Soc.* **1991**, *113*, 7823.
(484) Chen, P.; Duesing, R.; Tapolsky, G.; Meyer, T. J. *J. Am. Chem. Soc.* **1989**, *111*, 8305.
(485) Chen, P.; Duesing, R.; Graff, D. K.; Meyer, T. J. *J. Phys. Chem.* **1991**, *95*, 5850.
(486) MacQueen, D. B.; Schanze, K. S. *J. Am. Chem. Soc.* **1991**, *113*, 7470.
(487) MacQueen, D. B.; Eyler, J. R.; Schanze, K. S. *J. Am. Chem. Soc.* **1992**, *114*, 1897.
(488) Yonemoto, E. H.; Saupe, G. B.; Schmehl, R. H.; Hubig, S. M.; Riley, R. L.; Iverson, R. L.; Mallouk, T. E. *J. Am. Chem. Soc.* **1994**, *116*, 4786.
(489) Chen, P.; Mecklenburg, S. L.; Duesing, R.; Meyer, T. J. *J. Phys. Chem.* **1993**, *97*, 6811.
(490) Chen, P.; Mecklenburg, S. L.; Duesing, R.; Meyer, T. J. *J. Phys. Chem.* **1993**, *97*, 13126.
(491) Piotrowiak, P.; Miller, J. R. *J. Phys. Chem.* **1993**, *97*, 13052.
(492) Chapman, C. F.; Maroncelli, M. *J. Phys. Chem.* **1991**, *95*, 9095.
(493) Ittah, V.; Huppert, D. *Chem. Phys. Lett.* **1990**, *173*, 496.
(494) Bart, E.; Huppert, D. *Chem. Phys. Lett.* **1992**, *195*, 37.
(495) Huppert, D.; Ittah, V.; Kosower, E. M. *Chem. Phys. Lett.* **1989**, *159*, 267.
(496) Gould, I. R.; Young, R. H.; Mueller, L J.; Albracht, A. C.; Farid, S. *J. Am. Chem. Soc.* **1994**, *116*, 3147.
(497) Gould, I. R.; Noukakis, D.; Gomez-Jahn, L.; Young, R. H.; Goodman, J. L.; Farid, S. *Chem. Phys.* **1993**, *176*, 439.
(498) Markel, F.; Ferris, N. S.; Gould, I. R.; Myers, A. B. *J. Am. Chem. Soc.* **1992**, *114*, 6208.
(499) Sutin, N. in *Electron Transfer in Inorganic, Organic and Biological Systems*; Bolton, J. R., Mataga, N., McLendon, G., Eds., Advances in Chemistry No. 228; American Chemical Society: Washington, DC, 1991; p 25.
(500) Brunschwig, B.; Ehrenson, S.; Sutin, N. *J. Am. Chem. Soc.* **1984**, *106*, 6858.
(501) Mussell, R. D.; Nocera, D. G. *J. Am. Chem. Soc.* **1988**, *110*, 2764.
(502) Mussell, R. D.; Nocera, D. G. *J. Phys. Chem.* **1991**, *95*, 6919.
(503) Zaleski, J. M.; Chang, C. K.; Nocera, D. G. *J. Phys. Chem.* **1993**, *97*, 13206.
(504) Zaleski, J. M.; Chang, C. K.; Leroi, G. E.; Cukier, R. I.; Nocera, D. G. *J. Am. Chem. Soc.* **1992**, *114*, 3564.
(505) Zaleski, J. M.; Wu, W.; Chang, C. K.; Leroi, G. E.; Cukier, R. I.; Nocera, D. G. *Chem. Phys.* **1993**, *176*, 483.
(506) Liang, N.; Miller, J. R.; Closs, G. L. *J. Am. Chem. Soc.* **1989**, *111*, 8740.
(507) Liang, N.; Miller, J. R.; Closs, G. L. *J. Am. Chem. Soc.* **1990**, *112*, 5353.
(508) Kirmaier, C.; Holten, D. *Photosynth. Res.* **1987**, *13*, 225.
(509) Youvan, D. C.; Marrs, B. L. *Sci. Am.* **1987**, *256*, 42.

(510) Parson, W. W.; Woodbury, N. W. T.; Becker, M.; Kirmaier, C.; Holten, D. In *Antennas and Reactions Centers of Photosynthetic Bacteria*; Michel-Beyerle, M. E., Ed.; Springer-Verlag: Berlin, 1985; p 278.
(511) Schweitzer, G.; Hucke, M.; Griebenow, K.; Muller, M. G.; Holzwarth, A. R. *Chem. Phys. Lett.* **1992**, *190*, 149.
(512) Miller, J. R.; Peeples, J. A.; Schmitt, M. J.; Closs, G. L. *J. Am. Chem. Soc.* **1982**, *104*, 6488.
(513) McGuire, M.; McLendon, G. *J. Phys. Chem.* **1986**, *90*, 2549.
(514) Strauch, S.; McGuire, M.; McLendon, G.; Guarr, T. *J. Phys. Chem.* **1983**, *87*, 3579.
(515) Guarr, T.; McGuire, M.; Strauch, S.; McLendon, G. *J. Am. Chem. Soc.* **1983**, *105*, 616.
(516) Dorfman, R. C.; Lin, Y.; Zimmt, M. B.; Baumann, J.; Domingue, R. P.; Fayer, M. D. *J. Phys. Chem.* **1988**, *92*, 4258.
(517) Wayne, E. J., Jr.; Chen, P.; Meyer, T. J. *J. Am. Chem. Soc.* **1992**, *114*, 387.
(518) Gaines, G. L., III.; O'Neil, M. P.; Svec, W. A.; Niemczyk, M. P.; Wasielewski, M. R. *J. Am. Chem. Soc.* **1991**, *113*, 719.
(519) Wasielewski, M. R.; Johson, D. G.; Svec, W. A.; Kersey, K. M.; Minsek, D. W. *J. Am. Chem. Soc.* **1988**, *110*, 7219.
(520) Harriman, A.; Heitz, V.; Ebersole, M.; Willigen, H. van, *J. Phys. Chem.* **1994**, *98*, 4982.
(521) Chen, P.; Meyer, T. J. Unpublished results.

CR941180W